POLITECNICO DI MILANO

Scuola di Ingegneria Industriale e
dell’Informazione

Corso di Laurea in
Ingegneria Meccanica

Development and implementation in Amesim® of the Model Predictive Control for the energy management of a HEV

Relatore: Prof. MAPELLI Ferdinando Luigi

Tesi di Laurea di:
DONI Diego Matr.783101

Anno Accademico 2013-2014

Acknowledgment

This thesis work marks the end of my university education which has been tough, long but awesome. Studying in Milan and Stockholm, carrying out the thesis at LMS Imagine in Lyon were great experiences and some people have had a crucial role to make it possible. For this and for other reasons, I would like to thank professor Annika Stensson Trigell from KTH, Royal Institute of Technology and professors Federico Cheli, Ferdinando Luigi Mapelli from Politecnico di Milano for their support both during the development of the work and to write this report. Their nice suggestions made me understand that the work was evolving in a good manner. They also encouraged me to analyze interesting topics which made the thesis project even more interesting and helped me to define a good layout for this report.

Let me thank all people I met at LMS Imagine in Lyon who were always kind, friendly and warm with me. They involved me in many activities which made me feel part of the company and made my time in France happier. Last but not least a special thank goes to Yerlan Akhmetov and Bruno Lecointre from LMS Imagine for the invaluable help and knowledge they gave me throughout my staying in Lyon, and Peter Mas from LMS Imagine who decided to hire me as intern.

… En del av mitt hjärta ligger där
och mina tankar flyger alltid dit…

Abstract

The rising price of fuel and the ever-restricting legislations on fuel consumption and amount of pollutant emissions have encouraged almost all automotive manufacturers to look for alternative propulsion systems which may replace the well-established internal combustion engine. Hybridization seems the most promising solution at least in the short term period. The term hybrid electric vehicle indicates a ground vehicle which is equipped with either one or two electric machines in addition to a conventional internal combustion engine. A hybrid electric vehicle guarantees a great flexibility in the energy management since both fuel energy and electric energy stored in a battery can be used together to provide the necessary traction effort; however the superior operating flexibility of the powertrain requires a complex control strategy which manages efficiently the power flow among the components of the powertrain. In addition hybrid vehicles establish new challenges for the designers in particular considering the passengers' quality perception of the vehicle, i.e. NVH (i.e. Noise and Vibration Harshness). This thesis develops a MPC-based control strategy for the energy management problem of a power-split hybrid electric vehicle where fuel economy and reduction of the discomfort felt by passengers during engine starting and stopping are the core objectives. The strategy is formulated according to an optimization problem driven by the two objectives above mentioned and subjected to multiple constraints. The constraints are related to the operating points of the machines, to the need of assuring charge sustenance of the vehicle and reduce the longitudinal oscillations due to engine start and stop. The strategy has been validated over some standard drive cycles and the performance have been compared to those achievable with a rule based strategy. The thesis assesses the potential of implementing additional information provided by interactive navigation systems like GPS and GIS in the optimization problem; moreover it investigates which parameters affect the most the numeric optimization. The results show a decrease in fuel consumption in all standard drive cycles in comparison to the rule based strategy. The MPC-based control strategy shows good robustness against vehicle parameters uncertainty nonetheless the analysis has highlighted few weaknesses of the linear MPC approach. All simulations have been carried out via co-simulation between Simulink® and Amesim®.

Keywords: model predictive control, power-split hybrid electric vehicle, energy management.

Sommario

Il crescente costo del carburante e l’introduzione di leggi restrittive in materia di consumo di combustibile ed emissione di sostanze nocive, sta spingendo i costruttori mondiali di veicoli terrestri allo sviluppo di sistemi di propulsione alternativi al consolidato motore a combustione interna. Nell’ultimo ventennio varie sono state le soluzioni ipotizzate, ciò nonostante l’ibridizzazione sembra attualmente la soluzione tecnica più promettente per raggiungere i traguardi di superiore efficienza energetica. Un veicolo elettrico ibrido é equipaggiato con un motore a combustione interna supportato da almeno un motore elettrico e da una fonte di potenza elettrica. Grazie alla possibilità di utilizzare contemporaneamente l’energia chimica del combustibile e l’energia elettrica immagazzinata in una batteria ad alto voltaggio, i veicoli ibridi elettrici (HEV) garantiscono elevata flessibilità operativa con potenzialità di ridurre in maniera significativa le emissioni nocive e il consumo rispetto a un veicolo convenzionale. Tuttavia la superiore efficienza energetica può essere raggiunta solo a patto che tutti i componenti del sistema di propulsione cooperino in sinergia. Questo richiede lo sviluppo di una strategia di controllo avanzata capace di ottimizzare il flusso di potenza tra le macchine. In aggiunta gli HEVs pongono nuove sfide nell’ambito della progettazione NVH dei veicoli. Questa tesi ha l’obiettivo di sviluppare una strategia di controllo basata su Model Predictive Control per la gestione del flusso di potenza del veicolo e la riduzione delle vibrazioni del corpo vettura associate agli eventi di attivazione e spegnimento del motore a combustione interna. La strategia risolve un problema di ottimizzazione guidato dai due obiettivi menzionati in precedenza e soggetto ai numerosi vincoli operativi delle macchine. La strategia é stata testata simulando 5 cicli di guida standardizzati e le prestazioni in termini di riduzione del consumo e delle vibrazioni del corpo vettura, sono state confrontate con quelle ottenibili da una strategia concorrente basata su un approccio euristico. La tesi analizza anche la potenzialità di integrare ulteriori informazioni rese disponibili da sistemi di navigazione quali GPS e GIS nella gestione ottimale del flusso di potenza. I risultati mostrano un decremento del consumo totale sui cicli di guida standardizzati quando la strategia MPC é implementata; essa mostra anche robustezza rispetto alla variabilità di alcuni parametri del veicolo e della strada. Tuttavia emergono delle limitazioni dovute allo sviluppo di una strategia linearizzata. Tutte le simulazioni sono state condotte in parallelo con i software Simulink® e Amesim®.

Parole chiave: model predictive control, power-split hybrid electric vehicle, energy management

Estratto in lingua italiana

Struttura della tesi

Questo lavoro di tesi ha lo scopo di sviluppare una strategia di controllo, basata sull'approccio Model Predictive Control, del flusso di potenza nel sistema di propulsione di un veicolo ibrido elettrico serie-parallelo, per migliorare l'efficienza così da ridurre il consumo di carburante. L'intero lavoro é svolto al calcolatore dove il veicolo di riferimento é rappresentato da un modello fisico-matematico dettagliato implementato nel software commerciale Amesim$^{®}$ distribuito da LMS International. Il progetto é stato interamente svolto presso LMS International nella sede di Lione, Francia.

La tesi, scritta in lingua inglese, inquadra dapprima il problema di definire una strategia di controllo per la gestione energetica di un veicolo ibrido elettrico, successivamente descrive i passaggi matematici necessari per sviluppare la strategia MPC. Nella terza parte vengono ampiamente discussi i risultati, mettendo in luce vantaggi e svantaggi della strategia. La tesi é organizzata in capitoli, in particolare i primi due capitoli inquadrano i veicoli ibridi elettrici nel panorama dell'industria automobilistica attuale, evidenziando pregi e difetti rispetto ad architetture concorrenti. Il terzo capitolo tratta in dettaglio l'architettura serie-parallelo power split utilizzata in questa tesi, descrivendo i componenti più importanti e le differenti modalità di guida. Il quarto capitolo introduce e spiega la strategia di controllo MPC dal punto di vista dell'ottimizzazione numerica necessaria per elaborare i comandi di controllo sul sistema. Il quinto capitolo discute i risultati principali quelli cioè che pongono in confronto le prestazioni della strategia MPC con quelle di una strategia concorrente. Questo capitolo é importante in quanto chiarifica il principio operativo della strategia. Il sesto capitolo affronta l'analisi in dettaglio dei parametri che influenzano il funzionamento della strategia. É fatto largo uso dell'analisi di sensibilità per estrarre informazioni utili circa la dipendenza delle prestazioni della strategia dai valori dei parametri. L'ultimo capitolo conclude la tesi riassumendo i punti principali e fornendo indicazioni su possibili sviluppi futuri. Le tre appendici finali illustrano i passaggi matematici necessari per implementare la strategia, eseguire l'analisi di sensibilità e i cicli di guida di riferimento adottati in tutte le simulazioni numeriche.

L'ibrido come soluzione

Un terzo dell'intero consumo energetico mondiale é attribuito al trasporto di merci e persone su gomma; ad esso si attribuisce anche una parte attiva nel processo di riscaldamento dell'atmosfera terrestre. Per fronteggiare l'elevato consumo energetico e ridurre l'emissione di sostanze inquinanti nell'atmosfera sono state emanate leggi stringenti volte a incentivare il progresso tecnologico nel campo automobilistico. Ad esempio l'unione europea ha fissato come obiettivo per il 2020 il limite massimo di emissione di CO_2 per gli autoveicoli pari a 95g/km. Tutti i costruttori mondiali di autoveicoli stanno lavorando instancabilmente alla ricerca di tecnologie innovative e soluzioni costruttive capaci di ridurre il consumo e i tassi di emissione di inquinanti dei veicoli stradali. Queste due problematiche sono principalmente collegate all'utilizzo di un motore a combustione interna per generare la necessaria potenza e coppia di propulsione. Per ridurre il consumo é necessario migliorare l'efficienza del processo di combustione; allo stesso modo l'abbattimento dei tassi di emissione di inquinanti é legato al trattamento dei prodotti della reazione chimica di combustione. Nonostante la ricerca nell'ambito dei motori a combustione interna abbia portato a notevoli progressi, é difficile pensare che in futuro sarà possibile rispettare gli obiettivi sempre più stringenti avendo come unica leva lo sviluppo del motore endotermico.

Per questa ragione nell'ultimo ventennio i costruttori automobilistici hanno cercato alternative alla sola propulsione fornita dal motore a combustione interna. La via privilegiata é quella dell'elettrificazione dove il sistema di propulsione del veicolo si arricchisce di componenti elettromeccanici che hanno lo scopo di affiancare o addirittura sostituire completamente il motore a combustione interna nella generazione di potenza al fine di ridurre l'impatto ambientale del veicolo. Le principali soluzioni proposte si distinguono in due classi: quella dei veicoli completamente elettrici e quella dei veicoli ibridi. Nel primo caso l'energia elettrica, ottenuta dalla conversione di energia chimica immagazzinata in una batteria, é l'unica fonte energetica del sistema che utilizza un motore elettrico per la conversione di quest'ultima in potenza meccanica utile alla propulsione. Nei veicoli ibridi elettrici invece il motore a combustione interna é utilizzato in sinergia con uno o più motori elettrici al fine di raggiungere una efficienza superiore rispetto a veicoli convenzionali e quindi minor consumo e riduzione dei tassi di emissione di inquinanti. Il bilancio energetico vede in questo caso due fonti primarie di energia rappresentate dall'energia chimica immagazzinata in una batteria ad alto voltaggio e l'energia chimica di un combustibile fossile. Grazie a queste due fonti energetiche distinte, i veicoli ibridi elettrici non soffrono dei tipici problemi che affliggono i veicolo elettrici e.g. limitata autonomia di guida data dalla ridotta capacità elettrica delle batterie, lunghi periodi di ricarica della batteria. I veicoli elettrici ibridi rappresentano dunque al giorno d'oggi la sola reale alternativa alla propulsione basata interamente su un motore a combustione interna. Essi pongono una grande sfida ingegneristica perché se da un lato la presenza contemporanea di un motore endotermico e di macchine elettriche, insieme a tutti i sottosistemi necessari al loro funzionamento e alla loro regolazione, rende l'architettura della trasmissione e del sistema di propulsione assai complessa, da un altro punto di vista la propulsione elettrica introduce un grado di libertà aggiuntivo nel bilancio energetico del veicolo e la maggiore flessibilità nella suddivisione del carico tra motore endotermico e macchine elettriche in base alle condizioni operative. La suddivisione della potenza nei due rami del sistema di propulsione é generalmente guidata da opportuni obiettivi che devono essere raggiunti lungo una missione di guida. Tipicamente la riduzione del consumo totale di combustibile e dei tassi di emissione istantanei di sostanze inquinanti rappresentano due obiettivi della gestione energetica di un veicolo ibrido. In parallelo occorre tenere conto dei molteplici vincoli esistenti sui punti di funzionamento dei componenti pertanto la definizione di una corretta ripartizione della generazione di potenza si riflette nella risoluzione di un problema di ottimizzazione vincolata. Questo problema é indicato con il termine *energy management.*

Il problema di ottimo

Data la complessità del problema, é richiesto lo sviluppo e l'implementazione di una strategia di controllo che coordini le funzioni di tutte le macchine preposte alla generazione di potenza meccanica al fine di raggiungere gli obiettivi rispettando tutti i vincoli operativi. Il controllo é organizzato a livelli. Ogni sottosistema (trasmissione, batteria, motore endotermico, macchine elettriche) é gestito da un suo controllore che imposta il punto di funzionamento della macchina in base alle istruzioni ricevute; tali controllori sono definiti di basso livello. Al livello più alto é posto l'autista che fornisce i comandi base tramite i pedali di acceleratore e freno ed eventualmente tramite il cambio marcia. L'interazione della struttura di controllo con altre logiche di controllo (ABS, ESP etc...) é gestita da una controllore di alto livello posto appena sotto l'autista sulla scala gerarchica. Il cuore della strategia é però il Vehicle Supervisory Controller. Questo elemento implementa la vera strategia di controllo del flusso di potenza; esso riceve le informazioni dai sensori e le specifiche dall'autista e interagisce con i controllori di basso livello per coordinare il funzionamento di tutte le macchine. La grande sfida consiste nel definire questa strategia di controllo e gli approcci finora sperimentati si racchiudono in due classi:

- Strategie *rule based*: sfruttando le informazioni fornite da vari sensori, il controllore riconosce lo stato di funzionamento del veicolo. Per ogni stato di funzionamento la strategia dispone di delle azioni di controllo reimpostate che vengono automaticamente applicate al sistema.
- Strategie di controllo ottimo: il rapporto di suddivisione della potenza tra motore endotermico e propulsione elettrica é il risultato di un problema di ottimizzazione. Questa classe é ulteriormente suddivisa in metodologie *globali* e *locali*, dove la denominazione é basata sulla lunghezza dell'orizzonte temporale futuro che viene considerato nel problema di ottimizzazione.

Data la natura statica delle strategie rule based, le azioni di controllo non sono ottimali per la particolare situazione di guida quindi il veicolo non lavora in genere nelle migliori condizioni di efficienza. Queste tecniche sono però le più semplici da implementare perché non sono computazionalmente dispendiose. Le tecniche di ottimizzazione globali quali Dynamic Programming assumono di conoscere in anticipo l’esatto profilo di potenza richiesta lungo tutta la missione di guida pertanto riescono a calcolare off line l’azione di controllo valida per tutta la missione. Nei casi in cui non intervengano perturbazioni esterne la strategia risulta essere la migliore in assoluto. Nella realtà é però impossibile conoscere con esattezza il profilo futuro di potenza richiesta pertanto queste strategie sono per lo più utilizzate nell’ambito della simulazione numerica per fornire la soluzione di riferimento, le cui prestazioni servono da metro di giudizio rispetto alle strategie real time, in modo da capire le effettive potenzialità del controllore sviluppato. Dal punto di vista dell’implementazione real time le strategie di ottimizzazione locale sono più interessanti. Esse limitano l’ottimizzazione a pochi istanti futuri cercando di prevedere l’evoluzione della richiesta di potenza, oppure limitano il problema di ottimo all’istante di campionamento. Model Predictive Control é un esempio del primo approccio invece A-ECMS é un esponente del secondo.

Questa tesi affronta la definizione di una strategia di controllo basata su Model Predictive Control per il problema energetico di un veicolo ibrido elettrico serie-parallelo power split. Questo tipo di ibrido garantisce la maggior flessibilità nella gestione della produzione di potenza, quindi é candidato a fornire la migliore evoluzione rispetto a un veicolo convenzionale motorizzato da un solo motore a combustione interna. Il Model Predictive Control é un metodo che elabora una strategia di controllo per un sistema dinamico che sia ottima rispetto a una funzione di merito e che soddisfi tutti i vincoli operativi agenti sul sistema. Il metodo MPC utilizza un modello di riferimento della dinamica del sistema per prevedere la sua risposta ad ingressi noti di controllo e di disturbo esterno lungo un orizzonte di previsione futuro. I soli valori di controllo che portano il sistema a soddisfare tutti i vincoli operativi lungo l’orizzonte di previsione sono presi in considerazione e tra questi si estraggono unicamente quelli che rendono ottima la funzione di merito lungo lo stesso orizzonte di previsione. MPC é già applicato con successo nell’industria chimica, a cui deve la sua nascita, ma grazie all’evoluzione nel campo dei microprocessori sta crescendo il suo impiego in ambito automobilistico. La decisione di applicare il metodo MPC per lo sviluppo di una strategia di controllo di alto livello nasce dalla forza di tale metodo di includere molteplici vincoli operativi già nella risoluzione del problema di ottimo, dunque la strategia rispetta i vincoli e può essere direttamente applicata al sistema. In più la natura previsionale del metodo suggerisce che l’adozione di sistemi di navigazione quali GPS, informazioni sul traffico etc.. possano migliorare la previsione della potenza richiesta in futuro dall'autista e quindi l'efficienza del veicolo.

Sviluppo della strategia MPC

Il metodo MPC é basato su 4 punti cardine:

- Modello di riferimento della risposta del sistema a ingressi noti
- Funzioni di vincolo
- Funzione di merito
- Ottimizzazione numerica

Come descritto brevemente in precedenza, il metodo MPC calcola i valori delle variabili di controllo da applicare al sistema all'istante immediatamente successivo a quello di campionamento basandosi sulla risoluzione di un problema di ottimizzazione. Il metodo utilizza le condizioni misurate all'istante di campionamento e un modello affidabile della risposta del sistema per prevedere la sua evoluzione lungo un orizzonte futuro di previsione sotto la guida di una sequenza di controlli. Esistono diverse possibili sequenze di controlli che possono portare il sistema dalle condizioni iniziali a quelle finali desiderate rispettando tutti i vincoli operativi; tuttavia esiste solo una sequenza che, svolgendo tale compito, rende ottima una funzione di merito assegnata. MPC risolve quindi un problema di ottimizzazione per calcolare questa sola sequenza ottima. Nella formulazione classica del metodo MPC la sequenza di controllo è applicata lungo un orizzonte di controllo futuro di lunghezza uguale o inferiore rispetto all'orizzonte di previsione. Dunque MPC risolve un problema di ottimizzazione basato sull'evoluzione futura del sistema, tuttavia esso applica solo i valori di controllo che corrispondono al primo passo di evoluzione andando poi a ripetere l'intero processo di ottimizzazione servendosi delle nuove informazioni disponibili al successivo campionamento e spostando in avanti di un passo l'orizzonte di previsione. Questa tecnica di calcolo ricorsiva prende il nome di *receding horizon* e porta a definire un controllo in retroazione.

Una delle problematiche dell'ottimizzazione numerica sta nel assicurare che l'algoritmo converga a un punto di ottimo del sistema e che tale punto sia l'ottimo globale. Qualora il problema godesse della proprietà di convessità allora esisterebbe un solo punto di ottimo e questo sarebbe di ottimo globale. É possibile garantire questa proprietà definendo il problema secondo la forma canonica della programmazione quadratica cioè con funzione di merito quadratica nelle variabili di progetto, i.e. le variabili di controllo, e definita positiva mentre i vincoli devono essere espressi sotto forma di disuguaglianze lineari. I quattro punti elencati in precedenza sono implementati numericamente cercando di rispettare queste condizioni per la convessità del problema di ottimizzazione; di seguito si fornisce una breve descrizione dei passaggi matematici che si rendono necessari.

Il modello di riferimento

Il veicolo analizzato in questa tesi é un ibrido elettrico serie-parallelo di tipo power split che non riflette nello specifico nessun veicolo reale. Lo scopo non é infatti quello di ottimizzare un veicolo specifico ma piuttosto sviluppare una strategia di controllo e valutarne le potenzialità. Si é utilizzato come riferimento un modello dettagliato implementato nel software Amesim® che consente di riprodurre la dinamica longitudinale del veicolo e il funzionamento dei suoi componenti principali quali motore a combustione interna, macchine elettriche, batteria ad alto voltaggio e trasmissione. In più il modello consente di eseguire analisi di base sul comfort limitate al campo di bassa frequenza e ai moti di beccheggio e scuotimento verticale della cassa. Il modello é costruito a blocchi dove ogni blocco descrive il comportamento di un componente mediante equazioni matematiche. Lo schema costruttivo del veicolo é rappresentato nella prossima figura.

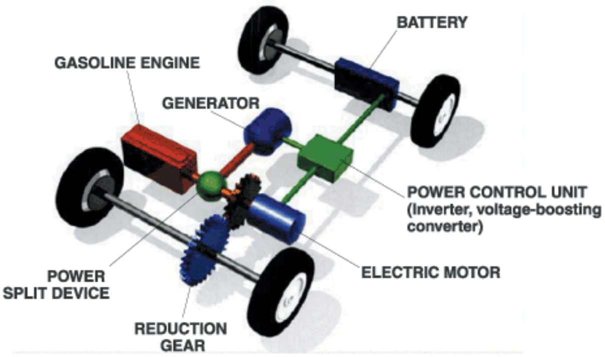

Figura 1: Sistema di propulsione di un ibrido elettrico power-split.

Un veicolo ibrido elettrico power split si compone di un motore endotermico e due macchine elettriche collegate a un rotismo epicicloidale (power splite device) che ha la scopo di ripartire la potenza tra queste tre macchine e la sala motrice anteriore. Le due macchine elettriche possono operare sia da motore che da generatore e definiscono il carico per la batteria ad alto voltaggio posta sulla sala posteriore. La power control unit é l'elettronica di potenza che, sulla base della strategia di controllo implementata al suo interno, fissa la ripartizione e il flusso di potenza tra motore endotermico e batteria elettrica in modo tale da bilanciare le richieste dell'autista e rispettare i vincoli operativi del veicolo. Grazie al rotismo epicicloidale e alla batteria ad alto voltaggio é consuetudine affermare che un ibrido power split ha due gradi di libertà nella gestione della potenza. Tramite il rotismo epicicloidale la velocità angolare dell'albero a gomiti é indipendente dalla velocità angolare delle ruote motrici consentendo di fissare liberamente la velocità angolare del motore endotermico e quindi dando un notevole vantaggio in termini di efficienza energetica. In più la batteria ad alto voltaggio funge da buffer energetico assorbendo l'eccesso di potenza prodotta dal motore endotermico rispetto a quanto richiesto alla ruota e fornendo invece potenza alle ruote motrici quando la potenza prodotta dal motore termico non é sufficiente. Questo si traduce in un ulteriore vantaggio in termini di efficienza energetica perché nelle condizioni di bassa richiesta di potenza il motore termico può produrre un surplus di potenza in condizioni di alta efficienza che viene immagazzinata nella batteria e riutilizzata nelle fasi di massima richiesta di potenza, andando così a supportare il motore endotermico che pertanto non deve pareggiare il carico massimo e può mantenere un punto operativo caratterizzato da basso consumo. Quanto descritto si attua tramite una opportuna strategia di controllo che utilizza il generatore elettrico e il rotismo epicicloidale per governare il punto di funzionamento del motore a combustione interna; dato che la velocità angolare dell'albero a gomiti può essere settata in maniera indipendente rispetto alla velocità angolare delle ruote motrici si suole indicare il gruppo rotismo epicicloidale - generatore elettrico come una e-CVT (electronic continuous variable transmission). Un veicolo di questo tipo dispone di numerose modalità di guida che spaziano da una modalità totalmente elettrica, alla modalità power-split dove motore endotermico e batteria cooperano per raggiungere la migliore efficienza energetica, alla modalità parallela dove tutta la potenza prodotta dal motore termico fluisce alle ruote motrici, alla frenata rigenerativa che rappresenta un'ulteriore guadagno in termini di efficienza energetica visto che parte dell'energia cinetica del veicolo é impiegata per ricaricare la batteria senza utilizzare parte della potenza prodotta dal motore a combustione interna. La sala motrice anteriore é collegata all'albero che reca la corona del rotismo epicicloidale e il rotore del motore elettrico tramite una cinghia non riportata nella figura precedente.

Il modello implementato in Amesim® consente di modellare tutte queste fasi di guida, tuttavia esso é troppo complesso per poter essere utilizzato come riferimento da MPC per prevedere la risposta del sistema eseguendo numerose valutazioni in poco tempo. Di conseguenza si é provveduto a estrarre un modello matematico più semplice in grado di cogliere gli aspetti fondamentali del problema energetico tralasciando quelli meno importanti. I seguenti componenti sono stati modellati:

- Motore a combustione interna
- Macchine elettriche
- Trasmissione
- Batteria ad alto voltaggio

La dinamica dell'albero a gomiti e l'andamento dello stato di carica della batteria sono stati modellati mediante due equazioni differenziali del primo ordine, invece tutti gli altri componenti sono stati descritti tramite una modellazione quasi statica. Il funzionamento della batteria ad alto voltaggio é stato descritto secondo il modello di un circuito elettrico equivalente come rappresentato nella prossima figura:

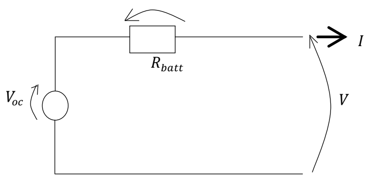

dove V_{oc} corrisponde al voltaggio di circuito aperto della batteria, R_{batt} corrisponde alla resistenza interna equivalente della batteria, V e I rappresentano rispettivamente il voltaggio e la corrente ai morsetti della batteria. Lo derivata temporale dello stato di carica della batteria é definita dalla seguente equazione differenziale:

$$\frac{dSOC}{dt} = -\frac{I}{Q_{batt}} = -\frac{V_{oc} - \sqrt{V_{oc}^2 - 4P_{batt}R_{batt}}}{2Q_{batt}R_{batt}} \tag{1}$$

dove SOC indica lo stato di carica della batteria, t é la variabile temporale, Q_{batt} é la capacità elettrica della batteria, P_{batt} é la potenza totale scambiata dalla batteria con le macchine elettriche. La potenza della batteria funge da collegamento con il sistema di propulsione, comprensivo del motore endotermico, delle macchine elettriche e della trasmissione alle ruote motrici. Esso é schematizzato come segue:

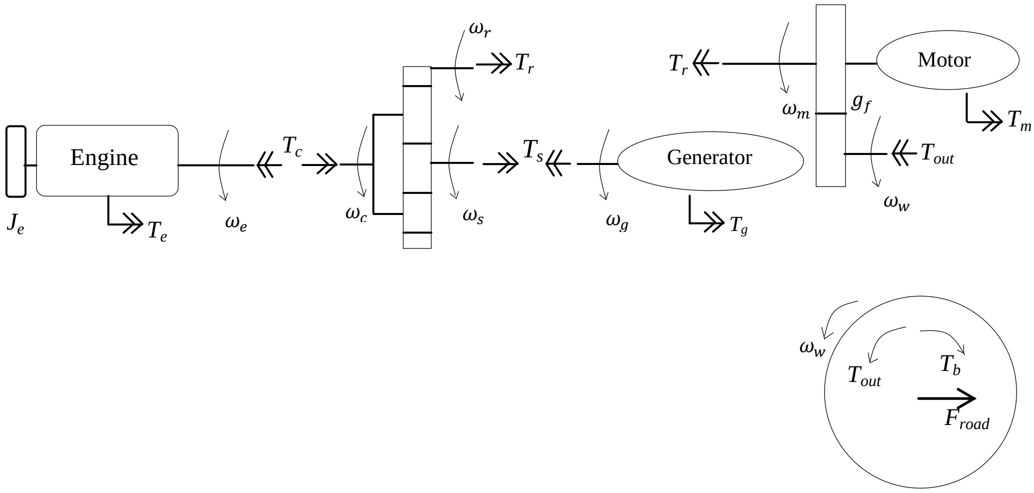

dove $J_e$rappresenta l'inerzia rotazionale del volano, T_e la coppia del motore endotermico all'albero, ω_e la velocità angolare dell'albero a gomiti, T_c la coppia del planetario, ω_c la velocità angolare del planetario, T_s la coppia del solare, ω_s la velocità angolare del solare, T_r la coppia della corona, ω_r la velocità angolare della corona, T_g la coppia del generatore al rotore, ω_g la velocità angolare del rotore del generatore, T_m la coppia del motore elettrico al rotore, ω_m la velocità angolare del rotore del motore elettrico, g_f il rapporto di trasmissione totale tra corona e ruote motrici, ω_w la velocità angolare delle ruote motrici, T_{out} la coppia totale all'uscita o in ingresso alla trasmissione, T_b la totale coppia frenante applicata dal sistema frenante di servizio, F_{road} la totale forza resistente esercitata dalla spinta aerodinamica e dalla resistenza al rotolamento. La dinamica longitudinale del veicolo é schematizzata servendosi dell'analogia del moto di avanzamento di un punto materiale soggetto alla forza di trazione e alle forze resistive date dalla resistenza al rotolamento e dalla spinta aerodinamica. La componente della forza peso parallela al terreno é stata trascurata in quanto si é assunto nella prima parte di questa tesi che la strategia di controllo non possa conoscere la pendenza della strada. Assumendo nota la coppia totale alle ruote richiesta dall'autista, definita come:

$$T_{driver} = T_{out} - T_b \tag{2}$$

é possibile integrare la velocità di avanzamento del veicolo lungo un orizzonte temporale $[t; t+T]$ a partire dalla equazione differenziale che governa la dinamica longitudinale del veicolo.

$$m^*\ddot{x} + \frac{1}{2}\rho_{air}C_x\dot{x}^2 + mgf_r = \frac{T_{driver}}{r_w} \tag{3}$$

dove m^* indica la ierzia equivalente del veicolo comprensiva del corpo vettura e di tutti gli organi in moto, x é il grado di avanzamento del veicolo, ρ_{air} la densità dell'aria, C_x il coefficiente adimensionale di resistenza aerodinamica, m la massa del veicolo, g l'accelerazione di gravità, f_r il coefficiente di resistenza al rotolamento, r_w il raggio di rotolamento della ruota.

Dalla conoscenza della coppia e della velocità si ricava il profilo della potenza richiesta dall'autista lungo l'orizzonte temporale $[t; t+T]$. Noto questo profilo in ingresso, è compito della strategia di controllo decidere come utilizzare la potenza prodotta dal motore endotermico e dalle macchine elettriche per bilanciarlo. Siano la coppia all'albero fornita dal motore endotermico, la coppia del generatore elettrico e la totale coppia frenante prodotta dal sistema frenante di servizio le variabili di controllo del sistema; siano la velocità di avanzamento del veicolo e la coppia totale richiesta dall'autista gli ingressi misurati. Tramite queste grandezze è possibile descrivere il funzionamento di tutti i componenti del sistema di propulsione. Le equazioni fondamentali sono riportate di seguito:

$$\begin{cases} \omega_g = \left(\dfrac{Z_r}{Z_s} + 1\right)\omega_e - \dfrac{Z_r}{Z_s}\dfrac{g_f}{r_w}\dot{x} \\[2ex] \omega_m = \dfrac{g_f}{r_w}\dot{x} \\[2ex] T_m = \dfrac{T_{driver}}{g_f} + \dfrac{T_b}{g_f} + T_g\dfrac{Z_r}{Z_s} \end{cases} \tag{4}$$

con Z_r, Z_s ad indicare il numero di denti della corona e del solare.

Assumendo la velocità angolare dell'albero a gomiti e lo stato di carica della batteria come stati del sistema, si ricava la forma di stato non lineare che caratterizza il comportamento del sistema:

$$\begin{cases} \dot{SOC} = -\dfrac{V_{oc} - \sqrt{(V_{oc})^2 - 4P_{batt}R_{batt}}}{2Q_{batt}R_{batt}} = f_1(x,u,v) \\[3ex] \dot{\omega}_e = \dfrac{T_e + \dfrac{Z_s + Z_r}{Z_s}T_g}{J_e} = f_2(x,u,v) \\[3ex] y = \begin{Bmatrix} SOC \\ \dot{m}_f \\ \omega_g \\ T_m \\ \omega_m \\ P_{batt} \\ \omega_e \end{Bmatrix} = g(x,u,v) \end{cases} \tag{5}$$

dove:

$$x = \begin{Bmatrix} SOC \\ \omega_e \end{Bmatrix} \quad u = \begin{Bmatrix} T_e \\ T_g \\ T_b \end{Bmatrix} \quad v = \begin{Bmatrix} T_{driver} \\ \dot{x} \end{Bmatrix}$$

x contiene gli stati del sistema, u le variabili di controllo mentre v le variabili esterne misurate.

Nonostante ai fini dello sviluppo di una strategia di controllo per lo *energy management* di un veicolo ibrido sia sufficiente considerare solo la dinamica dello stato di carica della batteria in quanto tutte le altre dinamiche del sistema sono molto più veloci, in questo modello viene anche descritta la dinamica dell'albero a gomiti in quanto si vuole utilizzare la strategia stessa per addolcire l'intervento del generatore elettrico nelle fasi di attivazione e spegnimento del motore endotermico così da ridurre il discomfort patito dai passeggeri. Lo scopo è sviluppare una strategia di controllo che incorpori anche alcuni obiettivi riguardanti il comfort a bordo e dunque non richieda delle modifiche ulteriori per poter essere applicata al veicolo.

Per definire completamente la forma di stato non lineare occorre determinare le espressioni analitiche delle funzioni f_1, f_2 e g. In particolare é necessario ricavare un modello di regressione del consumo istantaneo di combustibile rispetto alla variabile di controllo T_e e allo stato ω_e, esprimere le perdite di potenza nelle macchine elettriche rispetto a x, u, v e la resistenza interna della batteria ad alto voltaggio come funzione dello stato SOC. Tutte queste relazioni sono reperibili in Amesim® sotto forma di tabella multi ingresso, non direttamente utilizzabili da un algoritmo numerico per la risoluzione del problema di ottimizzazione. É necessario dunque sostituire tali tabelle con modelli di regressione polinomiale; di seguito sono riportati i modelli di regressione utilizzati.

Il consumo istantaneo di combustibile $\dot{m}_f$ [kg/s] é espresso come funzione della coppia [Nm] erogata dal motore a combustione interna e la velocità angolare [rad/s] dell'albero a gomiti secondo la relazione seguente:

$$\dot{m}_f = p_1 + p_2\omega_e + p_3T_e + p_4\omega_e^2 + p_5\omega_eT_e + p_6T_e^2 + p_7\omega_e^2T_e + p_8\omega_eT_e^2 + p_9T_e^3 \tag{6}$$

I coefficienti del polinomio valgono:

Tabella 1: Coefficienti di regressione polinomiale del consumo di combustibile.

Coefficiente	Valore
p_1	$7.275\ e-3$
p_2	$9.843\ e-4$
p_3	$8.277\ e-3$
p_4	$1.148\ e-6$
p_5	$1.979\ e-5$
p_6	$-1.820\ e-4$
p_7	$6.222\ e-8$
p_8	$2.067\ e-7$
p_9	$1.610\ e-6$

La potenza persa nelle macchine elettriche, espressa in W, é legata alla coppia erogata dalla macchina [Nm] e alla velocità angolare del rotore [rad/s] dalla seguente relazione:

$$P_m^{loss} = P_g^{loss} = 2.3477\,\omega + 0.00182\,T^2\omega - 4.87^{-8}\,T^4\omega \tag{7}$$

Da ultima, la resistenza interna [Ω] di una singola cella della batteria é espressa in funzione dello stato di ***scarica*** della batteria stessa [%]:

$$R_{cell} = 1.977e - 08 * SoD\hat{}2 \; - \; 9.056e - 07 * SoD \; + \; 5.47e - 04 \tag{8}$$

La resistenza interna equivalente della batteria si ricava conoscendo la disposizione dei banchi di celle in serie e parallelo.

L’onere computazionale nell’utilizzare una forma di stato non lineare come modello di riferimento per MPC è elevato, in più non è garantita la convessità del problema di ottimizzazione. Di conseguenza la forma di stato è linearizzata ad ogni istante di campionamento sfruttando ogni volta le nuove informazioni rese disponibili dai sensori. La strategia MPC, dunque, utilizza la forma di stato linearizzata per prevedere la risposta del sistema dalle condizioni definite all’istante di campionamento fino al termine dell’orizzonte di previsione sotto l’effetto degli ingressi misurati e delle variabili di controllo. Tale tecnica prende il nome di LTV-MPC (Linear Time Varying). L’evoluzione della coppia totale richiesta dall’autista è calcolata dalla strategia stessa secondo un andamento a decadimento esponenziale a partire dal valore misurato all’istante di campionamento mentre la velocità di avanzamento è ottenuta tramite integrazione della dinamica longitudinale del veicolo. La forma di stato è linearizzata secondo una serie di Taylor troncata al termine lineare:

$$\begin{cases} \dot{x} \approx F + Ax + B_u u + B_v v \\ y \approx G + Cx + D_u u + D_v v \end{cases} \tag{9}$$

con:

$$A = \left.\frac{\partial f}{\partial x}\right|_0 \quad B_u = \left.\frac{\partial f}{\partial u}\right|_0 \quad B_v = \left.\frac{\partial f}{\partial v}\right|_0 \quad C = \left.\frac{\partial g}{\partial x}\right|_0 \quad D_u = \left.\frac{\partial g}{\partial u}\right|_0 \quad D_v = \left.\frac{\partial g}{\partial v}\right|_0$$

$$F = f(x_o, u_o, v_o) - Ax_o - B_u u_o - B_v v_o \tag{10}$$

$$G = g(x_o, u_o, v_o) - Ax_o - B_u u_o - B_v v_o$$

L’approccio canonico del metodo MPC è nel dominio discreto del tempo pertanto la forma di stato linearizzata è discretizzata tramite Eulero avanti che approssima la derivata temporale continua come una differenza finita in avanti con periodo di discretizzazione T_s:

$$\dot{x}(t) \approx \frac{x(t\ +\ \delta) - x(t)}{T_s}$$

$$\begin{cases} x(k+1) = \ (I + AT_s)x(k) + \ T_sB_uu(k) + T_sB_vv(k) + T_sF \\ y(k) = Cx(k) + \ D_uu(k) + D_vv(k) + G \end{cases} \tag{11}$$

Tramite dei passaggi matematici descritti nell'Appendice A, la strategia MPC utilizza la forma di stato linerizzata e discretizzata per prevedere la risposta delle uscite del sistema lungo l'orizzonte di previsione, $\mathcal{Y}$, in funzione della sequenza dei valori delle variabili di controllo lungo l'orizzonte di controllo, U, e della sequenza dei valori degli ingressi noti lungo l'orizzonte di previsione, V. La sequenza ottimale U^* é quella che guida il sistema lungo una triettoria che ottimizzi la funzione di merito e rispetti contemporaneamente tutti i vincoli operativi.

I vincoli operativi

Le principali limitazioni derivano dalle caratteristiche intrinseche delle macchine del sistema di propulsione. I vincoli sono stati espressi come disuguaglianze lineari per essere coerenti con la formulazione del QP problem. Di seguito l'elenco dei vincoli:

Outputs:

$$SOC_{min} \leq SOC \leq SOC^{max}$$
$$\omega_g^{min} \leq \omega_g \leq \omega_g^{max}$$
$$T_m \leq f(V, \omega_m)$$
$$\omega_m^{min} \leq \omega_g \leq \omega_m^{max}$$
$$P_{batt}^{min} \leq P_{batt} \leq P_{batt}^{max}$$
$$\omega_e^{min} \leq \omega_e \leq \omega_e^{max}$$

Variabili di controllo**:**

$$T_e \leq f(\omega_e)$$
$$T_g \leq f(V, \omega_g)$$
$$T_b^{min}\ \leq\ T_b \leq T_b^{max}$$

I vincoli sulle uscite del sistema contemplano la banda entro la quale deve trovarsi lo stato di carica della batteria; é importante che durante la missione di guida lo stato di carica non oltrepassi tali limiti in quanto ne deriverebbe un degrado della vita utile della batteria. La velocità angolare del rotore del generatore elettrico deve essere compresa tra i due valori limite, lo stesso vale per la velocità angolare del motore elettrico e i limiti superiore ed inferiore sono identici essendo le due macchine elettriche uguali tra loro. La coppia massima che il motore elettrico può produrre in funzione del voltaggio applicato alla macchina e alla velocità angolare del rotore rappresenta un altro vincolo che viene duplicato anche per valori negativi della coppia quando il motore opera come generatore. Un ulteriore vincolo é rappresentato dalla massima potenza prodotta ed assorbita dalla batteria ad alto voltaggio. Infine i limiti superiore ed inferiore della velocità angolare dell'albero a gomiti chiudono i vincoli sulle uscite del sistema. Per quanto riguarda i vincoli sulle variabili di controllo vengono considerate le curve di coppia massima del motore a combustione interna e del generatore elettrico espresse rispettivamente in funzione della velocità angolare dell'albero a gomiti e della velocità angolare del rotore e del voltaggio. Da ultimo la massima coppia frenante che il sistema frenante di servizio é in grado di produrre alle ruote rappresenta il limite superiore per tale coppia mentre la coppia nulla é il limite inferiore. Le curve caratteristiche di coppia delle macchine sono fornite dal modello in Amesim®; per poterle implementare sotto forma di disuguaglianze lineari é necessario linearizzare le curve tramite un'approssimazione lineare a tratti e prescrivere che la coppia effettiva sia inferiore oppure superiore ad una data retta in funzione della velocità angolare dell'albero. Grazie alle relazioni lineari é possibile raccogliere i vincoli nella seguente forma matriciale:

$$AU \leq b \tag{12}$$

La funzione di merito

La funzione di merito é quadratica nei termini di costo che sono elencati nella prossima formula:

$$\begin{aligned} J(U) = \sum_{i=1}^{H_p-1} \Big[& \left(SOC(k+i) - SOC^{ref}\right)^2_{w_{SOC}} + \left(\dot{m}_f(k+i)\right)^2_{w_{\dot{m}_f}} \\ & + \left(\omega_g(k+i) - \omega_g^{ref}\right)^2_{w_{\omega_g}} + \left(\omega_e(k+i)\right)^2_{w_{\omega_e}} \Big] \\ & + \sum_{i=0}^{H_c-1} \left[\left(u(k+i)\right)^2_{w_u} + \left(\Delta u(k+i)\right)^2_{w_{\Delta u}} \right] \end{aligned} \tag{13}$$

Ogni termine ha per pedice il relativo peso w_i. I termini che compaiono nella funzione di merito sono, in ordine, la deviazione dello stato di carica della batteria rispetto al suo valore di riferimento, la portata massica di combustibile, la deviazione della velocità angolare del rotore del generatore elettrico rispetto al suo valore di riferimento, la velocità angolare dell'albero a gomiti, i livelli delle variabili di controllo e le variazioni da un istante di previsione al successivo delle variabili di controllo. I primi due termini governano il problema energetico decretando la ripartizione di produzione di potenza tra batteria e combustibile mentre tutti gli altri termini servono per migliorare la stabilità della strategia oppure per migliorarne le prestazioni in particolare situazioni di guida e sono stati aggiunti a seguito di numerose simulazioni preliminari che hanno consentito la comprensione più approfondita del funzionamento della strategia. La funzione di merito considera la somma dei quadrati dei termini su tutto l'orizzonte di previsione per le uscite del sistema, mentre la somma é estesa a tutto l'orizzonte di controllo per le variabili di controllo.

Sfruttando la notazione matriciale discreta della forma di stato é possibile esplicitare le uscite del sistema in funzione dei livelli delle variabili di controllo e in definitiva esprimere la funzione di merito come una funzione quadratica nelle variabili di controllo.

$$J(U) = U^t H U + 2q^t U + \ b_o \tag{14}$$

dove b_o raccoglie i termini costanti non importanti ai fini dell'ottimizzazione.

Algoritmo Active-set

Il problema di ottimizzazione vincolata é dunque formulato come un problema di programmazione quadratica nella forma canonica:

$$\min_{U}\{\ J(U) = U^t H U + 2q^t U + \ b_o \ \}$$

soggetto a:

$$AU \leq b$$

Le matrici H, A e i vettori q, b_o sono inizializzati a ogni istante di campionamento sfruttando le informazioni misurate sul sistema. Il vettore U^* delle variabili di controllo che risolve il problema di ottimo é calcolato mediante algoritmo active-set.

Risultati

Il modello dettagliato in Amesim® implementa una strategia di tipo rule based per la gestione del flusso di potenza; scopo della strategia MPC é rimpiazzare l'approccio euristico garantendo prestazioni superiori. La validazione della strategia MPC é quindi stata condotta secondo i seguenti punti principali:

- Valutazione del consumo totale del veicolo rispetto a cicli di guida standardizzati di cui é nota la lunghezza, l'altimetria e la velocità desiderata.

- Confronto del consumo totale ottenuto dalle due strategie per ogni ciclo di guida standard in condizioni di equilibrio energetico.

L’utilizzo di cicli di guida standardizzati consente di eliminare la variabilità dello stile di guida dell’autista nella valutazione dei consumi. L’autista é modellato mediante un regolatore PI sull’errore istantaneo tra la velocità desiderata e la velocità attuale del veicolo, questo tipo di simulazione é detta “*in avanti*” ed é molto utile per analizzare le prestazioni e la stabilità della strategia di controllo. Al contrario un approccio “*all’indietro*” escluderebbe l’autista dal modello assegnando direttamente il profilo di velocità desiderato e i calcoli procederebbero a ritroso lungo il flusso di potenza per determinare le coppie motrici necessarie a realizzare il moto. I cicli di guida standardizzati che sono stati impiegati in questo lavoro di tesi sono NEDC, HWFET, UDDS, SC03, US06; i loro profili di velocità desiderata sono riportati nell’Appendice C, la quota altimetrica é sempre stata presa costante a 0 m su livello del mare.

Tutti i risultati fanno riferimento ad un veicolo in equilibrio energetico cioè il livello finale dello stato di carica della batteria coincide con il livello iniziale. Il veicolo preso in esame é classificato “*a sostentamento di carica*” dunque non é prevista una fonte esterna di energia che ricarichi la batteria ad alto voltaggio ma viene utilizzata parte della potenza prodotta dal motore endotermico per questo scopo. Una valutazione del consumo nella situazione in cui livello iniziale e finale dello stato di carica siano uguali é preferibile perché illustra completamente la ripartizione del flusso di potenza tra le macchine. Per raggiungere tale situazione é sufficiente ripetere la medesima missione di guida aggiornando ogni volta il livello iniziale dello stato di carica con il livello finale dell’ultima missione. L’analisi completa delle prestazioni della strategia MPC ha cercato di coprire quanti più aspetti possibili che verranno ad uno ad uno affrontati qui di seguito. É doveroso sottolineare come la strategia MPC campiona le informazioni dai sensori di misura in maniera discreta con periodo di campionamento pari a 0.1s, al contrario la strategia rule based lavora in continuo campionando gli ingressi e aggiornando i valori delle variabili di controllo ad ogni passo di integrazione numerica. Questo conferisce un piccolo vantaggio alla strategia rule based mentre rende la strategia MPC più vicina ad una reale applicazione.

Fuel economy

Dall’informazione sulla massa di combustibile consumato, si determina la fuel economy tramite la relazione riportata di seguito.

$$\left({}^{l}/_{100km}\right) = \frac{m_{fuel}[g]}{\rho_{fuel}[\frac{g}{dm^3}]} * \frac{100km}{distance\ [km]} \tag{15}$$

dove ρ_{fuel} corrisponde alla densità del combustibile liquido mentre *distance* indica la distanza totale percorsa dal veicolo lungo la missione di guida considerata.

La prossima tabella e il prossimo istogramma illustrano le differenze tra le due strategie in termini di efficienza energetica.

Tabella 2: Consumo di carburante ottenuto dalle due strategie sui 5 cicli di riferimento.

	Rule based				**MPC**		
Cycle	SOC_{level}[%]	$M_{fuel}[g]$	${}^{l}/_{100km}$		SOC_{level}[%]	$M_{fuel}[g]$	${}^{l}/_{100km}$
NEDC	59.86	509.03	5.927		59.49	493.6	5.742
HWFET	59.65	751.25	5.837		59.73	741.62	5.762
SC03	47.97	286.47	6.378		57.34	261.16	5.815
UDDS	58.14	546.0	5.840		57.46	541.59	5.793
US06	42.00	901.59	8.973		56.17	741.53	7.380

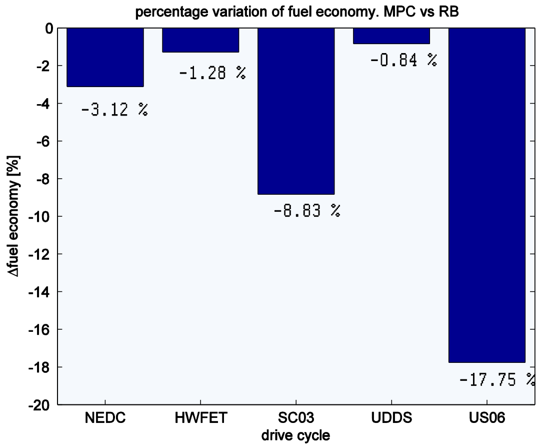

Figura 2: Riduzione percentuale di consumo ottenuta con MPC rispetto alla strategia euristica.

Entrambe le strategie soddisfano tutti i vincoli operativi, unica eccezione la strategia rule based che non riesce a mantenere il livello di carica della batteria entro il limite inferiore sul ciclo US06. L'istogramma dimostra che la riduzione percentuale di consumo totale ottenuta mediante MPC varia a seconda del ciclo di guida, con risultati migliori per situazioni di guida extra-urbana caratterizzate da alte velocità e alta richiesta di potenza. I cicli SC03 e US06 alternano brusche accelerazioni a tratti di alta velocità dove la strategia di controllo é chiamata a gestire il flusso di potenza in condizioni di alta richiesta di potenza su un limitato periodo di tempo. Il ciclo UDDS rappresenta una condizione di guida urbana dove il vantaggio portato da MPC é risibile. La spiegazione a questi risultati é da cercare nel principio operativo attuato da MPC.

Tale strategia sfrutta costantemente i gradi di libertà forniti da rotismo epicicloidale e dal buffer di energia rappresentato dalla batteria ad alto voltaggio. Un esempio lampante di questo comportamento é fornito dalle prossime figure che mostrano alcuni risultati tratti dal ciclo autostradale HWFET per le due strategie di controllo. Il tratto di ciclo a cui fanno riferimento i risultati considera una prima parte di accelerazione in cui la velocità cresce fino a superare i 90 km/h, seguita da un tratto a velocità pressoché costante. Il profilo di velocità é riportato nella prossima figura.

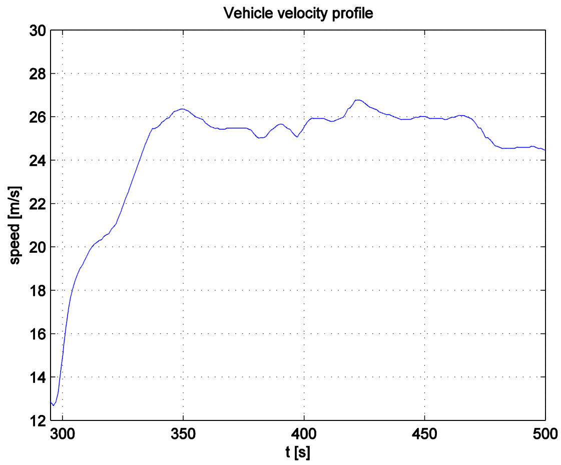

Figura 3: Profilo di velocità nel tratto di guida considerato.

Le prossime due figure riportano il flusso di potenza attraverso il sistema di propulsione per la strategia rule based a sinistra e per MPC a destra.

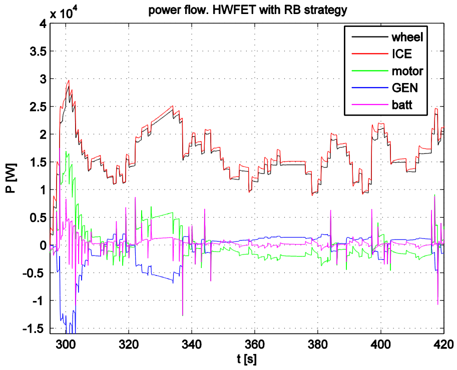

Figura 4: Bilancio di potenza ottenuto con la strategia euristica.

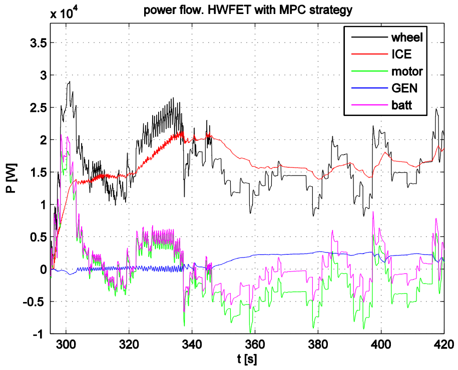

Figura 5: Bilancio di potenza ottenuto con MPC.

La strategia rule based utilizza la potenza prodotta dal motore endotermico (linea rossa) per seguire quasi fedelmente il profilo di potenza richiesta dall’autista (linea nera). La potenza che fluisce nel ramo elettro-meccanico del sistema di propulsione é inferiore, si nota come la potenza media associata alla batteria sia prossima al valore nullo e le fluttuazioni siano contenute. Quindi la strategia euristica ricorre principalmente al motore endotermico quando la richiesta di potenza cresce e continuamente adatta il suo punto operativo per seguire il trend di potenza. Al contrario la strategia MPC utilizza la potenza fornita dal motore a combustione interna per bilanciare la potenza media richiesta dall’autista e ricorre al supporto delle macchine elettriche per bilanciare le fluttuazioni di potenza. L’utilizzo della batteria é massiccio come dimostra la figura a destra; essa funge da buffer quando la potenza istantanea é inferiore al valore medio mentre fornisce potenza quando questa cresce oltre il valore medio. Motore endotermico e batteria dunque lavorano in stretta sinergia.

Le prossime due figure illustrano invece i punti operativi del motore endotermico in questa situazione di guida, così come definiti dalle due strategie.

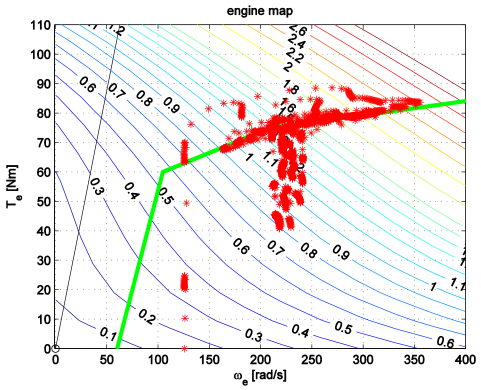

Figura 6: Mappa dei punti operativi del motore a benzina ottenuti con la strategia euristica.

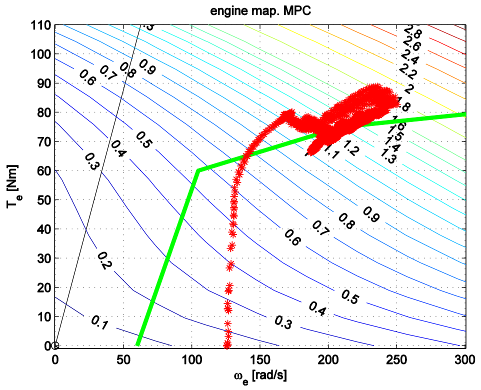

Figura 7: Mappa dei punti operativi del motore a benzina ottenuti con la strategia MPC.

Come già evidenziato in precedenza, la strategia rule based modifica continuamente il punto operativo del motore a combustione interna cercando di farlo cadere sempre sulla curva verde che collega i punti a più alta efficienza. Questo metodo ha però lo svantaggio di ricorrere ad una velocità angolare dell’albero a gomiti alta quando la potenza richiesta cresce molto; in tale regione operativa l’efficienza della combustione decresce molto. Al contrario MPC limita lo spostamento del punto operativo del motore e riesce a mantenerlo prossimo alla curva di alta efficienza con una velocità angolare dell’albero a gomiti inferiore a 250 rad/s. questo si traduce in un’efficienza istantanea del motore endotermico superiore rispetto a quanto ottiene la strategia rule based; il confronto é evidenziato nella prossima figura.

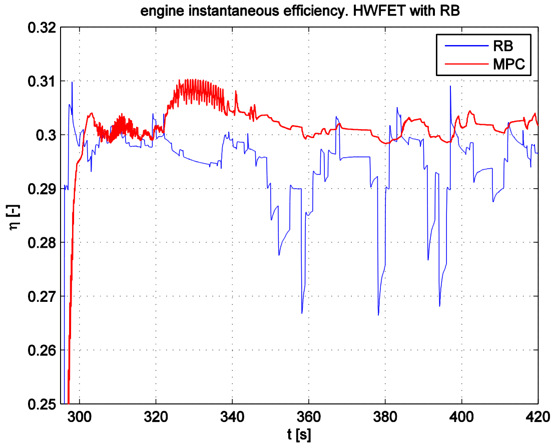

Figura 8: Efficienza del motore a combustione interna. Confronto tra le due strategie.

Quindi MPC riesce a ridurre il consumo totale di combustibile su tutti i cicli di guida perché sfrutta al massimo la sinergia tra macchine elettriche e motore a combustione interna, utilizzando quest'ultimo per bilanciare la potenza media richiesta dall'autista. Tale approccio garantisce risultati migliori quanto maggiore é la richiesta di potenza mentre le differenze si appianano nei tratti urbani dove il carico é limitato.

Problema legato alla linearizzazione

Il tratto di guida illustrato nelle figure in precedenza consente di visualizzare un problema legato alla linearizzazione della forma di stato da usare come modello previsionale per la strategia MPC. Tra 300s e 340s la strategia MPC decide di condurre il veicolo in modalità parallela dove la rotazione del generatore elettrico é arrestata e si ottiene un rapporto fisso tra il motore endotermico e le ruote motrici. In questa condizione dunque la velocità angolare del rotore del generatore é prossima a 0 rpm e può accadere che essa oscilli attorno al valore nullo tra due istanti di campionamento successivi. Il modello di regressione polinomiale per la potenza persa in una macchina elettrica contiene il valore assoluto della velocità angolare del rotore in quanto la potenza persa deve sempre risultare positiva.

$$P_m^{loss} = P_g^{loss} = 2.3477\,|\omega| + 0.00182\,T^2|\omega| - 4.87^{-8}\,T^4|\omega| \tag{16}$$

Di conseguenza questo modello polinomiale non é lineare ed é necessario definire due espressioni linearizzate differenti in base al segno della velocità angolare del rotore all'istante di campionamento i.e. i termini sono cambiati di segno se $\omega < 0\, rad/s$ all’istante di campionamento. Quando la velocità angolare del rotore cambia segno continuamente a causa di piccole fluttuazioni ma le condizioni di guida si mantengono pressoché invariate, l’adozione di due modelli previsionali differenti crea incertezza in quanto le previsioni possono essere significativamente diverse tra loro. In più la potenza persa nelle macchine elettriche può risultare negativa lungo l’orizzonte di previsione. Questo aspetto é molto più evidente in modalità di guida parallela dove il veicolo procede generalmente a velocità costante, dunque tutti gli ingressi sono pressoché invariati tra due istanti di campionamento successivi, mentre la velocità angolare del rotore del generatore é prossima al valore nullo.

É possibile ridurre questo fenomeno, eliminando le oscillazioni, introducendo un valore di riferimento per la velocità angolare del rotore in modalità di guida parallela e penalizzando nella funzione di merito la differenza tra questo riferimento e il livello attuale di velocità angolare. Il valore di riferimento é volutamente molto piccolo (0.1 rad/s). Questo é il motivo per cui tale differenza compare nella formulazione della funzione di merito ma il termine é attivo solo nella modalità di guida parallela. Lo svantaggio di questa soluzione tampone é ritardare il passaggio ad una modalità di guida differente, questo induce in alcuni casi una efficienza inferiore rispetto alle simulazioni in cui non é presente.

Comfort

La strategia MPC é stata sviluppata con un occhio di interesse anche al comfort a bordo. Infatti i veicoli ibridi elettrici introducono nuove problematiche in merito al comfort e alla percezione della qualità dei passeggeri, ad esempio nel caso di un veicolo ibrido power-split l’avviamento e l’arresto del motore a combustione interna avviene generalmente con il veicolo in movimento quindi é importante mascherare quanto più possibile questi eventi agli occupanti del veicolo. L’avviamento e l’arresto della rotazione dell’albero a gomiti é comandato dalla coppia del generatore elettrico; la coppia si scarica sul telaio generando vibrazioni che si trasmettono ai passeggeri. L’avviamento e l’arresto repentino dell’albero a gomiti corrispondono a un picco di coppia del generatore elettrico, dunque, a una sgradevole sensazione per i passeggeri a bordo. Per attenuare questo problema la coppia del generatore elettrico é annoverata tra le variabili di controllo del sistema mentre la dinamica rotazionale dell’albero a gomiti é inclusa nella forma di stato. In questo modo, agendo con opportuni pesi sul livello e sulla variazione della coppia del generatore elettrico, é possibile addolcire l’intervento del generatore all’attivazione e allo spegnimento del motore endotermico. Le prossime figure mostrano il progresso ottenuto in una fase di avviamento.

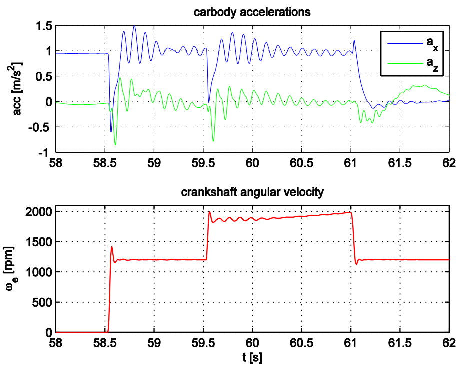

Figura 9: Accelerazioni del corpo vettura e velocità angolare dell'albero a gomiti. Strategia euristica.

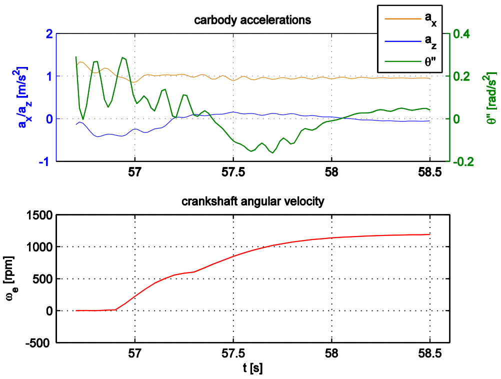

Figura 10: Accelerazioni del corpo vettura e velocità angolare dell'albero a gomiti. Strategia MPC.

La figura a sinistra mostra che la strategia rule based comanda repentinamente la variazione della velocità angolare dell’albero a gomiti causando ampie oscillazioni sia dell’accelerazione longitudinale che verticale del corpo vettura. Lo stesso evento di avviamento comandato da MPC é rappresentato nelle figure a destra. La curva seguita dalla velocità angolare é molto più dolce e l’effetto sulle accelerazioni del corpo vettura é limitato. Questo comportamento é raggiunto grazie ad un utilizzo completamente diverso della coppia del generatore elettrico come mostrato nelle prossime due figure.

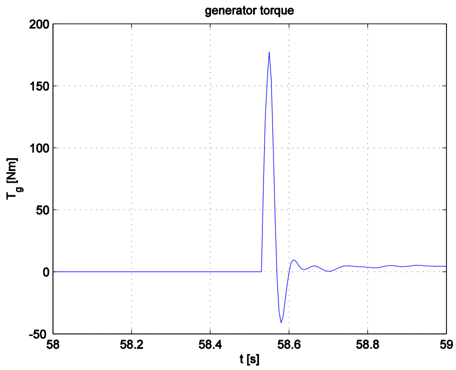

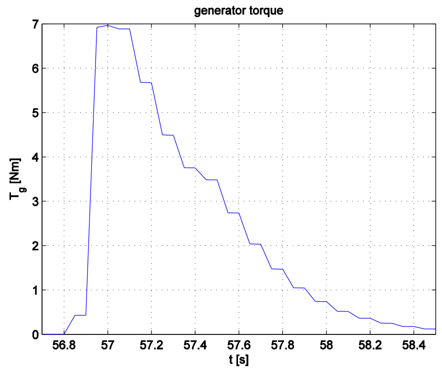

Figura 11: Utilizzo della coppia del generatore elettrico durante l'avviamento del motore endotermico. Strategia euristica.

Figura 12: Utilizzo della coppia del generatore elettrico durante l'avviamento del motore endotermico. Strategia MPC.

Nel primo caso il picco della coppia é ben visibile e supera i 150 Nm, il periodo di attivazione é limitato a 0.1 s. Nel secondo caso, il massimo valore di coppia é inferiore a 7 Nm e poi MPC abbassa gradualmente il livello per raggiungere la velocità di rotazione di minimo dopo circa 1s. il tempo totale di attivazione é dunque molto più lungo ma se si osserva con attenzione le figure 9, 10 si nota come in entrambi i casi le funzioni del motore endotermico comincino a circa 58.5 s dunque MPC comincia la fase di avviamento prima rispetto alla rule based per poi attivare la coppia allo stesso istante di tempo. Anche la strategia rule based é in grado di raggiungere la medesima crescita dolce della variabile ω_e modificando il guadagno proporzionale del controllore di basso livello che comanda la coppia del generatore; dunque, trovando una soluzione al di fuori della strategia stessa.

Seguendo le indicazioni riportate nella norma ISO 2631-5 e prendendo come riferimento le fasi di Start&Stop del ciclo NEDC, é stata calcolata l'accelerazione equivalente pesata a partire dalla accelerazione longitudinale, verticale e di beccheggio del corpo vettura ed applicando le funzioni di peso specificate nella norma per le suddette direzioni di misura. Per convenzione la norma specifica che l'accelerazione equivalente dovrebbe risultare inferiore a 0.5 m/s^2 per non generare una sensazione sgradevole a bordo vettura. Tutte le accelerazioni calcolate sono risultate inferiori a tale livello di soglia.

Stabilità della strategia MPC

A causa dei vincoli operativi e del fatto che la strategia é linearizzata ad ogni istante di campionamento, non é possibile applicare alcuna regole della teoria del controllo per garantire la stabilità della strategia. A tal scopo si é provveduto a testare la strategia rispetto a differenti condizioni operative variando alcuni parametri del modello. Ancora una volta si sono confrontati i risultati con quelli ottenuti dalla strategia rule based. Tramite l'approccio One-At-a-Time si sono ripetute una serie di simulazioni variando di volta in volta il livello di un parametro solo, utilizzando il ciclo NEDC come ciclo di riferimento. I parametri presi in esame sono stati la massa del corpo vettura, la pendenza della strada, il coefficiente adimensionale di resistenza aerodinamica, la rigidezza della cinghia di trasmissione, l'inerzia rotazionale delle ruote e il coefficiente di adesione pneumatico - superficie stradale. Soltanto per i primi tre parametri si é osservato una influenza sul consumo totale pertanto si riportano di seguito i risultati relativi alle corrispondenti simulazioni.

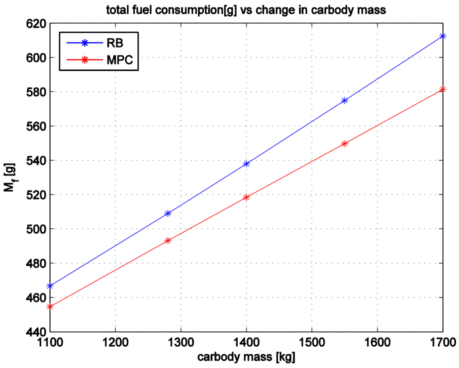

Figura 13: Massa di combustibile consumata in funzione alla massa del corpo vettura. Confronto tra le strategie.

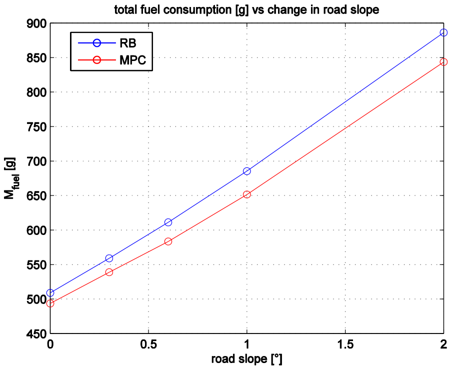

Figura 14: Massa di combustibile consumata in funzione della pendenza della strada. Confronto tra le strategie.

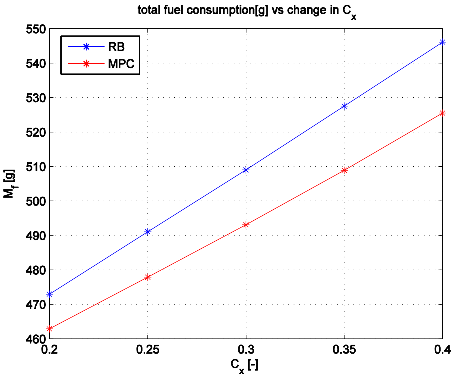

Figura 15: Massa di combustibile consumata in funzione del coefficiente adimensionale di resistenza all'aria. Confronto tra le strategie.

Tutti i vincoli operativi sono soddisfatti e non si registrano oscillazioni o instabilità nelle decisioni elaborate dal problema di ottimizzazione, dunque si può concludere che la strategia MPC lavora bene anche a fronte di variazioni dei parametri del veicolo e/o della strada. In più, come si nota dalle figure in alto, il consumo totale di combustibile in grammi é sempre inferiore rispetto a quanto ottenuto dalla strategia euristica, quindi MPC garantisce prestazioni migliori anche per queste condizioni operative.

Analisi del comportamento della strategia

Lo sviluppo della strategia MPC ha riguardato anche lo studio dei parametri interni alla strategia che influenzano il problema di ottimizzazione e dunque le prestazioni della stessa. In particolare si é voluto investigare il ruolo della previsione della coppia richiesta dall'autista e classificare l'importanza dei parametri interni.

Previsione della coppia alle ruote

Il metodo MPC si basa sulla previsione degli accadimenti futuri per risolvere un problema di ottimizzazione e calcolare le azioni di controllo da applicare al sistema quindi é interessante capire l'influenza del modello adottato per prevedere la coppia richiesta dall'autista alle ruote. Il modello previsionale impiegato nello sviluppo della strategia descrive la coppia richiesta secondo un decadimento esponenziale il cui valore iniziale coincide con il livello campionato mentre il tasso di decadimento varia in relazione al livello di potenza richiesto. In alternativa si é assunto che il veicolo disponga di sistemi di navigazione quali GPS e GIS e che esso ripetesse assiduamente la stessa missione di guida giorno per giorno. Questo é il caso ad esempio degli autobus che seguono sempre lo stesso percorso. Con questa ipotesi é possibile assegnare alla strategia MPC l'andamento preciso della potenza richiesta lungo l'orizzonte di previsione. Infatti é lecito assumere che il profilo desiderato di velocità corrisponda alla velocità media registrata su una serie di ripetizioni della medesima missione di guida e allo stesso modo la coppia richiesta dall'autista e ottenuta con precedenti simulazioni, rappresenti la coppia richiesta in media dall'autista. Per semplificare l'analisi e per consentire alla strategia MPC di lavorare nelle migliori condizioni operative possibili, sono stati forniti in ingresso sia il profilo desiderato di velocità che un profilo di coppia ottenuto da una simulazione test. In tal modo la previsione di queste due variabili lungo l'orizzonte di previsione é pressoché esatta a meno di piccolissime e trascurabili differenze nella coppia. Questa situazione é irrealistica ma lo scopo di questa analisi é quello di investigare l'influenza della previsione della coppia, e conseguentemente della velocità di avanzamento, sulle prestazioni della strategia di controllo. I cicli NEDC e HWFET sono stati scelti come riferimento, entrambi modificati per includere una variazione altimetrica lungo il percorso. I risultati mostrati di seguito fanno riferimento alle simulazioni realizzate con la strategia nominale e alle simulazioni realizzate con la strategia che riceve in ingresso la descrizione esatta del profilo di coppia e di velocità.

Tabella 3: Confronto del consumo totale tra la strategia MPC nominale e la strategia supportata da GPS/GIS.

Ciclo / **Strategia**	**NEDC**	**HWFET**
	$M_{fuel}\ [g]$	$M_{fuel}\ [g]$
Nominal	518.72	761.35
Exact prediction	518.50	761.0

Dai risultati emerge inaspettatamente un'influenza pressoché nulla della previsione sulle prestazioni della strategia. La spiegazione a questa conclusione si può trovare osservando, ad esempio, le sequenze dei valori ottimi della coppia del motore a combustione interna lungo l'orizzonte di controllo ottenuti da successivi problemi di ottimo. La prossima figura riporta alcune di queste sequenze definite sul ciclo NEDC per un tratto di accelerazione.

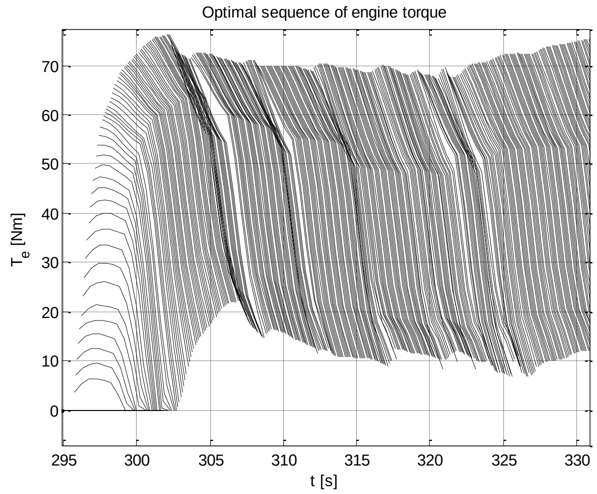

Figura 16: Sequenze dei valori ottimi della coppia del motore endotermico calcolate come soluzione di successivi problemi di ottimizzazione.

Queste sequenze sono state ottenute dalla strategia che riceve in ingresso gli andamenti corretti delle variabili esterne misurate; si nota come MPC definisca un andamento crescente della coppia nella primissima porzione dell’orizzonte di controllo mentre nella seconda parte riduce velocemente la coppia. Ricordando che lo scopo della strategia é quello di minimizzare la funzione di merito quadratica lungo tutto l’orizzonte di previsione, questo andamento della sequenza ottima si può spiegare con il tentativo da parte della strategia di ridurre la deviazione dello stato di carica della batteria nella prima porzione dell’orizzonte di previsione utilizzando la potenza del motore a combustione interna, invece nella seconda porzione essa riduce la coppia erogata dal motore endotermico per minimizzare il consumo totale su tale orizzonte. In quest’ottica il problema di ottimizzazione sembra essere governato principalmente dal livello di potenza richiesto e dall’entità della deviazione dello stato di carica della batteria, all’istante di campionamento. Questa conclusione spiega il motivo per cui modificando la previsione degli ingressi misurati non si registra un cambiamento nei valori ottimi delle variabili di controllo determinati dalla strategia.

Analisi di sensibilità dei parametri interni

La strategia di controllo MPC é caratterizzata da molti parametri interni quali ad esempio la lunghezza dell’orizzonte di controllo, i pesi dei termini della

funzione di merito, il tasso di decadimento esponenziale della previsione della coppia richiesta alle ruote etc...
I valori di tutti questi parametri sono stati fissati mediante una lunga messa a punto manuale basata sulla ripetizione di numerose simulazioni, pertanto é interessante capire se esistono altri set di valori tali da garantire prestazioni migliori della strategia i.e minor consumo di combustibile. Inoltre vale la pena investigare la possibilità che, a seconda delle condizioni di guida e del veicolo, il set ottimale dei valori dei parametri possa cambiare; in particolare in relazione alla massa del veicolo può essere opportuno modificare il valore di uno o più parametri per raggiungere una migliore efficienza energetica. Questa ultima considerazione può rivelarsi utile negli autocarri dove é possibile avere una stima della variazione della massa trasportata sfruttando le valvole sensibili alla variazione di carico.

Per trovare una risposta a questi due punti é stata condotta una ampia analisi di sensibilità su alcuni parametri interni della strategia con lo scopo di identificare una superficie di risposta tra due uscite del sistema (i.e. consumo totale e livello di equilibrio dello stato di carica) e alcuni parametri importanti della strategia. Sfruttando l’esperienza maturata durante la procedura di messa a punto manuale, 5 parametri sono stati considerati più importanti: la lunghezza dell’orizzonte di previsione, il numero di step nell’orizzonte di previsione per i quali i pesi della funzione di merito sono modulati da un andamento a decadimento esponenziale, la lunghezza dell’orizzonte di controllo, i pesi applicati sulla deviazione dello stato di carica della batteria e sul consumo istantaneo di combustibile. Per questi due ultimi parametri si é considerato la variazione rispetto al valore nominale. I cicli NEDC e HWFET sono stati scelti come riferimento, due valori della massa del corpo vettura sono stati considerati, in questo modo l’analisi ha sperimentato diverse condizioni di guida per trarre il maggior numero di informazioni. Inoltre le analisi hanno testato un ampio campo del dominio di ogni parametro al fine di catturare eventuali dipendenze non lineari tra le uscite del sistema e i parametri.

Le tecniche consolidate della Design Of Experiment sono state ampiamente impiegate, partendo con un’analisi su due livelli a fattoriale completo dei cinque parametri e proseguendo con la determinazione si superfici di risposta delle due uscite basate su campionamento Central Composite Design. Le superfici di risposta sono stati ottenute per soli 4 parametri siccome l’analisi a fattoriale completo ha mostrato la ridotta influenza della lunghezza dell’orizzonte di controllo.

Le conclusioni che si possono trarre sono innanzitutto una generale insensibilità delle uscite del sistema dal particolare ciclo di guida considerato oppure dalla massa del veicolo. In questo senso la strategia MPC non é legata a particolari condizioni di guida ma il suo comportamento si ripete inalterato per diversi cicli di guida. Importante é osservare che variando il livello dei parametri interni rispetto alla condizione nominale definita nella messa a punto manuale si producono larghe variazioni del livello di equilibrio dello stato di carica della batteria, i.e. fino a ± 3 livelli. Al contrario la massa totale di combustibile non mostra la stessa dipendenza, si registrano variazioni contenute nell'ordine dei pochissimi grammi o frazioni del grammo anche per ampi intervalli dei livelli dei parametri interni. In particolare l'utilizzo delle superfici di risposta consente di concludere che il set ottimale dei parametri interni che minimizza il consumo totale é molto vicino al set definito mediante la messa a punto manuale. I parametri interni che hanno la maggiore influenza sul livello di equilibrio dello stato di carica della batteria sono la lunghezza dell'orizzonte di previsione e il peso della deviazione dello stato di carica della batteria.

Conclusioni

La strategia di controllo basata su MPC ha dimostrato di raggiungere un consumo totale inferiore rispetto a una strategia euristica quando testate su cicli di guida standardizzati. Sul ciclo di guida urbano UDDS la riduzione percentuale di consumo é pari a -0.84 %, sul ciclo di guida autostradale HWFET la riduzione percentuale é pari a -1.28 %. I cicli NEDC, SC03 e US06 coinvolgono condizioni di guida miste urbane ed extraurbane e soprattutto richiedono un maggior sforzo da parte del sistema di propulsione. In questi casi la strategia MPC ottiene i risultati migliori grazie alla profonda sinergia tra motore endotermico e batteria; la riduzione percentuale di consumo totale é pari a -3.12 %, -8.83 %, -17.75 % rispettivamente. Rispetto alla strategia euristica, la strategia MPC é stata sviluppata per essere potenzialmente implementabile in un controllore real time in quanto lavora a tempo discreto, ricorre a semplici modelli di regressione polinomiale. La strategia si é dimostrata stabile rispetto alla variabilità dei parametri del veicolo e/o della strada e la messa a punto dei suoi parametri interni non é in alcun modo legata a un ciclo di guida specifico, da questo punto di vista la strategia é più robusta rispetto, ad esempio, a A-ECMS. La strategia si é dimostrata molto potente sapendo anche controllare le fasi di avviamento e spegnimento del motore a combustione interna al fine di limitare le vibrazioni conseguenti agenti sui passeggeri attraverso il corpo vettura. L'accelerazione equivalente calcolata secondo le equazioni fornite dalla norma ISO 2631-5, é risultata sempre essere inferiore al valore soglia 0.5 m/s^2 che indica una percezione sgradevole di una oscillazione ripetuta nel tempo.

Tuttavia emerge il problema di ricorrere ad una forma di stato linearizzata per prevedere la risposta del sistema che introduce incertezza nella soluzione ottima definita dal controllore. Le simulazioni al calcolatore hanno dimostrato che il problema di ottimizzazione é risolvibile con successo entro il periodo di campionamento di 0.1 s anche se rimane ancora da definire come dovrebbe comportarsi la strategia in tutte quelle situazioni in cui il problema risolta essere mal posto, non risolvibile. Questo problema é ad ogni modo comune a tutte le strategie di controllo basate sulla risoluzione di una funzione di merito. Non di meno il problema di ottimo sembra essere governato principalmente dal valore di deviazione dello stato di carica della batteria e dalla potenza richiesta dall'autista, all'istante di campionamento rendendo la strategia piuttosto statica e non potendo sfruttare le informazioni aggiuntive fornite dai sistemi di navigazione. Eventualmente questi dati potrebbero essere impiegati a un livello di controllo superiore sulla scala gerarchica rispetto alla strategia MPC che in base alle informazioni acquisite possa modificare alcuni parametri, ad esempio il livello di riferimento dello stato di carica della batteria, escludere uno dei termini della funzione di costo. Un'altra limitazione é rappresentata dal fatto che MPC é un metodo model based quindi é necessario sviluppare un modello semplice ma affidabile del sistema di propulsione del veicolo e ogni modifica apportata a questo assieme implica la definizione di un modello nuovo con conseguente validazione.

Table of contents

1 Introduction 1

2 Alternative propulsion systems 3

  2.1 The importance of hybridization 3

  2.2 Hybrid electric vehicles 6

  2.3 Control structure for energy management 7

    2.3.1 The hardware 7

    2.3.2 The formulation as a problem of optimum 8

    2.3.3 The algorithms - State of the art 10

  2.4 Drivability metrics 15

3 Architectures of hybrid electric vehicles 17

  3.1 Classification of hybrid electric vehicles 17

    3.1.1 Series hybrid electric vehicle 19

    3.1.2 Parallel hybrid electric vehicle 20

    3.1.3 Series/parallel hybrid electric vehicles 21

    3.1.4 Plug-In hybrid electric vehicles 23

  3.2 Driving modes of a power-split hybrid electric vehicle 23

  3.3 Main components of the analyzed HEV 27

    3.3.1 Power-split drive 27

    3.3.2 Internal combustion engine 30

    3.3.3 Electric machines 31

    3.3.4 High voltage battery 32

    3.3.5 The vehicle assembly 34

4 The MPC-based control strategy 37

  4.1 Background 37

  4.2 Formulation of the MPC strategy 40

    4.2.1 The reference simplified model 40

    4.2.2 The operating constraints 56

    4.2.3 The cost function 61

    4.2.4 The linearized state space form 62

4.2.5 Quadratic Programming and Active set method 65
4.3 How the strategy works 66
5 Results 71
5.1 Validation of the models 71
5.2 Fuel economy 74
5.2.1 Drive cycles and charge sustenance 74
5.2.2 Comparison of the results 75
5.2.3 The operating principles of the two control strategies 78
5.2.4 A problem related to linearization 86
5.3 Drivability 88
5.3.1 Velocity tracking error 88
5.3.2 Passengers discomfort related to engine starting and stopping 88
6 Additional analyses 97
6.1 Robustness of the control strategy 97
6.1.1 Carbody mass 98
6.1.2 Road slope 101
6.1.3 Dimensionless coefficient of aerodynamic drag 103
6.1.4 Parameters with low influence 105
6.2 Analysis of internal parameters 107
6.2.1 Sensitivity analysis 107
6.2.2 Integration of GPS/GIS 122
7 Conclusions and future works 127
Appendix A - Matrix approach to MPC 131
Appendix B - Sensitivity analysis and RSM 139
Appendix C - Standard drive cycles 147
Bibliography 151

List of figures

Figure 2.1: Mitshubishi i-Miev [4]..4
Figure 2.2: Tesla Roadster [4]..4
Figure 2.3: Control structure for the energy management of a hybrid electric vehicle 7
Figure 2.4: The eight working states of the rule based strategy [6]..................11
Figure 3.1: Layout of the powertrain of a series HEV......................................19
Figure 3.2: Layout of the powertrain of a parallel HEV...................................21
Figure 3.3: Components of a power-split hybrid electric vehicle......................22
Figure 3.4: Components of a 2x2 series/parallel HEV 22
Figure 3.5: 3D view of the powertrain of a power-split HEV [19]....................23
Figure 3.6: Power flow in electric mode [19] 24
Figure 3.7: Positive split mode. C and B mark two paths for engine power to the wheels [19]...26
Figure 3.8: Positive split mode. the engine power is used to charge the battery [19]...26
Figure 3.9: Regenerative braking. Part of vehicle's kinetic energy is recovered in the high voltage battery [19]..27
Figure 3.10: Planar view of the transaxle. The engine is connected to the carrier, the generator to the sun while the ring gear and the motor deliver the traction torque to propel the vehicle [19]..28
Figure 3.11: Simplified model of a planetary gear set type I............................28
Figure 3.12: Fuel mass flow rate [g/s] as function of engine torque and speed. The engine OOL is the green curve. 30
Figure 3.13: Characteristic curves of the engine. Maximum, minimum torque and engine OOL...30
Figure 3.14: Output torque as function of input voltage and rotor angular velocity...32
Figure 3.15: Power losses as function of output torque, rotor angular velocity [19]...32
Figure 3.16: Arrangement of battery banks. Equivalent electric circuit of a single battery cell [19]..33
Figure 3.17: Internal resistance of a cell as function of state of discharge and temperature...33
Figure 3.18: Open circuit voltage of a cell as function of state of discharge and temperature...33
Figure 4.1: (a). (left) A system may move from Xo to X_N following three possible different trajectories. (b) (middle) the constraints are dynamic and the optimal trajectory needs to be recomputed. (c) (right) MPC updates the optimal control action at each sampling time...38

Figure 4.2: Equivalent electric circuit which models the battery 43
Figure 4.3: Simplified scheme of the mechanical side of the powertrain 45
Figure 4.4: Original (blue) and new (red) grid of values of engine torque and speed. 49
Figure 4.5: 11 Experimental curves which represent fuel mass flow rate as function of engine speed and engine torque. 50
Figure 4.6: An example of interpolation of fuel consumption over the new set of engine torque values for curve number 8. 50
Figure 4.7: Extrapolation to calculate the new value of fuel consumption for a null value of engine torque. 51
Figure 4.8: The new values of mf are connected to one another by a surface for a better visualization and the surface is superimposed to the original curves. ... 51
Figure 4.9: Polynomial regression model of fuel flow rate over the entire operating domain of the engine. 52
Figure 4.10: Regression surface of power loss in the electric machines. 53
Figure 4.11: Rgression surface of power loss in the electric machines. Second view.. 53
Figure 4.12: Experimental values of power loss (blue circles) and regression model (red curve). Discrepancies between the experimental values and the estimated values using the regression model. 54
Figure 4.13: Cell internal resistance. Experimental data (blue circles) and correspondent data obtained from the regression model (red circles). 55
Figure 4.14: Characteristic curves of the engine and correspondent simplification with lines. 57
Figure 4.15: Characteristic curve of the electric machines................................ 59
Figure 4.16: Complete operating domain of the electric machines. 59
Figure 4.17: Example of linearization of the characteristic curve of the electric machines. 59
Figure 5.1: Battery SOC as obtained with Amesim® and the nonlinear model.. 72
Figure 5.2: Crankshaft angular velocity as obtained with Amesim® and the nonlinear model. 72
Figure 5.3: Comparison of power loss in the motor. 72
Figure 5.4: Comparison of fuel mass flow rate. 72
Figure 5.5: Power loss in the generator. Comparison between Amesim® and the linearized SS form. 73
Figure 5.6: Percentage reduction of fuel consumption given by MPC with respect to the rule based strategy. 75
Figure 5.7: Comparison of battery state of charge level over the 5 considered drive cycles as obtained with the rule based strategy (blue curves) and the MPC-based strategy (red curves). a) top left NEDC, b) top right HWFET, c) mid left SC03, d) mid right UDDS, e) low US06 77
Figure 5.8: Velocity profile of the driving situation used to analyze the operating principle of the MPC strategy. 78

Figure 5.9: Correspondent power flow in the powertrain. 79
Figure 5.10: Battery state of charge and engine torque for two repetitions of the same velocity profile. 80
Figure 5.11: Velocity profile which corresponds to the considered driving situation. 81
Figure 5.12: Power flow in the powertrain as obtained with the rule based strategy (left)and with MPC (right)..81
Figure 5.13: Engine operating points as obtained with the rule based strategy (left) and with MPC (right). 82
Figure 5.14: Velocity profile of the considered portion of HWFET.................83
Figure 5.15: Power flow with the rule based strategy in HWFET. 83
Figure 5.16: Power flow with MPC in HWFET. 83
Figure 5.17: Engine operating points defined by the rule based strategy. 84
Figure 5.18: Engine operating points obtained with MPC................................84
Figure 5.19: Engine efficiency over the analyzed driving situation. 85
Figure 5.20: Generator angular velocity during parallel driving mode in HWFET. 86
Figure 5.21: Generator angular velocity once its reference value is included in the cost function. 87
Figure 5.22: Power flow in the powertrain once the reference value of generator angular velocity is introduced. 87
Figure 5.23: Carbody accelerations during engine starting. 89
Figure 5.24: Carbody jerks during engine starting..89
Figure 5.25: Carbody accelerations with a lower proportional gain. 90
Figure 5.26: Carbody jerks with a lower proportional gain. 90
Figure 5.27: Generator torque for a unitary proportional gain...........................90
Figure 5.28: Generator torque for a proportional gain equal to 0.1. 90
Figure 5.29: Carbody accelerations due to engine starting obtained with MPC. 93
Figure 5.30: Generator torque defined by MPC to start the engine. 94
Figure 5.31:Longitudinal acceleration 94
Figure 5.32: Vertical acceleration. 94
Figure 5.33: Pitch acceleration...94
Figure 5.34: Carbody accelerations during engine stopping.............................96
Figure 6.1: Battery SOC equilibrium level as function of carbody mass change. 99
Figure 6.2: Total fuel consumption as function of carbody mass change..........99
Figure 6.3: Engine power as function of carbody mass levels........................100
Figure 6.4: Engine torque as function of carbody mass..................................101
Figure 6.5: Engine speed as function of carbody mass...................................101
Figure 6.6: Road height as function of vehicle absolute position. Road slope is equal to 0.6° and the absolute position of carbody center of gravity is 3422.85 m...102

Figure 6.7: SOC equilibrium level as function of road slope. 102
Figure 6.8: Fuel consumption as function of road slope. 102
Figure 6.9: Time history of the SOC level as function of road slope. 103
Figure 6.10: SOC equilibrium level as function of Cx 104
Figure 6.11: Fuel consumption as function of Cx. 104
Figure 6.12: SOC equilibrium level correspondent to the 11 configurations listed above. 106
Figure 6.13: Total fuel consumption correspondent to the 11 configurations listed above. 106
Figure 6.14: Coefficients of influence on SOC. NEDC 1280kg. 113
Figure 6.15: Coefficients of influence on fuel consumption. NEDC 1280kg . 113
Figure 6.16: Coefficients of influence on SOC. NEDC 1650kg. 114
Figure 6.17: Coefficients of influence on fuel consumption. NEDC 1650kg. 114
Figure 6.18: Coefficients of influence on SOC. HWFET 1280kg. 114
Figure 6.19: Coefficients of influence on fuel consumption. HWFET 1280kg. 114
Figure 6.20: 25 values of SOC final level. NEDC 1650kg. 116
Figure 6.21: 25 values of fuel consumption. NEDC 1650kg. 116
Figure 6.22: 25 values of SOC final level. HWFET 1650kg Conf. B. 116
Figure 6.23: 25 values of fuel consumption.HWFET 1650kg Conf B. 116
Figure 6.24: Normal probability plot of the residuals. 118
Figure 6.25: Total fuel consumption for low, base and high level of Hp. 119
Figure 6.26: Total fuel consumption as function of Hp. HWFET. 120
Figure 6.27: Total fuel consumption as function of Hp. NEDC. 120
Figure 6.28: Road slope and velocity profile for NEDC. 123
Figure 6.29: Road slope and velocity profile for HWFET. 123
Figure 6.30: Sequence of optimal values of engine torque. HWFET. 124
Figure B.1: Full factorial design 141
Figure B.2: CCD-design. 141
Figure B.3: The test configurations taken by three different design matrices. 144
Figure C.1: Reference velocity profile of cycle NEDC 147
Figure C.2: Reference velocity profile of cycle HWFET 147
Figure C.3: Reference velocity profile of cycle SC03 148
Figure C.4: Reference velocity profile of cycle UDDS 148
Figure C.5: Reference velocity profile of cycle US06 149

List of tables

Table 2.1: Technical data of two electric vehicles 5
Table 4.1: Regression coefficients of the polynomial regression model for fuel flow rate. 53
Table 4.2: Coefficients used to define the linear constraints of the engine characteristic curves. 58
Table 4.3: Coefficients used to define the linear constraints of the electric machines on maximum torque. 60
Table 4.4: Penalty weights defined in the cost function. 68
Table 5.1: Comparison of fuel economy. Final results. 75
Table 5.2: Fuel economy and battery state of charge equilibrium level over the urban portion of NEDC. 82
Table 5.3: Velocity tracking error. Mean value and standard deviation. 88
Table 5.4: Equivalent accelerations related to engine start&stop events. 96
Table 6.1: Performance of the two strategies against carbody mass variation. ..99
Table 6.2: Fuel economy percentage variation with respect to carbody mass. .100
Table 6.3: Values of the results displayed in the two figures above. 102
Table 6.4: Fuel economy and percentage variation with respect to the base case. 103
Table 6.5: Values of SOC level and fuel consumption shown in the two figures above. 104
Table 6.6: Fuel economy and percentage variation with respect to the base case. 104
Table 6.7: SOC equilibrium level and total fuel consumption as function of wheels rotary inertia. 105
Table 6.8: SOC equilibrium level and total fuel consumption as function of silent chain stiffness. 105
Table 6.9: SOC equilibrium level and total fuel consumption as function of adhesion coefficient tyre-road. 105
Table 6.10: The 11 configurations that have been tested in this analysis. 106
Table 6.11: Low and high levels of each factor. 109
Table 6.12: Levels of each parameter taken for Configuration A. 110
Table 6.13: Levels of each parameter taken for Configuration B. 111
Table 6.14: Design matrix of the DOE-CCD analysis. 112
Table 6.15: Ci on SOC.NEDC 1280kg 113
Table 6.16: Ci on fuel. NEDC 1280kg. 113
Table 6.17: Ci on SOC. NEDC 1650kg. 114
Table 6.18: Ci on fuel. NEDC 1650kg. 114
Table 6.19: Ci on SOC. HWFET 1280kg. 114
Table 6.20: Ci on fuel. HWFET 1280kg. 114

Table 6.21: Coefficients of the regression model of fuel consumption and SOC minimum level. 117
Table 6.22: Comparison of the nominal against the optimal set of internal parameters. 120
Table 6.23: Fuel consumption with the nominal MPC strategy and the strategy which knows perfectly the future power request. 124
Table B.1: Design matrix of full factorial 142
Table B.2: Design matrix of CCD-design 142

Nomenclature

J: Cost function
SOC: Battery state of charge [%]
T: Simulation time [s]
$\dot{m}_f$: Fuel mass flow rate [g/s]
t: Time [s]
x: System states
u: Control inputs
v: External measured disturbances
LHV: Fuel low heating value [J/kg]
P_{el}: Electric power at battery's terminals [W]
T_c: Torque applied at the carrier [Nm]
T_r: Torque applied at the ring gear [Nm]
T_s: Torque applied at the sun gear [Nm]
ω_c: Angular velocity of the carrier [rad/s]
ω_r: Angular velocity of the ring gear [rad/s]
ω_s: Angular velocity of the sun gear [rad/s]
Z_s: Number of teeth of the sun gear [-]
Z_r: Number of teeth of the ring gear [-]
Z_c: Number of teeth of the carrier [-]
T_{table}^{e}: Engine torque read from the look-up table [Nm]
T_{target}: Set point of the engine torque [Nm]
$T_{losses,t_{hot}}$: The engine friction torque at hot temperature read from a proper table [Nm]
$T_{losses,t_{cold}}$: The engine friction torque at cold temperature read from a proper table [Nm]
$T_{dynamic}$: Engine torque obtained from a first order lag [Nm]
T_{output}^{e}: Engine output torque at crankshaft [Nm]
ρ_{air}: Air density [kg/m^3]
ρ_{air}^{0}: Reference air density value [kg/m^3]
τ_{engine}: Engine time constant [s]
τ_m: Time constant of the electric machines [s]
T_{table}^{m}: Set point of the electric machine torque read from a look-up table [Nm]
T_{out}^{rotor}: Output torque produced at the rotor of the electric machines [Nm]
I_{cell}: Electric current through one cell of the battery [A]
V_{cell}: Electric voltage across one cell of the battery [V]
R_{cell}: Internal resistance of one cell of the battery [Ω]
V_{cell}^{0}: Open circuit voltage of one cell of the battery [V]
P_{bank}: Number of bans in parallel [-]

S_{bank}: Number of banks in series [-]
S_{cell}: Number of cells in series within each bank
V_{bank}: Voltage across a bank
I: Battery electric current [A]
V: Battery output voltage [V]
R_{batt}: Battery internal resistance [Ω]
V_{oc}: Battery open circuit voltage [V]
P_{batt}: Power released/absorbed by the battery [W]
q: Charge of the battery [C]
Q_{batt}: Battery rated capacity [As]
$m_{carbody+engine}$: Mass of the carbody plus mass of the engine [kg]
$m_{unsprung}^{front}$: Inertia of the front unsprung mass [kg]
$m_{unsprung}^{rear}$: Inertia of the rear unsprung mass [kg]
m_v: Total mass of the vehicle [kg]
J_{wheels}^{axle}: Combined rotary inertia of the two wheels of one axle [kgm^2]
r_w: Static rolling radius of the wheel [m]
$g_{silent\ chain}$: Gear ratio introduced by the silent chain [-]
g_{FD}: Gear ratio of the final drive [-]
g_f: Total gear ratio between the motor and the driven wheels [-]
J_{motor}: Rotary inertia of the rotor of the motor [kgm^2]
J_e: Rotary inertia of the flywheel [kgm^2]
C_x: Dimensionless coefficient of aerodynamic resistance [-]
S: Vehicle front area [m^2]
f_r: Dimensionless coefficient of rolling resistance [-]
H_p: Length of the prediction horizon [#samples]
H_c: Length of the control horizon [#samples]
T_e: Engine output torque at the crankshaft [Nm]
ω_e: Angular velocity of the crankshaft [rad/s]
T_m: Motor output torque [Nm]
ω_m: Angular velocity of the rotor of the electric motor [rad/s]
T_g: Generator output torque [Nm]
P_m: Power released/absorbed by the electric motor [W]
P_g: Power released/absorbed by the electric generator [W]
ω_g: Angular velocity of the rotor of the electric generator [rad/s]
T_{out}: Driveline output torque [Nm]
ω_w: Angular velocity of the driven wheels [rad/s]
T_b: Total braking torque applied by the service braking system [Nm]
F_{road}: Total resistive force [N]
SoD: Battery state of discharge [%]
P_{loss}: Total power loss in the electric machines [W]
P_m^{loss}: Power loss in the electric motor [W]

P_g^{loss}: Power loss in the electric generator [W]
T_{sample}: Driving torque required by the driver at the sampling time [Nm]
T_{driver}: Total driving torque requested by the driver in the continuous time domain [Nm]
P_{sample}: Power required by the driver at the sampling time [W]
ρ_{fuel}: Fuel density [kg/m^3]
SOC_{level}: Equilibrium level of battery state of charge at the end of a cycle [%]
SOC^{ref}: Reference level of the battery state of charge [%]
ω_g^{ref}: Reference value of the angular velocity of the rotor of the generator [rad/s]
M_{fuel}: Total fuel consumption [g]
k_{chain}: Linear stiffness of the silent chain [N/m]
$\mu_{adhesion}$: Dimensionless adhesion coefficient tyre-road [-]
w_i: Penalty weight applied to the i-th term in the cost function [-]
a_w: Weighted acceleration signal in the time domain [m/s^2]
rms: Root means square of the acceleration signal in the time domain [m/s^2]
CF: Crest factor of the acceleration signal [-]
$\mathcal{Y}$: Sequence of system outputs over the prediction horizon
U: Sequence of control inputs over the control horizon
V: Sequence of external disturbances over the prediction horizon

1 Introduction

Sustainable mobility is an impelling issue for the worldwide scientific community and for the automotive industry. The reservoirs of hydrocarbons that are currently exploited are expected to be consumed within few decades and it is not guaranteed that new reservoirs will be found in the future. Furthermore global warming is strongly affected by ground vehicles which are included among the most important sources of pollutant gases in the atmosphere.

Automotive manufacturers are looking for new designs to produce environmental-friendly vehicles and the research has been pointing towards electrification of conventional powertrains to achieve highly efficient and less polluting vehicles. This trend has brought to the introduction of full electric vehicles, fuel cell electric vehicles and hybrid electric vehicles; however just for the hybrid ones it is correct to talk of large production volume and they are the most promising solution to the energy management problem now. The reason for hybrid electric vehicles success over the other two types is that they match the numerous objectives and constraints that driving a vehicle involves. The most important objective is drivability, namely the powertrain should match the driver’s power request in any driving situation provided that it is within its operating boundaries.

For a hybrid vehicle traction power is produced by the electric machines and the engine, therefore the additional targets is to produce power in the most efficient way. The power split between electric machines and engine is constrained by the characteristic curves of the machines, the necessity to guarantee a charge sustaining hybrid and the necessity to limit the force transmissibility between the powertrain and the passengers of the vehicle. As a consequence finding a proper way to produce the traction power while satisfying all operating constraints becomes a tough issue and it calls for an advanced strategy which can set the correct power split for any driving situation.

In the past the control strategy was defined upon engineers’ experience on the basis of pre-determined rules. Recently the theory of optimization has been applied to the energy management problem and different approaches have been used. Model Predictive Control is an approach to define a control action for a dynamic system which is optimal in some sense; it has been recently applied to the energy management problem since it can successfully handle multiple constraints and objectives while attaining high performance. In literature it is claimed that MPC can guarantee lower fuel consumption with respect to existing approaches moreover due to its intrinsic predictive nature it may take advantage of the cooperation with auxiliary navigation systems like GPS and GIS.

As a result the aim of this thesis is to develop a MPC-based control strategy for the energy management of a power-split hybrid electric vehicle in order to assess its capability to deal with this problem. For this purpose the performance of the strategy has been compared to those achievable with a rule based strategy over some standard drive cycles. The high fidelity model of the whole powertrain has been implemented in Amesim® while the control strategy in Simulink® and the two software have been run in co-simulation. MPC is based on a simplified linear model of the powertrain which allows the solver to compute an optimal solution within a limited period of time. The linear matrix approach allows the optimization problem to be expressed as a quadratic programming problem where the property of convexity is guaranteed. An improved Active-set algorithm has been used to solve the numeric optimization.

The results show that MPC manages to reduce total fuel consumption over all standard drive cycles with respect to the rule based strategy. However the strategy suffers from few weaknesses that should be taken into account in case of real time implementation.

The thesis is organized in chapters; the next chapter, the second one of the report, treats the energy management problem most while the third chapter introduces the most typical hybrid powertrain architectures giving more insight into the power-split architecture to highlight its strong sides and operating modes. The fourth chapter introduces the MPC-based control strategy. The theoretical background is briefly discussed while more insight is given into the mathematical steps which enable to set up the optimization problem. The fifth chapter shows the results in terms of fuel economy and drivability and compare the rule based strategy to the MPC one. The sixth chapter cope with additional analyses; in the first part a sensitivity analysis is used to catch the influence of some factors on the performance of the strategy. In the second part a simple implementation of additional input information coming from GPS and GIS is presented. In the end some conclusions and comments are provided together with an overview of possible future works.

2 Alternative propulsion systems

Ground transportation is accounted for one-third of the worldwide energy usage [1] and fossil fuels still represent the primary energy source for ground vehicles motion. The engine-powered vehicle is the most common architecture in automotive industry due to its flexibility, compact design and ease of transportation and storing of fuel. The energy necessary to drive a vehicle is obtained from a combustion process which takes place in the combustion chamber of an internal combustion engine. This process has two main important drawbacks: the low efficiency and the pollutants which are generated as products of the process. It is therefore not astonishing that the automotive industry has been investing lots of resources on continuous refinement of engine design and combustion process.

Specific targets in terms of fuel consumption and pollutant emission rates reduction should be satisfied by any new vehicle that is put on the market. Satisfying these constraints by improving solely the technology of engines and combustion process is quite challenging, for this reason almost all automotive manufacturers have already begun developing alternative propulsion systems which can meet current and future environmental regulations. During the last two decades electrification of automotive powertrain has been seen as a viable solution to achieve better fuel economy and lower pollutant emissions. Three main paths that have been followed by automotive manufactures and scientific community:

- Electric vehicles
- Hybrid electric vehicles
- Fuel cell hybrid electric vehicles

2.1 The importance of hybridization

The first solution is the most extreme one since it replaces the internal combustion engine with an electric motor while the other two configurations provides for using an internal combustion engine in collaboration with at least one electric machine to achieve better overall efficiency and lower pollutant emission rates. An internal combustion engine can provide maximum torque and power within a limited speed range, in addition it can work efficiently only within a limited domain of specific values of torque and angular velocity of the crankshaft. Moreover an engine cannot deliver torque if the crankshaft is not rotating meaning that it is necessary to install a clutch and a transmission in-between the engine and the driven axle. On the other hand an electric motor for traction application is characterized by a constant output torque, which corresponds to the maximum output torque, at low rotor angular velocity. The motor can provide maximum torque even when the rotor is not rotating and thus it is possible to couple directly the rotor to the driven wheels. The time response of an engine to change in the operating point is rather slower compared to the settling time of an electric motor, furthermore an electric motor can provide much higher torque and power than the rated ones for a limited period of time before it gets overheated. These two latter features supports the idea that an electric motor can guarantee quick response to driver's request and thus quick acceleration with constant output torque over a certain speed range. The efficiency of an electric machine is on average higher than 90% for most of the operating domain while an internal combustion engine can hardly achieve an efficiency higher than 40% [2].

In an electric vehicle (EV) the energy source is chemical and is converted into electric energy inside a battery. From the battery, electricity is used to power an electric motor and an electric drive regulates the bi-directional power flow between the battery and the electric motor which produces the traction effort but can also operate as generator to charge the battery. The limited electric capacity of a battery, the high cost for its substitution and the lack of infrastructures for quick battery charging still present unsolved problems which limit drastically the diffusion of EVs. The typical range of a full electric vehicle is limited to 70 kilometers [3] which represent an unfeasible value for a passenger vehicle needs. The life expectancy of energy storage battery is limited to few years after which the battery set has to be substituted and the time required to recharge a battery is still long, on average it takes few hours. Few electric vehicles have made their appearance on the market, among others Mitsubishi i-Miev and Tesla Roadster represent two opposite examples. Tesla roadster is a pioneer in electric vehicles since it is the first electric vehicle on the market equipped with Li-ion batteries. It is a sporty vehicle whereas Mitsubishi i-Miev aims at piercing the market of urban cars.

Figure 2.1: Mitshubishi i-Miev [4]

Figure 2.2: Tesla Roadster [4]

Few data about these vehicles [4]:

Table 2.1: Technical data of two electric vehicles

Mitsubishi i-Miev	Tesla Roadster
• Top speed: 130 km/h • Range: 144 km • Charging time: 6-8 hours • Quick charge: 1 hour • Battery: Li-ion 16 kWh • Price: ~ 20000 €	• Top speed: 250 km/h • Range: 350km • Charging time: 6/8 hours • Battery: Li-ion 53 kWh • Battery weight: 450 kg • Price: 90000€ (no more in production)

These two vehicles represent the-state-of-the-art as the quite long driving range proves, however the long charging time and the high price are not affordable for most of the people. Tesla claimed in 2011 that battery life was around 5 years and the price to replace the battery pack was 10000 €.

In order to overcome the problem of short driving range a fuel cell can be installed instead of a battery pack. A fuel cell operates as a standard battery, it exploits a chemical reaction to convert the chemical energy of a fuel into electric energy. Hydrogen is typically used as fuel even if other hydrocarbons like methanol or natural gas are sometimes used; oxygen is the main oxidizing agent. The big advantage represented by a fuel cell in comparison to a standard battery is that it can continuously release electric energy provided that the chemical reactants are supplied. Since oxygen can easily be found in air, a fuel cell vehicle can in practice run with the same operating principle of conventional engine-powered vehicles since it only requires a fuel storage unit. As a result longer driving range is achievable with respect to a battery electric vehicle and higher efficiency is obtainable in comparison to an engine-powered vehicle since fuel energy is converted into electricity by means of a chemical reaction which does not burn the fuel and thus has a much higher efficiency. The main limitation to fuel cell electric vehicle spreading is represented by the high cost during the transformation process to obtain hydrogen from water or hydrocarbons and to produce fuel cells which can meet the desired needs for ground transportation like quick start-up, high power density. Nowadays fuel cells are built with composite materials which have high cost of production.
Moreover, as for electric vehicles, the lack of specific infrastructure to store hydrogen represents another strong issue.

2.2 Hybrid electric vehicles

Hybrid electric vehicles represent instead a feasible response to current and future problems related to everyday urban mobility and environmental issues.
The definition hybrid electric appeals to the architecture of the vehicle powertrain which includes both a conventional powertrain based on an internal combustion engine and an innovative powertrain based on electric and mechanical components. The main reason to introduce additional components in the powertrain is to support the internal combustion engine during all its operations in order to shift its operating point to a region of high efficiency and low emission rates.

It is straightforward to understand that by sharing the total power request between the electric and the mechanical transmission paths a hybrid electric vehicle can achieve better fuel economy than a conventional vehicle where the engine has to balance the overall external load, however there is a number of reasons which can justify the improvement of overall efficiency from tank-to-wheel (1). Firstly, the main operating principle is *load-leveling* [1] meaning that the total power request is split between the internal combustion engine and the electric powertrain in such a way that the engine can always operate in a region of high efficiency or at least close to it. The power split ratio is, for most of the cases, not fixed but it can be varied depending on driving conditions. This corresponds to a degree of freedom in the energy management of the vehicle since the engine power can be either primarily sent to the driven wheels or used to charge the battery. The battery power represents the second degree of freedom. Suppose the engine worked always in its most efficient operating point, during low power request it can provide more power than the required one which is stored in the battery. During high power request the engine would not generate the total traction effort because the battery would support it by providing the necessary amount of power to match the total power request and let the engine work in a region of high efficiency. The power split allows the designer to install a downsized engine which can be optimized to work in a specific speed range rather than assuring a good compromise between performance and efficiency over the entire operating range.

Regenerative braking is applied in both electric and hybrid electric vehicles in order to recover part of the mechanical energy of the vehicle during braking and store it as electric energy into the battery; hence it is another possibility to achieve better fuel economy since battery state of charge can be replenished without using additional engine power. Lastly, full electric mode is available for example during low speed driving and low power request, reverse motion; the engine can be switched off during protracted stops if the battery is well charged.

---

[1] The overall efficiency of a vehicle should be evaluated considering the whole energy transformation process which is organised n two steps: well-to-tank and tank-to-wheel. However the current analysis considers only the latter.

The most important components of the powertrain are an internal combustion engine that is flanked by at least one electric machine, an energy storage battery, power electronics and a mechanical driveline. Hybrid vehicles can use the already existing infrastructures for fuel replenishment and they can successfully overcome typical limitations of EVs by using the internal combustion engine power to charge the battery and run the vehicle. These improvements are achieved at a price of higher complexity in the design and control of the powertrain components and operations. In fact in order to exploit the benefits that a hybrid architecture can guarantee in terms of fuel economy it is necessary to blend the operations of all powertrain components so that they can cooperate successfully. This requires the definition of a precise control strategy for energy management which has to decide how the power flow should be split within the powertrain, namely to what extent each machine should contribute to the production of total power required. A similar control strategy is not needed in a conventional engine powered vehicle since the internal combustion engine is the unique power unit.

2.3 Control structure for energy management

2.3.1 The hardware

Due to the high complexity of the system and multiple input/output information that have to be defined, the control is organized in a hierarchical structure which is depicted in Figure 2.3.

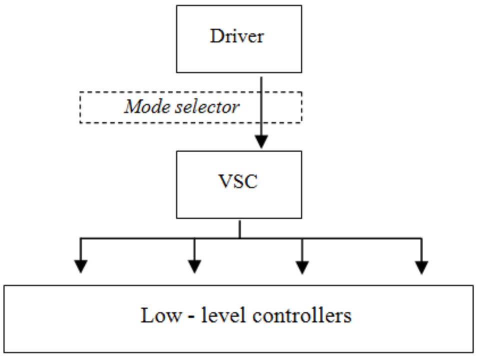

Figure 2.3: Control structure for the energy management of a hybrid electric vehicle

The driver is at the top level of this structure. It is outside the system but it defines the desired operating conditions of the powertrain in terms of torque and power request. The driver behaves like a feedback controller since the driver pushes either the throttle or the brake pedal depending on the error between the actual vehicle velocity and the desired velocity which is in his mind. Moreover sudden acceleration or braking commands can be provided depending on the driving situations. A mode selector is placed in-between the driver and the *vehicle supervisory controller* (VSC) [1] to change some internal parameters of this latter depending on driving situations; for example if a sudden hard braking is detected or a fault is detected in the system then the energy management problem has no more the priority but vehicle safety and stability has to be guaranteed. Therefore this additional controller takes over the control strategy and drives the vehicle to a safe state. In addition it coordinates the operations of the vehicle supervisory controller which considers only the energy management problem with other active control systems that are implemented in the vehicle.

The lowest level comprises the control algorithms of all machines in the powertrain. Each component in the powertrain has its dedicated control unit; these units are regarded to as low-level controllers and some typical examples are the engine controller, the gearbox controller, the electric machines controller. These controllers have the task to regulate the behavior of a machine in order to achieve a desired operating point. However these controllers have a limited view and understanding of what is happening in the system; they are only tuned to make a machine reach quickly the desired operating point while satisfying operating constraints but they are not able to define the desired set point on their own. For this reason a high level controller has the responsibility to define the target operating point of each component of the powertrain; this high level controller called vehicle supervisory controller has a global view of the operations of the powertrain, the status of the vehicle and the requests from the driver so it can properly define these desired operating points. The vehicle supervisory controller is the module which translates the driver's requests into specific control signals for the powertrain. It communicates with both entities and receives inputs from them. Throttle and brake pedal position are mapped to obtain the desired torque request; for parallel hybrids an additional input from the driver might be represented by the gear shifting command. Multiple signals from sensors spread in the vehicle are used to analyze the vehicle status. All inputs are processed and correspondent output control signals are provided to low level controllers through the vehicle *controller area network* (CAN).

2.3.2 The formulation as a problem of optimum

The energy management problem is addressed directly in the VSC and it can be idealized as a constrained optimization problem. It is designed in order to achieve specific objectives like lower fuel consumption, lower pollutant emissions while satisfying at the same time a number of constraints which are defined by the characteristics of the machines and drivability (i.e. how the vehicle responds to driver's requests). A typical constraint for a charge sustaining hybrid is that the battery state of charge level has to remain within two boundaries throughout the driving mission and the final level should be close to the initial level. The objectives are usually defined by metrics or mathematical functions: the definition depends on the objective itself; for example fuel economy involves the minimization of the total fuel consumption over the entire driving mission and the deviation of the battery state of charge at the end of the mission with respect to a target value. An integral objective plus a terminal cost on state of charge deviation summarize these targets:

$$J = \phi\left(SOC_f\right) + \int_0^T \dot{m}_f(x,u,t)\,dt = \phi(x,u,v,t) \tag{2.1}$$

Drivability may instead introduce objectives like attenuation of longitudinal jerk during gear shifting or number of gear shifting. In this case the objective is to minimize the total number of gear shifting events (GSE) within a driving mission and the cost function may represent this total number.

$$J = \sum_0^T GSE \tag{2.2}$$

In addition several constraints should be satisfied throughout the driving mission. The constraint on sustenance of battery state of charge has already been mentioned furthermore each component of the powertrain has a specific operating domain which should be taken into account when power split is defined otherwise desired setting points may not be achieved because they lie outside this domain. Operating constraints are easily translated into mathematical functions of system states and control inputs; depending on the type of the problem external measured disturbances can also be considered. Constraints can be represented via nonlinear functions as follows:

$$\psi(x,u,v,t) = 0 \tag{2.3}$$

where ψ is usually a vector of nonlinear functions.

Lastly, the energy management refers to a specific powertrain configuration where control inputs, system states and external disturbances are connected to one another. Different approaches are available to model a system; however a state space form is the most useful one since it highlights the relationships among system states, control inputs, external disturbances and system outputs.

$$\begin{cases} \dot{x} = f(x,u,v,t) \\ y = g(x,u,v,t) \end{cases} \tag{2.4}$$

Eventually the energy management problem consists in finding an optimal control strategy u which can minimize the objective function (2.1) while satisfying all constraints imposed by (2.3) and (2.4). In a mathematical form it corresponds to:

$$\min_{u} \{ \; J(u) = \phi(x,u,v,t) \; \}$$

subject to:

$$\psi(x,u,v,t) = 0 \tag{2.5}$$

$$\begin{cases} \dot{x} = f(x,u,v,t) \\ y = g(x,u,v,t) \end{cases}$$

The VSC has the task to find an optimal solution to this optimization problem consequently most of the success of an energy management strategy depends on the decisions taken by it which hence has to be designed in a proper way.

2.3.3 The algorithms - State of the art

A lot of work has been published on the energy management problem of a hybrid electric vehicle and a bunch of alternative control strategies have been developed and, in some cases, tested on real vehicles or prototypes. The following classification based on [5] identifies:

a) Rule based strategies
b) Optimization based strategies

The second family can be further distinguished into:

a) Global optimization methods: past, present and future driving conditions are supposed to be known exactly, namely the entire drive cycle is known in advance. These methods includes for instance dynamic programming and Pontryagin’s minimum principle.
b) Local optimization methods: past and present driving conditions are known while future driving conditions may be either predicted over a limited time period or not used in the analysis. The former case refers to

MPC and stochastic dynamic programming while the latter case refers to ECMS.

Rule based strategies

A rule based strategy is also known as a heuristic control strategy since in most of the cases it is defined upon engineers' experience and personal judgment. The control commands (desired operating points of the powertrain components) are defined by a set of rules depending on the input information coming from driver and vehicle sensors. These rules are similar to *if-then* [6] programming structures because the power split ratio between engine and battery is decided depending on the required traction power and the battery state of charge level.

Once a driving condition is recognized, correspondent rules are triggered. As a result these strategies do not try to find a numeric solution to the optimization problem illustrated in (2.5), so it is not guaranteed that the resulting control strategy is the optimal one moreover a tough tuning procedure of several parameters is required to achieve decent fuel economy over different driving scenario. Nonetheless due to their ease of implementation for real-time application, heuristic rule based strategies are extensively applied to hybrid electric vehicles available on the market today. In [6] a 8 states rule based strategy is compared to other three control strategies. The scheme of the heuristic control is reported in Figure 2.4.

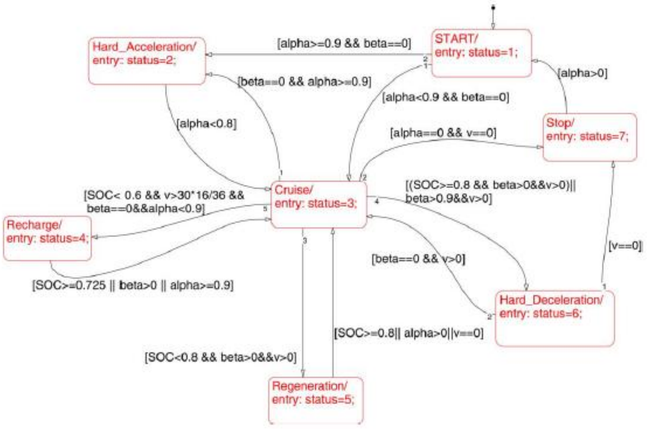
Hard_Acceleration/
entry: status=2;
[alpha>=0.9 && beta==0]
START/
entry: status=1;
[beta==0 && alpha>=0.9]
[alpha>0]
[alpha<0.9 && beta==0]
[alpha<0.8]
Stop/
entry: status=7;
[alpha==0 && v==0]
[SOC< 0.6 && v>30*16/36 &&
beta==0&&alpha<0.9]
Cruise/
entry: status=3;
[(SOC>=0.8 && beta>0&&v>0)||
beta>0.9&&v>0]
Recharge/
entry: status=4;
[v==0]
[beta==0 && v>0]
[SOC>=0.725 || beta>0 || alpha>=0.9]
Hard_Deceleration/
entry: status=6;
[SOC>=0.8|| alpha>0||v==0]
[SOC<0.8 && beta>0&&v>0]
Regeneration/
entry: status=5;
1
2
3
4
5

Figure 2.4: The eight working states of the rule based strategy [6]

Alpha and beta represent respectively the normalized acceleration pedal position and the normalized braking pedal position. The control output is the torque split between engine and electric motor. As the scheme illustrates, the power split is decided merely upon throttle and brake pedals position, torque request and battery state of charge level.

Dynamic programming

Dynamic programming is a method which calculates an optimal solution to (2.5) which holds for the entire driving mission since it is assumed that power request is completely know in advance. This corresponds to a huge limitation for real-time applications because it is impossible to know in advance the whole effort which is asked to the powertrain, nevertheless the optimal solution obtained with dynamic programming can be used as benchmark for assessment of other methods like for instance rule based. Dynamic programming has been widely used in many papers where the known driving mission corresponds to one of the standard drive cycles. If the system were not subjected to external disturbances then the solution obtained with dynamic programming would be the optimal one with the piece of advantage of being computed off-line. Unfortunately any real system is subjected to external disturbances whose properties cannot be completely known in advance; as a consequence if the optimal control strategy were computed off-line using dynamic programming and then applied to the system, it would produce poor performance and it may not guarantee the stability of the system.

In order to overcome this problem either stochastic dynamic programming or predictive dynamic programming [7] can be applied. Stochastic dynamic programming predicts the future outcome of external disturbances according to a Markov process. The stochastic properties of the probability distribution of random external variables should be known in advance and this represents a limitation for real-time application to the energy management problem. In fact this requires knowing the stochastic properties of power request at wheels which is very difficult when the driving mission is completely unknown. A partial description of road, traffic conditions can be provided by navigation systems however for the ease of real-time application the integration of all these tools represents a stringent constraint. In [6] dynamic programming is used to set a benchmark to assess the goodness of other three control strategies. In [8], however, DP is used in combination to standard optimal control theory to provide a control strategy for a parallel hybrid electric vehicle. On the other hand a promising application of stochastic dynamic programming appeals to those vehicles which are meant to repeat steadily the same route. In this case the average power request can be described on the basis of collected measurements of past repetitive driving missions. In [9] it is shown how stochastic dynamic programming can be applied to the energy management problem of a bus for public transportation whose mean power request profile can be determined in advance by collecting data of several driving missions along the same route. In [10], instead, Markov chains and Stochastic Dynamic Programming are even applied to a series hybrid electric vehicle whose driving mission is unknown a priori and power demand is obtained through a Markov process where stochastic properties are derived from the information acquired on different standard drive cycles. Dynamic programming is a powerful tool to derive an off-line optimal solution which can be later used for benchmark comparison in the design of a causal real-time controller. However the necessity to known exactly or at least the stochastic properties of all external disturbances and the heavy computational load required by the algorithm, makes it almost impossible to apply directly dynamic programming to the design of a real-time controller.

ECMS – equivalent consumption minimization strategy

ECMS was developed in order to simplify the global optimization problem in (2.5) to a local instantaneous problem that is much easier to handle and implement in real-time applications. The solution calculated with this approach is obtained from an optimization problem which is limited to the current time rather than to the entire driving mission which is unknown in most of the cases. Theoretically ECMS does not need to know past and future driving conditions to find an optimal power split between the electric and the mechanical paths. ECMS fits well for a charge sustaining hybrid electric vehicle because it treats the electric energy storage unit as an energy buffer which can help to reduce fuel consumption. In a charge sustaining hybrid electric vehicle the difference between initial and final levels of battery state of charge should be small meaning that part of fuel energy should be used to charge the battery. Consequently the energy discharged by the battery at a given instant in time should be replenished by part of fuel energy at a later phase while the electric energy recovered can be used afterwards to reduce engine load. These relations can be represented by a total fuel mass flow rate [5]:

$$\dot{m}_f^{total} = \dot{m}_f + \dot{m}_f^{eq} = \dot{m}_f + \frac{s}{Q_{lhv}} P_{el} \tag{2.6}$$

An equivalent fuel mass flow rate is introduced in order to include the cost of battery charging or discharging in the evaluation of the overall fuel consumption. $\dot{m}_f^{eq}$ can be either positive or negative depending on whether the battery is discharging or is being charged, thus $\dot{m}_f^{total}$ can be higher or lower than the actual engine fuel consumption. This strategy therefore tries to balance the usage of electric power by considering its equivalent effect on fuel mass flow rate and it defines the optimal power split among several combinations as the one which produces the lowest total fuel mass flow rate. A crucial parameter for this evaluation is the *equivalency factor* 's' which converts electric power into an equivalent fuel mass flow rate. In the early development of this strategy, the value of s was tuned according to the particular characteristics of the drive cycle, namely the driving mission was supposed to be known in advance and the equivalency factor was determined from an optimization process. Later in time adaptive ECMS, or A-ECMS, was developed to deal with real applications where driving mission is not known a priori. As example is provided in [11]. The equivalency factor is adapted to driving conditions and style by using recent past information and possibly future information to detect the cycle type. Another improvement considers route recognition where driving conditions are acknowledged according to their mean characteristics and the equivalency factor is updated from a table of stored values. A shifting time interval is considered for route recognition so that the value of s can be updated frequently. Despite the ECMS algorithm is much less computational demanding than dynamic programming, still there are some issues related to its implementation. The online route recognition and equivalency factor updating may require large memory usage, moreover the optimal control inputs are found among a set of discrete candidates similarly to DP. Therefore there is no assurance that the optimal values are included in this group.

MPC – model predictive control

MPC was developed in chemical industry as preferred control strategy for slow chemical processes. Model predictive control is undoubtedly a powerful tool to control dynamic systems characterized by several constraints on systems states, control inputs and outputs when a desired objective function should be minimized. Nonetheless it solves continuously a numeric optimization problem, hence its application in automotive industry is increasing besides the improvement of computational capability of microcontrollers. In [12] it is used to smoothen the transition between electric driving mode and hybrid mode which causes torque fluctuations and undesired longitudinal accelerations in a parallel hybrid electric vehicle. Many other examples of applications to automotive industry are available in [13].

When applied to the energy management problem of a hybrid electric vehicle, MPC can be seen as a step forward with respect to ECMS since it reduces the global optimization problem in (2.5) to a local problem limited to a short future time period where it uses predictions of future driving conditions to find an optimal control action which can both satisfy all constraints and minimize the objective function. In contrast with ECMS and DP, control inputs are not discretized in values but they can assume any value inside the admissible domain (although discretization is introduced by the computational capability of the software). Applications of MPC to the energy management of a hybrid vehicle is quite recent; among others, interesting examples of application to series and power-split hybrids are [14], [15], [16]. In particular [14] gives some insight into real-time application of MPC to this type of problem by highlighting the strong limitations that exist.[15] shows the capability of MPC to deal with multiple constraints while [16] assumes that torque equilibrium at the driveline may not be satisfied at each instant and therefore vehicle velocity tracking is introduced as additional objective in the cost function. This latter approach seems to be however not helpful since it augments the number of states and therefore the computational time. Due to the intrinsic predictive nature of the approach, it is claimed that the integration of MPC with navigation systems may result in better fuel economy than ECMS because future driving conditions may be predicted better [16],[17].

2.4 Drivability metrics

The hybridization of conventional vehicles does not only represent a promising way to improve fuel economy and reduce pollutant emissions but it has also caused new important challenges regarding NVH (i.e. noise and vibration harshness) [3]. Some of the NVH issues are peculiar of HEV and they have to be taken into account in the design phase since the customer’s perception of a vehicle product relies strictly on vehicle’s NVH characteristics. Torsional and bending vibrational modes of the powertrain are affected by the introduction of electric machines and operating modes of a hybrid vehicle. Electric machines add inertia to the system and this means that natural torsional and bending frequencies of the powertrain shift downwards and it is necessary to assure that they do not couple dangerously to rigid modes of the chassis. Moreover engine starting and stopping occur generally when the vehicle is already running depending on the battery state of charge and driver’s power demand. This implies that engine cranking and starting cannot occur in neutral position and the resulting torque may produce undesirable vibrations and torque fluctuations along the driveline.

Some of these problems are treated and solved at local levels by adopting for example dampers, advanced control of engine cranking torque and combustion onset. Nevertheless some of the modifications that need to be introduced to improve general vehicle’s NVH can affect and degrade fuel economy, namely the control actions decided by the vehicle supervisory controller may be later modified in order to satisfy any drivability restrictions. In particular gear shifting quality and engine start&stop events, which are commonly referred to as *drivability metrics* [18], may interfere with optimal energy management. Upshifting to reduce engine speed as function of vehicle speed in a parallel hybrid electric vehicle is seen as an important measure to improve overall energy efficiency however excessive gear shifting degrades passengers’ comfort and quality perception of vehicle’s performance. A customary drivability metric limits the number of gear shifting at the price of less efficient engine operating point. Most of control strategies for energy management focuses solely on fuel economy but this is useless from a production perspective since as above mentioned NVH restrictions are as important as fuel economy. In [18] it is shown that when drivability metrics are already included into the optimization problem (2.5), fuel consumption can be reduced by 10% in comparison to a control strategy which has been only based on fuel economy aspects and later modified to respect some NVH restrictions.

Due to the multiple constraints that characterize the energy management of a hybrid electric vehicle and the appealing property of being predictive by nature and suitable for implementation with auxiliary navigation systems, MPC has been chosen to develop a control strategy for the vehicle supervisory controller.

3 Architectures of hybrid electric vehicles

There is a rather large nomenclature for hybrid electric vehicles depending on the arrangement of the components in the powertrain and the rate of hybridization of the propulsion system. In this chapter a short description of the available classifications is provided then the different architectures of a hybrid powertrain are introduced and briefly explained. In particular emphasis is put on the comparison between series, parallel and series-parallel hybrid electric vehicles with the aim to highlight advantages and disadvantages of each configuration with respect to one another. Afterwards more insight on series-parallel hybrid electric vehicles is provided since this architecture is analyzed deeply in this thesis work. The driving operating modes are discussed and the technical terminology, which is useful to understand some key concepts that appear in the next chapters, is introduced and clarified. Lastly the layout of the analyzed power-split hybrid electric vehicle is introduced and the main components of the powertrain are characterized.

3.1 Classification of hybrid electric vehicles

A hybrid electric vehicle is equipped with an internal combustion engine and at least one electric motor which contributes to generate the necessary traction power. An electric energy storage unit provides electric power to the electric motor and works as an energy buffer for the engine. Most of the time a battery accomplishes this task however supercapacitors or fuel cell can also be used in placed of a conventional battery. Moreover the battery technology can range from lead acid to Li-ion batteries [1]. The powertrain that is discussed afterwards implements a lead-acid battery. With respect to a conventional passenger vehicle, the powertrain of a hybrid electric one can be seen as composed by a mechanical and an electric path for power flow which are connected to each other by mechanical and electric nodes. A planetary gear set or another device for mechanical power transformation is a mechanical node while power electronics represent an electric node. Blending of power between these two paths is crucial to achieve high efficiency and match power and torque requests from the driver.

A number of alternative classifications are available to distinguish the different types of hybrid electric vehicles that are currently available on the market. A first classification ranks hybrid vehicles on the basis of the characteristics of the electric side of the powertrain. Depending on the energy management of the battery, a vehicle can be either charge sustaining or charge depleting. A charge sustaining vehicle does not need of an external source of electric energy to restore the charge level of the battery because the engine can provide the whole necessary power to charge the storage unit. As a result a charge sustaining hybrid only needs of an external source of fuel to be driven. On the opposite a charge depleting vehicle utilizes the electric energy from the battery as much as possible and then it switches to engine driving mode as soon as the battery state of charge is too low. In this mode it operates as a charge sustaining hybrid so the engine power in also used to maintain the battery state of charge inside a prescribed safety band while the battery works as energy buffer to support the engine during driving. Plug-in hybrid electric vehicles (2) are charge depleting hybrids; they are operated in full electric mode at the beginning of the driving mission until the battery charge level diminishes to a low threshold and then the engine is activated to power the vehicle and keep the battery state of charge close to the low threshold. Engine power is not used to replenish the battery energy till a desired value since it is assumed that at the end of the driving mission the vehicle can be plug in an external source of electricity. Similarly full electric vehicles can be referred to as charge depleting vehicles but in this case there is no alternative available operating mode.

Being charge sustaining or charge depleting vehicle depends also on the rated characteristics of the electric components that are implemented in the powertrain with respect to the rated power of the internal combustion engine. This proportion can be referred to as *degree of hybridization* [1] and a hybrid electric vehicle can be classified as e.g. micro, mild, power or energy hybrid. A micro hybrid has no electric power assist during traction; fuel consumption can be mainly reduced by means of engine start&stop during traffic stops. A mild hybrid has the lowest degree of hybridization, the traction effort is mainly due to the engine and electric machines give a limited support during acceleration phases. The electric rated power is in the range of 5-10 kW with a battery rated capacity of 1-3 kWh. Power hybrids are intermediate since electric machines can provide a valuable support to the engine during all driving conditions with a rated power up to 40 kW but the battery has a low rated capacity (3-4 kWh) which does not allow long driving range in full electric mode. Energy hybrids are meant to guarantee long driving range in full electric mode thanks to high rated electric power (70-100 kW) and high electric capacity of the battery (15-20 kWh) [1]. This latter definition corresponds to a charge depleting vehicle while a power or mild hybrid usually corresponds to a charge sustaining hybrid. The most common classification is actually the one based on the arrangement of the components in the powertrain. As already mentioned in chapter 2 a hybrid electric vehicle is regarded to as the union of a conventional vehicle with a full

---

[2] A PHEV has an additional interface which allows the battery to be directly connected to the external electric grid without using the fuel energy to charge the battery.

electric vehicle (3) however the assembly of the two powertrains can be organized in a variety of different configurations. The most common ones are:

- Series hybrids
- Parallel hybrids
- Series/parallel hybrids

3.1.1 Series hybrid electric vehicle

When an internal combustion engine is added to the powertrain of a full electric vehicle with the target to extend the driving range of the vehicle but the engine is not mechanically coupled to the driven wheels, then a series hybrid configuration is achieved. The goal of the engine is to run an electric generator, which is placed downstream the crankshaft, in order to produce electric energy that can either charge a battery or directly feed an electric motor. Consequently the engine in a series hybrid does not directly contribute to generate the traction effort whereas it serves to extend the driving range of the vehicle by generating the on board electric energy that is used to charge the battery as soon as the charge level drops. The whole traction power is provided by the electric motor which can also work as a generator during braking by recovering part of the vehicle kinetic energy. The electric power flow through the generator, the battery and the motor is regulated by power electronics which decides the direction of the flow depending on the battery state of charge and driving conditions. The power flow is bi-directional between the battery and the driven wheels while power can only flow from the engine to the battery, namely it is not possible to replenish the tank with new fuel by transforming the vehicle’s mechanical energy. The driveline is placed downstream the electric motor and it usually comprises a transmission, a final gear and a differential to deliver the traction torque to the driven wheels. The next figure illustrates a scheme of a typical series hybrid powertrain; the engine and the generator are marked with red color in order to highlight the different layout of the powertrain in a series hybrid with respect to a full electric vehicle.

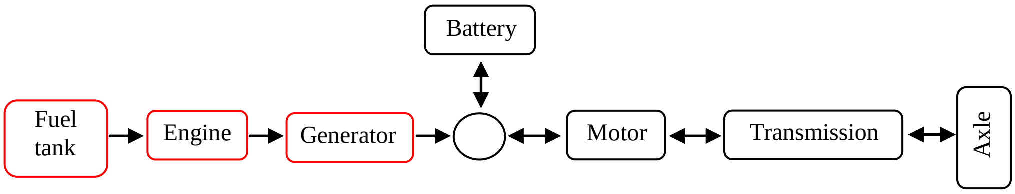

Figure 3.1: Layout of the powertrain of a series HEV

---

[3] The term *“conventional vehicle”* is used here to indicate a ground vehicle which has an internal combustion engine as unique power unit.

A series hybrid vehicle is therefore a charge sustaining vehicle and it has the main advantage that the engine operating point is completely decoupled with respect to the velocity of the vehicle. The engine is only used to run a generator consequently the only input command is represented by the power that has to be produced to recharge the battery. As a result the engine operating point can always fall on the engine optimal operating curve thus high efficiency is always achieved. Moreover the engine is small in size and the layout of the powertrain is rather simple. Nonetheless the electric motor has to be designed for the maximum power request and the battery should have high capacity otherwise the charge would drop quickly and the engine should be used regularly. Series hybrids perform well in urban drive cycles characterized by frequent start and stop events, whereas the double energy conversion from chemical to electric and then from electric to mechanical from the fuel tank down to the driven wheels produces lower overall efficiency than conventional engine powered vehicles on highway routes. It is therefore not surprising that this architecture has been designed for busses of public transportation.

3.1.2 Parallel hybrid electric vehicle

Two power transmission paths are used to deliver the necessary traction power to the driven axle. One path comprises the fuel tank and the internal combustion engine while the second path is the electric one which includes the battery and the motor which can be operated as generator during regenerative braking. A planetary gear set usually blends the power between the two paths and thus different operating modes are available ranging from full electric mode to parallel driving where engine and motor power the same axle to provide traction. A belt or a chain combined with a fixed gear ratio can also be used. With respect to a series hybrid the main advantage is represented by the smaller size that both engine and motor have since the overall power request is split between these two machines. Moreover there is no need to install a generator in the powertrain since the motor can work as generator to charge the battery by using the surplus of power produced by the engine. On the opposite the complexity of the powertrain is higher and the energy management requires a refined control strategy. Moreover a fixed step mechanical transmission is installed since the engine is directly connected to the driven wheels; as a consequence the overall efficiency of the driveline is likely to be lower than for a series hybrid since the engine operating point cannot be set independently on the vehicle speed. A continuously variable transmission can however overcome this issue. The next figure illustrates a simplified scheme of a parallel architecture.

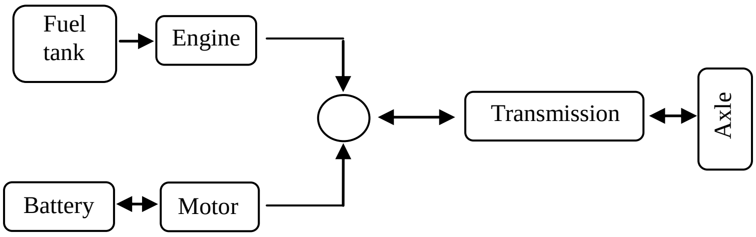

Figure 3.2: Layout of the powertrain of a parallel HEV

Power flow is bidirectional in the electric path while energy recovery is impossible through the engine. Thanks to the synergy of engine and electric motor the driving range of parallel hybrids is longer than series hybrids. Research around parallel hybrids is intensive since they represent a good balance between driving range, reduction of pollutant emissions, fuel consumption and driving performance. Several modifications to the basic layout are available, for example transmission can be based on manual, automatic or CVT. The rotor of the motor can be coupled to the driveshaft upstream or downstream the transmission. Drivability issues like engine start&stop and gear shift quality has to be taken into account when an energy management control strategy is defined otherwise it can lead to poor on board comfort due to excessive gear shifting or engine start&stop events.

3.1.3 Series/parallel hybrid electric vehicles

This configuration is regarded to as the most promising one since it collects the advantages of series (the engine operating point is independent on the vehicle speed) and parallel hybrids (synergy between engine and electric motor), giving high flexibility of power management for better fuel economy. These improvements are at the cost of higher complexity in the design and control of the powertrain and also of higher cost of the vehicle for customers. Series-parallel hybrids use extensively the engine in combination with the electric machines but at the same time the engine operating point is decoupled from vehicle speed; this enables to achieve high efficiency for all operating modes. As for series hybrids an electric generator is added to the powertrain; it works as starter for the engine and as source of electric energy to charge the battery when it is commanded by the vehicle supervisory controller. It can also support the engine and the electric motor to provide traction power for a limited time when power request is very high. Series-parallel hybrid electric vehicles are distinguished between power-split and 2x2. The next two figures report two simplified schemes of the layout of the powertrain in these two cases.

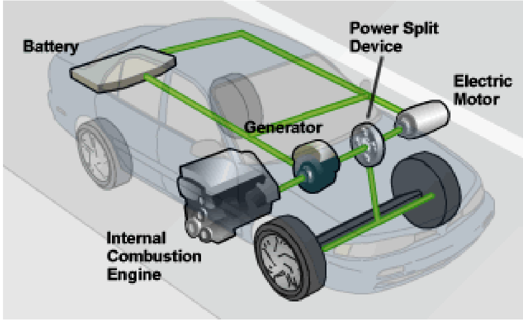

Figure 3.3: Components of a power-split hybrid electric vehicle

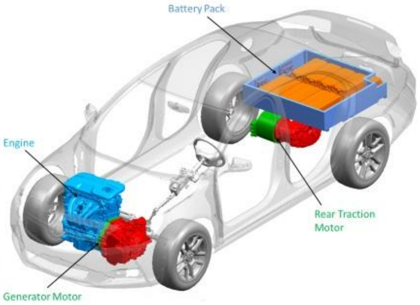

Figure 3.4: Components of a 2x2 series/parallel HEV

The key component of the power-split architecture is the planetary gear set which connects with one another the engine, the generator and the electric motor. The power-split drive guarantees high flexibility in the design because it can successfully disengage the engine from the driven wheels and at the same time it divides the engine power between the driven wheels and the generator. The powertrain has two degrees of freedom [15] since engine power and engine speed can be chosen almost independently on the vehicle operating point. The battery works as a buffer of energy; it absorbs the power produced in excess by the engine when power request is load while it releases power to support the engine during traction. At the same time the rotary velocity of the crankshaft can be adjusted independently on the vehicle speed by setting properly the operating point of the generator and using the power-split drive as an electronic continuous variable transmission. A power-split hybrid collects all operating modes of series and parallel hybrids, namely the vehicle can run in full electric mode, series, parallel, power-split mode and regenerative braking is exploited during brakings. Power-split architecture is used in passenger vehicles having a front driven axle; on the opposite the 2x2 series/parallel architecture is applied to sporty vehicles.

This latter configuration can be operated with the same operating modes of a power-split hybrid however both front and rear axle are driven. The internal combustion engine and the electric generator are mechanically coupled to the front axle and similarly to the power-split case the engine power is used to both power the front axle and charge the battery through the generator. The electric motor provides extra traction torque to the rear axle to support the engine during acceleration phases and fluctuations in power request furthermore it can charge the battery using part of the vehicle kinetic energy during braking. Power blending between front and rear axle is easier than a power-split hybrid since it is electronically controlled and it does not require additional mechanical components. The transaxle of a power-split hybrid, which includes the engine, the generator, the planetary gear set and the electric motor, is a compact assembly whereas packaging is more complicated in a 2x2 architecture.

3.1.4 Plug-In hybrid electric vehicles

A further interesting development which raises the interest in hybrid propulsion systems is the possibility to plug in the vehicle to an external source of electric energy. Even better fuel economy and lower pollutant emissions can be achieved because the vehicle can run in full electric mode for longer mileage by exploiting the electric energy of the battery according to a charge depleting mode. Less power from the engine has to be used to charge the battery during driving because it is assumed that once the vehicle reaches its final destination, the battery will be charged by an external source. The same architectures used for charge sustaining hybrid electric vehicles are exploited with the addition of an external interface to enable connection to a power grid. Nonetheless the complexity of the powertrain increases due to additional components and in order to achieve consistent improvement in fuel economy and emissions it is necessary to provide updated information to the vehicle supervisory controller by means of navigation systems like GPS and traffic information.

3.2 Driving modes of a power-split hybrid electric vehicle

As mentioned above a power-split hybrid electric vehicle offers several different operating modes which are described here below. The electromechanical powertrain of a power-split hybrid electric vehicle is simply represented in the next figure.

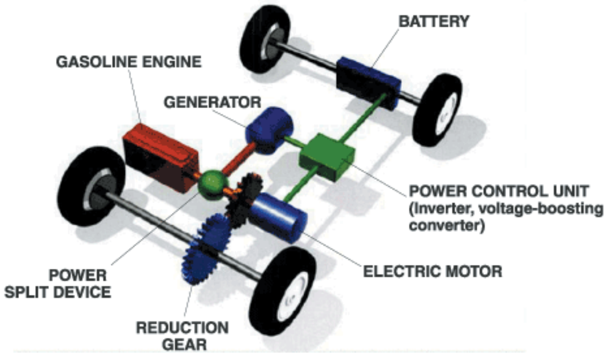

Figure 3.5: 3D view of the powertrain of a power-split HEV [19]

The following driving modes can be identified in a power-split hybrid electric vehicle [20].

Electric mode

When power request is limited and vehicle speed is low the whole traction power is produced by the electric motor provided that the battery has sufficient energy.

In this mode the engine does not intervene and the carrier of the planetary gear set is locked. If a brake is not applied to the sun gear the rotor of the generator rotates freely but the machine does not produce power. The electric motor draws power from the battery therefore the duration of this operating mode depends a lot on the battery state of charge level and on the rated capacity of the battery. Electric driving mode is exploited for reverse motion too. The next figure represents the power flow within the powertrain during this driving mode. The letter A stands for 1st driving mode.

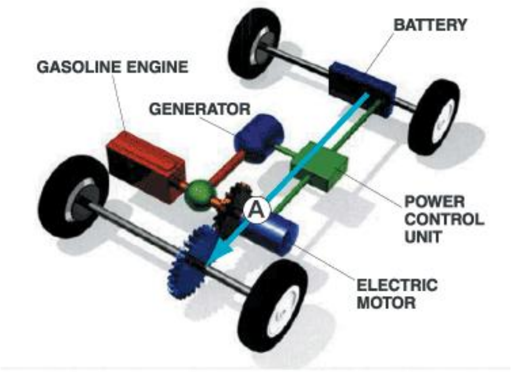

Figure 3.6: Power flow in electric mode [19]

Hybrid mode

In this driving mode the engine, the generator and the motor work together in order to achieve the highest engine efficiency according to the driving conditions. The engine power is split between a mechanical path that through the ring gear delivers power to the driven axle and an electric path that through the generator delivers power either to the battery or to the motor. A number of alternative solutions exist for the power flow among the three machines and the battery; the vehicle supervisory controller uses the generator torque to set the engine operating point and blend the engine power between the two paths. In fact the generator torque is used to control the crankshaft angular velocity which ultimately defines the engine power split ratio between the mechanical and the electric path. The higher the engine speed the more power is delivered to the battery, similarly it is possible to increase engine efficiency by reducing engine speed and let the generator operate as a motor. The hybrid mode occurs during acceleration, cruising phases but also when the vehicle is standing still and the battery needs to be charged. The hybrid mode is an example of the intrinsic flexibility of a power-split hybrid electric vehicle and two main behaviors can be recognized: positive and negative split mode.

a) Positive split mode

This is the standard driving mode which applies to most of driving conditions.

In positive split mode the crankshaft rotates quicker than the driven wheels (if they are referred to the same shaft) and the resulting generator angular velocity is opposite to the generator torque (4), as a result this machine releases electric power to the power electronics. The final usage of the engine power flowing through the generator depends on the driving conditions. During acceleration phases, the motor supports the engine to provide the total required traction torque; as a result the engine does not produce the total required torque and the power which flows in the electric path is used to feed the motor. During hard accelerations the battery can provide additional power to the motor which can therefore support more the engine. On the other hand when the vehicle is cruising the power produced by the generator is used to charge the battery. The split of electric power is decided by power electronics depending on acceleration effort and battery state of charge.

b) Negative split mode

In this mode the angular velocity of the generator has the same sign of the generator torque meaning that this electric machine works as a motor. This situation can occur either during engine starting when the generator works as engine starter or during high speed cruise. In this latter case the generator velocity becomes negative and creates an overdrive ratio which allows the vehicle to maintain high speed while the crankshaft can still rotate slowly. In this configuration the power produced by the engine flows to the driven wheels via the ring gear while the generator is fed by the battery which also provides power to the motor. The next two figures represent respectively the positive split mode for normal driving when extra power from the battery is not needed to feed the motor and the positive split mode when it is used to charge the battery.

---

[4] The behaviour of the power split drive is described afterwards.

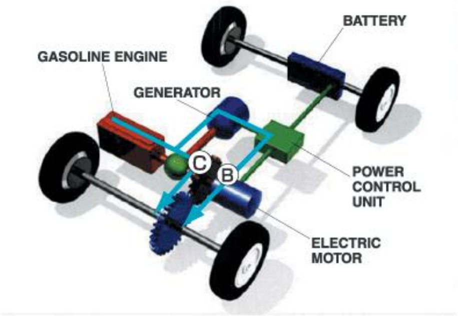

Figure 3.7: Positive split mode. C and B mark two paths for engine power to the wheels [19].

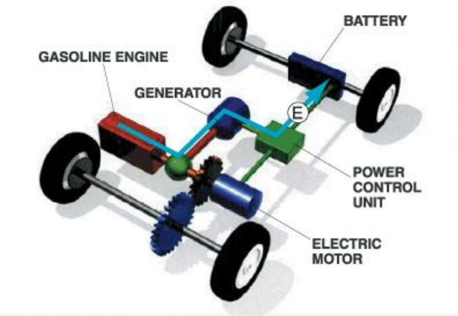

Figure 3.8: Positive split mode. the engine power is used to charge the battery [19].

Parallel mode

The sun gear can be locked by means of a brake and thus the rotor of the generator cannot rotate. In this situation the whole engine power is delivered to the driven axle which represents a more efficient operating condition rather than delivering power to the wheels via the generator and the motor. This operating mode is mostly applied when the vehicle is being driven at rather high constant velocity; a null generator angular velocity helps to keep the crankshaft angular velocity low and therefore to make the engine operate in a region of high efficiency. The motor can support the engine either with a positive torque to cope with an increase in power request by drawing energy from the battery or with a negative torque to absorb the extra torque produced by the engine. Again the battery provides an additional degree of freedom to achieve higher fuel economy than a conventional vehicle. The power flow is equal to the case of positive split mode except for the fact that the entire engine power flows to the driven axle.

Regenerative braking

During braking, part of vehicle kinetic energy can be recovered at the axle powered by the electric motor by using this machine as generator. For a power-split architecture the motor powers the front axle and during regenerative braking the engine rotates freely meaning that no power flows in the planetary gear set. The motor can therefore absorb power and deliver it to the battery to replenish the state of charge.

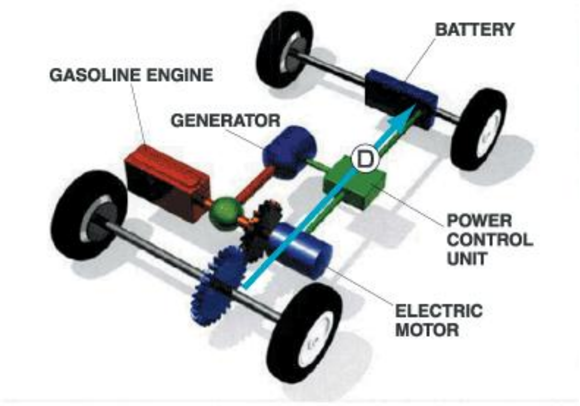

Figure 3.9: Regenerative braking. Part of vehicle's kinetic energy is recovered in the high voltage battery [19].

Engine braking

During long braking on strongly inclined road or when the battery is overcharged and regenerative braking cannot be carried out, engine braking is accomplished. In this mode the motor does not apply any load to the axle and rotates freely while the engine is idling and absorbs power. Again the engine speed is controlled according to the vehicle speed in order to set the amount of power that should be absorbed. Conventional service braking system can intervene during both regenerative braking and engine braking to add an additional braking torque.

3.3 Main components of the analyzed HEV

A power-split hybrid electric vehicle has been analyzed deeply through a high fidelity model implemented in Amesim®. The Amesim® model represents the architecture of a front wheel drive power-split powertrain whose architecture resembles the one represented in Figure 3.5 even if the model includes a silent chain in-between the front axle and the ring gear. Consequently the final transmission introduces a fixed gear ratio, which is obtained as the series of the silent chain and the set of gear wheels, but also it adds elasticity and damping to the driveline. The engine, the power split drive, the electric machines and the battery are the most important components in the powertrain for this reason their properties are introduced now, while the vehicle assembly is treated afterwards.

3.3.1 Power-split drive

The next figure illustrate a planar view of the transaxle of a common power-split hybrid electric vehicles which comprise the three power units and the planetary gear set or power-split drive.

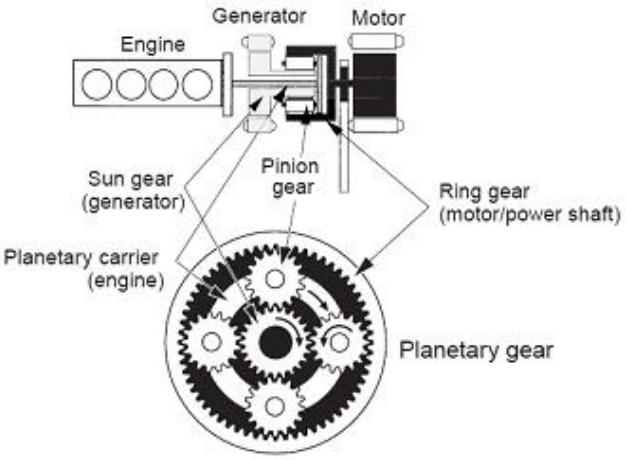

Figure 3.10: Planar view of the transaxle. The engine is connected to the carrier, the generator to the sun while the ring gear and the motor deliver the traction torque to propel the vehicle [19].

The rotor of the electric generator is coaxial to the engine output shaft and both machines are installed on the same side with respect to the planetary gear set. The engine output shaft is the inner shaft and it passes through the planetary gear to match the carrier on the other side. The rotor of the generator represents the sun gear while the ring gear is directly connected to the rotor of the electric motor and both have a fixed connection to the driven wheels. The power split drive is regarded to as an electric continuous variable transmission because thanks to the particular design of the planetary gear set it is possible to decouple the engine speed from the vehicle speed..In order to model the behavior of the planetary gear set, a quasi-static approach is used where the inertia of the gears and the internal losses are neglected and thus they do not appear in the torque equilibrium equation. According to this approach three torques and three angular velocities are needed to describe the behavior of the component [21]. The layout represented in fig. Figure 3.10 corresponds to a planetary gear set of type I whose simplified model is represented in the next figure.

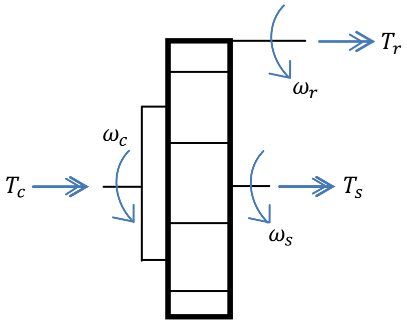

Figure 3.11: Simplified model of a planetary gear set type I

The following kinematic relationship holds for the three angular velocities.

$$\frac{Z_r}{Z_s} = -\frac{\omega_s - \omega_c}{\omega_r - \omega_c} \tag{3.1}$$

The sun gear, the carrier and the ring gear are parallel and coaxial therefore the following torque equilibrium holds:

$$T_r + T_c + T_s = 0 \tag{3.2}$$

Assuming no power loss inside the planetary gear set, the inlet power flow has to be balanced by the outlet power flow as follows:

$$T_r\omega_r + T_c\omega_c + T_s\omega_s = 0 \tag{3.3}$$

By rearranging the set of equations (3.1), (3.2), (3.3) it is possible to express the angular velocity of the carrier and the outlet torque at the ring gear and at the carrier as function of the angular velocity of the ring gear, sun gear and the inlet torque at the sun gear.

$$\begin{cases} \omega_c = \dfrac{Z_s}{Z_s + Z_r}\omega_s + \dfrac{Z_r}{Z_s + Z_r}\omega_r \\[2ex] T_c = -\dfrac{Z_s + Z_r}{Z_s}T_s \\[2ex] T_r = \dfrac{Z_r}{Z_s}T_s \end{cases} \tag{3.4}$$

The angular velocity of the carrier corresponds to the angular velocity of the crankshaft while the angular velocity of the ring is related to the vehicle speed through a fixed gear ratio, therefore the angular velocity of the generator can be used to decouple these two former variables and thus it enables to achieve higher efficiency of the engine. In practice the engine is speed controlled meaning that the generator torque is used to set the desired angular velocity of the crankshaft. The planetary gear set that is modeled here has the following characteristics:

- $Z_r = 78$
- $Z_c = 23$
- $Z_s = 30$

3.3.2 Internal combustion engine

The vehicle is equipped with a 1.2 liters gasoline atmospheric engine.

This gasoline engine produces a maximum torque of 174 Nm at 4500 rpm and delivers a maximum output power of 89.21 kW at 5000 rpm. The characteristic curves of engine torque are defined by means of tables as well as the fuel mass flow rate; the next two figures report respectively a contour plot of the fuel mass flow rate as function of the engine operating point and the engine characteristic curves. The engine Optimal Operating Line is defined as the set of operating points which release a given power with the lowest fuel mass flow rate; this curve is also represented in the next figures by means of a green piecewise linear envelope.

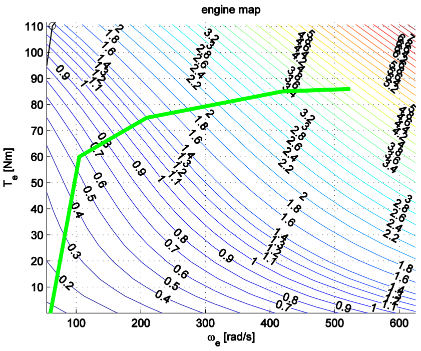

Figure 3.12: Fuel mass flow rate [g/s] as function of engine torque and speed. The engine OOL is the green curve.

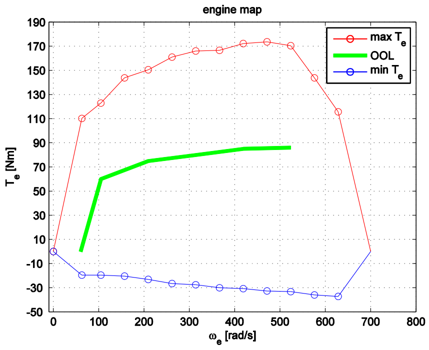

Figure 3.13: Characteristic curves of the engine. Maximum, minimum torque and engine OOL.

The torque that the engine can produce at a given angular velocity of the crankshaft is controlled by the admission rate or engine load. Negative torques are controlled by values of the engine load between -0.1 and 0 where -0.1 corresponds to the minimum curve. A load equal to 1 defines the maximum achievable engine torque while all other torque values are obtained as linear interpolation between these two curves for a specific value of the engine speed. Negative engine torques represent friction and pumping losses inside the combustion chamber. The engine output torque is calculated from a value read in a table which is modified by a first order dynamics in order to take into account the delay in engine response. The value from the table is read as function of engine admission rate and input engine speed; this value is modified in order to take into account possible variation of air density in comparison to the default value and the time lag due to the combustion process. Consequently the engine torque delivered at the crankshaft is obtained as a result of these two subsequent steps:

$$T_{target} = T^{e}_{table} + T_{losses,t_{hot}} - T_{losses,t_{water}}$$

$$\tau_{engine}\dot{T}_{dynamic} + T_{dynamic} = T_{target}$$

$$T^{e}_{output} = T_{dynamic}\frac{\rho_{air}}{\rho^{0}_{air}}$$

where ρ^{0}_{air} is $1.205\ kg/m^{3}$ while τ_{engine} is equal to $0.01s$

Similarly the fuel mass flow rate and the pollutant emission rates are read from correspondent tables as function of the engine operating point.

These output values are modified according to the engine wall temperature in case a thermal management analysis is carried out. In this thesis work the engine wall temperature and the cooling fluid temperature are kept constant throughout the simulations consequently these changes are not applied; similarly the air density is set equal to its default value so it does not introduce any additional changes.

3.3.3 Electric machines

The generator and the electric motor are represented by the same type of electric machine; this designing solution holds for many series-parallel hybrid vehicles on the market since it reduces the production costs. The functionalities of the machine is described by means of tables and equations; in particular a table contains the maximum torque values as function of the rotor angular velocity and the input voltage while the power losses are expressed as function of the operating point (torque and speed) of the machine. The following two figures illustrate the characteristic curve of the electric machines and the power loss as function of the operating point.

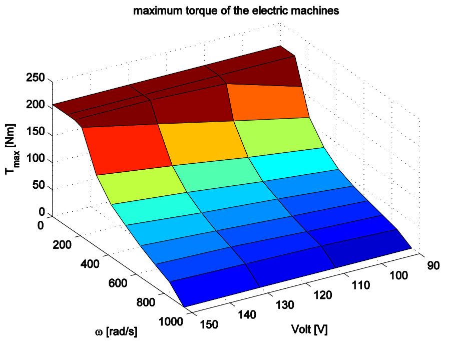

Figure 3.14: Output torque as function of input voltage and rotor angular velocity.

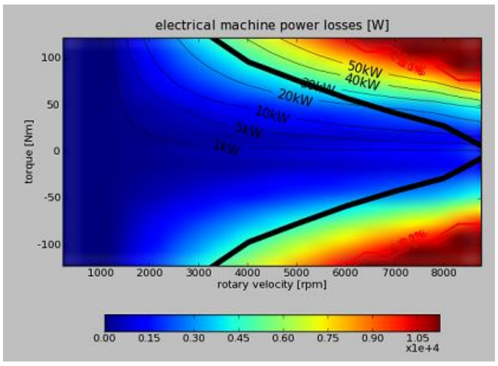

Figure 3.15: Power losses as function of output torque, rotor angular velocity [19].

The characteristic curve of the electric machines is expressed as function of input voltage and angular velocity of the rotor. The torque value obtained from the table is applied to the powertrain according to a first order dynamics which is meant to model the time delay that is always present in a real machine. This first order dynamics and the table substitute the power electronics that control a real electric machine but which are not included in this model.
The output shaft torque is calculated as follows:

$$\tau_m \dot{T}_{out}^{rotor} + T_{out}^{rotor} = T_{table}^{m}$$

where τ_m is equal to 0.001s
The electric machines are connected to the battery via electric coils and set the electric load for the battery while this latter defines the input voltage to the machine. The rotary inertia of the rotor is simply modeled through a 1D disc which is placed downstream the electric machine.

3.3.4 High voltage battery

A hybrid electric vehicle is equipped with two batteries. The high voltage battery is involved in the power management of the vehicle while a 12V battery feeds few auxiliary components. Regarding the energy management only the high voltage battery is important and in the following this component is named simply as battery. The battery is modeled as an assembly of equivalent electric circuits [21] where each circuit represents a single cell of the battery. The internal properties of internal resistance and open circuit voltage of the battery are determined by the arrangement of the cell banks which can be placed in parallel and in series together with additional data which describe these variables as functions of the battery internal fluid temperature and the battery state of charge. The next figures illustrate an example of banks arrangement with 4 banks in series, 7 banks in parallel and 3 cells per battery bank; moreover the equivalent electric circuit that is used to model a cell of the battery is shown too.

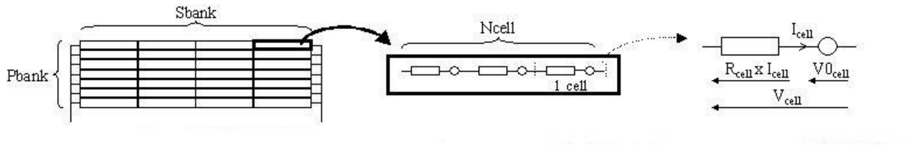

Figure 3.16: Arrangement of battery banks. Equivalent electric circuit of a single battery cell [19].

Each cell is modeled as an equivalent electric circuit with an internal resistance and a voltage source represented by the open circuit voltage.
The equation of the circuit can be written as follows:

$$V_{cell}^{0} = V_{cell} + R_{cell} I_{cell} \tag{3.5}$$

The values of R_{cell} and V_{cell}^{0} are read from correspondent tables as function of battery state of charge and battery internal temperature. Throughout the analysis none temperature change has been considered hence the temperature has been kept constant to 80°C. The next two figures represent the values of the two parameters as function of temperature and depth of discharge which is defined as 100% – state of charge [%].

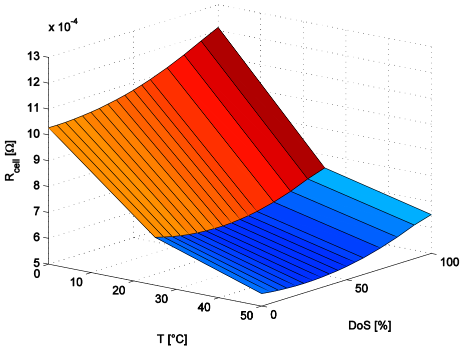

Figure 3.17: Internal resistance of a cell as function of state of discharge and temperature.

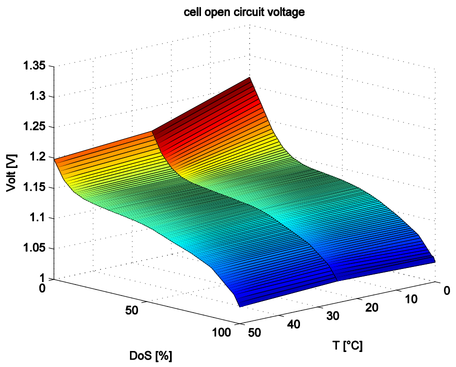

Figure 3.18: Open circuit voltage of a cell as function of state of discharge and temperature.

Under the assumption that the cells behave in the same way, it is possible to obtain the battery output quantities from the electric behavior of a single cell and the banks arrangement. As a result the battery total current, the battery output voltage and the battery total resistance are calculated as follows:

$$\begin{gathered} I = I_{cell}P_{bank} \\ V_{bank} = V_{cell}S_{cell} \\ V = V_{bank}S_{bank} \\ R_{batt} = R_{cell} * S_{bank} * \frac{S_{cell}}{P_{bank}} \end{gathered} \tag{3.6}$$

The battery open circuit voltage is defined through the following equation:

$$V_{oc} = V_{cell}^{0}S_{cell}S_{bank} \tag{3.7}$$

The battery total current is negative when the battery discharges as a consequence the time derivative of the battery charge is defined as follows:

$$\frac{dq}{dt} = I \tag{3.8}$$

By comparing this time derivative with the battery rated capacity it is possible to define the time derivative of the battery state of charge as a function of the battery load:

$$\frac{dSOC}{dt} = \frac{dq}{dt}\frac{100}{Q_{batt}} \tag{3.9}$$

3.3.5 The vehicle assembly

The vehicle assembly comprises the wheels, the suspension system and the carbody. The torque delivered by the driveline is applied to the driving wheels which are characterized by a rotary inertia while the tyre properties are modeled by means of Pacejka 89. The wheel normal load is a function of the carbody pitch motion and it is used inside the Pacejka model. The wheels are connected to the carbody via the suspension assembly which comprises for each axle an unspung mass, tyre and suspension stiffness, viscous dampers. The carbody is subjected to the aerodynamic drag and to the reaction torques and forces from the engine block, suspension system. The engine block is connected to the chassis by means of three bushings thus the model computes the transmissibility of forces and oscillations between the engine and the carbody. The overall dynamics in the vehicle symmetry plane is solved by using the Euler equations, while the vehicle lateral dynamics is not analyzed in this model.

The nominal values of the most important parameters which characterize the vehicle are provided in the following list:

- $m_{carbody+engine} = 1280\ kg$

- $m_{unsprung}^{front} = m_{unsprung}^{rear} = 40\ kg$
- $m_v = m_{carbody} + m_{engine} + m_{unsprung}^{front} + m_{unsprung}^{rear} = 1360\ kg$
- $J_{wheels}^{axle} = 2\ kgm^2$
- $r_w = 0.2977\ m$
- $g_{silent\ chain} = 0.9231\ [-]$
- $g_{FD} = 4.2308\ [-]$
- $g_f = g_{silent\ chain} \cdot g_{final} = 3.905\ [-]$
- $J_{motor} = 0.01\ kgm^2$
- $J_e = 0.1\ kgm^2$
- $\rho_{air} = 1.2\ kgm^3$
- $C_x = 0.3\ [-]$
- $S = 2\ m^2$
- $f_r = 0.025\ [-]$
- $P_{bank} = 1\ ,\ S_{bank} = 6\ ,\ S_{cell} = 40$

4 The MPC-based control strategy

In this chapter it is described how predictive control can be used to develop a control strategy which manages the power split of a hybrid electric vehicle in order to achieve the desired objectives. Model predictive control relies on a mathematical formulation of the system, thus the chapter illustrates the physical and mathematical modeling that has been applied to set up the optimization problem in order to calculate the optimal control strategy.

4.1 Background

In chapter 2 it is underlined how the energy management of a hybrid electric vehicle can be formulated as a constrained optimization problem whose solution is generally computed by means of numeric algorithms. Different approaches have been tested so far to get a suitable optimal control action and Model Predictive Control (MPC) is included in this list. Model Predictive Control belongs to the family of model based optimal control theory where a numeric optimization problem is solved to compute the control action which can drive a dynamic system to a desired set point while achieving the best performance defined by a proper index. In fact a system usually has to be driven to a desired set point starting from an initial configuration. The trajectory that the system can follow from this initial state to the final desired one is usually constrained by a number of state constraints; however even in this situation there is normally a bunch of alternative control actions which can lead the system to the final state. Each control action makes the system follow a different trajectory once it is applied. Besides the desired final set point additional requests are usually specified on some performance that the system should achieve while moving along a trajectory; therefore the control action which can achieve the best performance indices is the optimal one and it is the only one which should be applied to the system. Model Predictive Control computes this optimal control strategy by combining predictions of future system response to an optimization problem. A simple example is described below to clarify the operating principle of MPC.

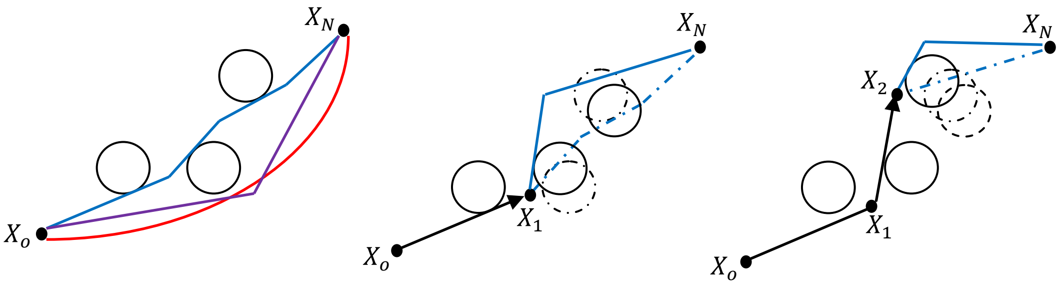

Figure 4.1: (a). (left) A system may move from Xo to X_N following three possible different trajectories. (b) (middle) the constraints are dynamic and the optimal trajectory needs to be recomputed. (c) (right) MPC updates the optimal control action at each sampling time.

Figure 4.1(a) represents the initial state $X_o$and the desired set point X_N that the system is supposed to achieve, while the blue circles represent the state constraints. MPC knows the initial and the desired final states moreover it includes models of the dynamics of the system and of the shape of the constraints. Using these models MPC can formulate three suitable control actions and by using the model of the system dynamics it can predict the correspondent trajectories that the system would follow once these control sequences were applied to the system. The three trajectories are represented in Figure 4.1(a) with blue, purple and red colours. In this example it is supposed that the control actions are defined in order to bring the system to the final state however in the classical MPC formulation the prediction can be limited to few future steps and thus the control action is meant to bring the system to an intermediate future state.

Suppose the performance index were the minimization of the total travel distance, then the trajectory represented in blue would minimize this objective while satisfying all constraints, thus the correspondent control action would be the optimal one. This optimal control action u_1^* is calculated as the solution of a constrained mathematical optimization problem where the objective function to be minimized corresponds to the total travel distance from X_o to X_N. Figure 4.1(b) shows that the state constraints are dynamic hence they change while the system evolves from X_o to X_1 under the input u_1^*. Therefore if the control action were not changed the system would violate one or more constraints along its trajectory. This is not an issue for MPC since it samples the new operating conditions of the system at X_1 and updates the model of the constraints, thus it can compute a new optimal control action to drive the system from X_1 to X_N by solving a new optimization problem. Once the system gets to X_2 the whole optimization problem is repeated once more in order to calculate a new optimal control action to drive the system from X_2 to X_N. This procedure is repeated even if the constraints do not alter their shape and thus the optimal control action defined at the previous step would still match the requests. Consequently MPC calculates by nature a feed forward control action which would bring the system from the given state to the final desired one however only the first element of the computed control sequence is applied to the system and then the optimization problem is repeated at the next sampling time using as inputs the new operating conditions and moving the prediction horizon one step forward. This approach is called *receding horizon* and it brings to a feedback control action.

This simple example highlights the core points of MPC:

- Reference model of the system: a model of system dynamics is used to predict its response under the effect of a control action and known external disturbances.
- Model of the constraints: it evaluates the prediction of system response against the constraints in order to understand if a control action would bring the system to an unfeasible operating condition.
- Objectives: typically a desired final state should be achieved, in parallel some performance indices should be either maximize or minimize, for example travel time or distance.
- Optimization: a constrained optimization problem is solved in order to calculate the optimal control action which can successfully drive the system to the desired state while satisfying all constraints and achieving the best performance according to the objectives.

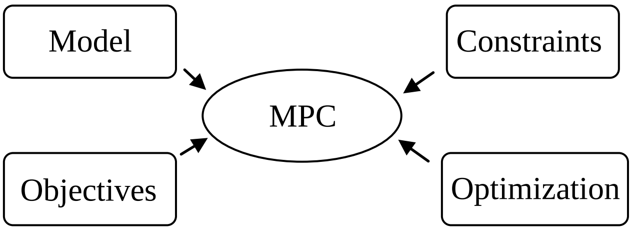

From the example above it is clear that the optimization problem should be solved numerically through a sequence of iterations which tries to diminish the cost function until its global optimum. However an optimization problem has generally many local minima and during the course of the optimization routine the algorithm may stuck in a local minimum without getting to the global optimum of the cost function. A convex optimization problem does not suffer from this drawback since convexity of the cost function assures that just one point of minimum exists thus the algorithm would reach this point provided that it converges successfully. A Quadratic Programming problem where the cost function is a quadratic function of the control variables while the constraints are linear functions of the control variables, is desirable for MPC application since it guarantees convexity of the optimization problem provided that few conditions are satisfied by the cost function and the constraints. There exist a number of efficient algorithms that have been developed to solve specifically quadratic programming problems hence the optimal solution can usually be computed quickly. Therefore the aim is to set up the optimization problem as a QP problem and the four core points should have a proper mathematical formulation. The remaining part of the chapter describes the mathematical procedures that are necessary to compute a suitable MPC-based control strategy for the energy management of a power-split hybrid electric vehicle, the conditions which guarantee the convexity are highlighted.

4.2 Formulation of the MPC strategy

4.2.1 The reference simplified model

The reference model should be simple to reduce the computational effort of the optimization problem but at the same time it should be reliable to guarantee a correct prediction of future responses of the system to input control commands and know external disturbances. In order to develop a state space form which enables the definition of a model based optimal control strategy a forward approach has been applied besides a quasi-static modeling of most of the powertrain components [21]. Forward approach has been used to model the longitudinal motion of the vehicle. According to this approach the actual vehicle speed is compared to the desired vehicle speed and the error is used by a PID controller to generate proper control commands. The PID controller models the driver and the output commands are sent to the components of the powertrain in order to generate the necessary tractive or braking torque to track the reference velocity profile. The driveline output torque is applied to the vehicle and the output of the simulation is the vehicle speed obtained from integration of the vehicle longitudinal dynamics. On the contrary a backward approach would assign the reference velocity profile as input and the equation of the vehicle longitudinal motion is used to calculate the correspondent torques produced by the engine and the electric machines, hence the outcomes of the simulation are the fuel consumption and the battery state of charge.

The forward approach is more realistic and is preferable when a control strategy is designed since it permits to evaluate the stability of the strategy because the commands produced by the driver are not known a priori. Moreover a backward approach assumes that the powertrain can always match instant by instant the desired velocity profile which is not generally true when the torque request exceeds the powertrain limits. Consequently the simple reference model is obtained under the assumption that the driver provides as input the desired torque request in order to track the reference velocity profile while the control strategy provides the control commands to the prime movers to match the torque and power request from the driver. Both the driver and the control strategy are outside the reference model even if the MPC-based control strategy uses this latter model to predict the response of the powertrain to a specific control action. The behavior of the components of the powertrain has been modeled either as quasi-static or as dynamic. In a dynamic approach the behavior of a component is modeled through a differential equation or a set of differential equations; this enables to capture high frequency dynamics of the component. On the other hand a quasi-static approach neglects any dynamics associated to the behavior of a component and the modeling exploits only equilibrium equations.

Eventually the following assumptions have been considered to derive the model:

- the dynamics associated to the rotary motion of the rotor of the generator and the rotor of the motor are much faster compared to the first rotary dynamics of the crankshaft and the response of the vehicle regarding its longitudinal motion. As a result the rotary inertia of the generator and the motor have been neglected.
- the engine block is assumed to be rigidly connected to the carbody meaning that the bushings are neglected and the inertia of the engine block is included in the inertia of the carbody. On the other hand the flywheel is modeled through a rotary inertia.
- the transmission (planetary gear set, final gear ratio and front differential) is assumed to have unitary efficiency.
- the rotary inertia of all components in the transmission is neglected.
- temperature effects are neglected
- the battery is modeled by means of an equivalent electric circuit
- damping, flexibility along the transmission and in the suspension assembly are neglected
- no tyre model is introduced. It is assumed that both the traction torque delivered by the driveline and the braking torque can always be immediately and completely discharged to the ground
- wind velocity and road slope are not considered since their values cannot be known by the MPC controller at this stage
- the rotary inertia of the four wheels is replaced by an equivalent linear inertia which augments the overall vehicle mass in the differential equation which describes the longitudinal motion of the vehicle
- the vehicle dynamics is solely described regarding the longitudinal motion of the vehicle, thus neither bounce nor pitch nor yaw motion is treated by this simplified model. As a consequence the effect of mass transfer on vehicle dynamics is neglected.
- similarly to the previous point the actual braking force distribution between the front and the rear axle is neglected and the total braking torque is assumed to be applied at the driven axle.

- the total braking torque is split between the torque provided by the service braking system and the torque obtained through regenerative braking at the front axle by using the motor as electric generator.
- the four wheels are merged together into a single wheel which combine the overall rotary inertia.
- the longitudinal dynamics of the vehicle is described as the motion of a point mass subjected to resistive forces given by rolling resistance, braking torque and air resistance together with a traction effort produced by the powertrain
- the only available information on driving conditions are represented by the driver's torque request and the vehicle actual longitudinal velocity at the sampling time.

For the energy management problem the dynamics of the battery state of charge is generally the only state variable that is taken into account, however the MPC strategy has been developed in order to address simple issues related to on-board comfort therefore the angular velocity of the crankshaft has been used as second state of the system. This choice comes mainly from [18] and from preliminary observations done besides some simulations carried out with the original rule based strategy. In these simulations it appears that every time the engine is activated or stopped the carbody experiences large oscillations of longitudinal, vertical and pitch accelerations due to a quick variation of generator torque which has the task to adjust the angular velocity of the crankshaft. In order to overcome this issue the rotary inertia of the crankshaft is introduced to define the engine torque and the generator torque as control inputs and thus smooth the action of this latter variable. If the dynamics of the crankshaft were not considered, then the engine and the generator torques would be simply related by an equilibrium equation and it would not be possible to achieve a smooth engine starting and stopping inside the control strategy itself. Considering these assumptions, the powertrain can be modeled using two separate models for the mechanical and the electrical side. These two sides can communicate through the battery power.

Electric side

The pure electric side of the system is represented by the battery. The simplest battery model is an equivalent electric circuit characterized by a total internal resistance and an overall open circuit voltage. The scheme of this circuit is reported in the next figure.

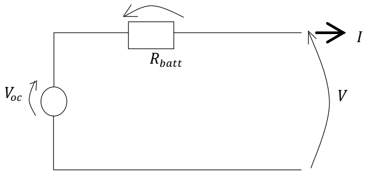

Figure 4.2: Equivalent electric circuit which models the battery

Applying the Kirchhoff's circuit law, the voltage equilibrium produces the following relation:

$$V_{oc} = V + IR_{batt} \tag{4.1}$$

In a battery power is lost due to electric and chemical processes; it is assumed that the equivalent internal resistance collects all these losses. Multiplying the latter equation on both sides by the battery output voltage and rearranging the terms, produces:

$$V^2 - V_{oc}V + R_{batt}P_{batt} = 0 \tag{4.2}$$

$$V = \frac{V_{oc}}{2} \pm \frac{1}{2}\sqrt{V_{oc}^2 - 4P_{batt}R_{batt}} \tag{4.3}$$

The only feasible solution is the one with sign "+" because when electric current does not flow in the circuit the output voltage equates the open circuit voltage.

By replacing this latter equation into the definition of the battery output current and by transforming the denominator using the rationalization formula, it results:

$$\begin{aligned} I = \frac{P_{batt}}{V} &= \frac{2P_{batt}}{V_{oc} + \sqrt{V_{oc}^2 - 4P_{batt}R_{batt}}} \\ &= \frac{2P_{batt}\left(V_{oc} - \sqrt{V_{oc}^2 - 4P_{batt}R_{batt}}\right)}{V_{oc}^2 - (V_{oc}^2 - 4P_{batt}R_{batt})} \\ &= \frac{V_{oc} - \sqrt{V_{oc}^2 - 4P_{batt}R_{batt}}}{2R_{batt}} \end{aligned} \tag{4.4}$$

The time derivative of the battery state of charge is defined as the ratio of the battery output current over the battery rated capacity, where positive current indicates that the battery is discharging power:

$$\frac{dSOC}{dt} = -\frac{I}{Q_{batt}} = -\frac{V_{oc} - \sqrt{V_{oc}^2 - 4P_{batt}R_{batt}}}{2Q_{batt}R_{batt}} \tag{4.5}$$

As a result the time derivative of the battery state of charge depends on the electric load acting on the battery, this load is defined by the battery power which corresponds to the summation of the power associated to the generator, motor and power losses inside these machines as follows.

$$\begin{aligned} P_{batt} &= P_m + P_g + P_m^{loss} + P_g^{loss} \\ &= T_m\omega_m + T_g\omega_g + f(T_m, \omega_m) + f\big(T_g, \omega_g\big) \end{aligned} \tag{4.6}$$

Power losses are always positive while electric power associated to the operating points of the machines can assume both positive and negative values as a consequence the electric machines can either draw of provide power to the battery. Since the electric machines contribute to produce the tractive force they are included in the mechanical side of the powertrain and thus the battery power is the variable which connects the two sides of the powertrain.

Mechanical side

The mechanical part of the powertrain can be represented according to the scheme reported here below.

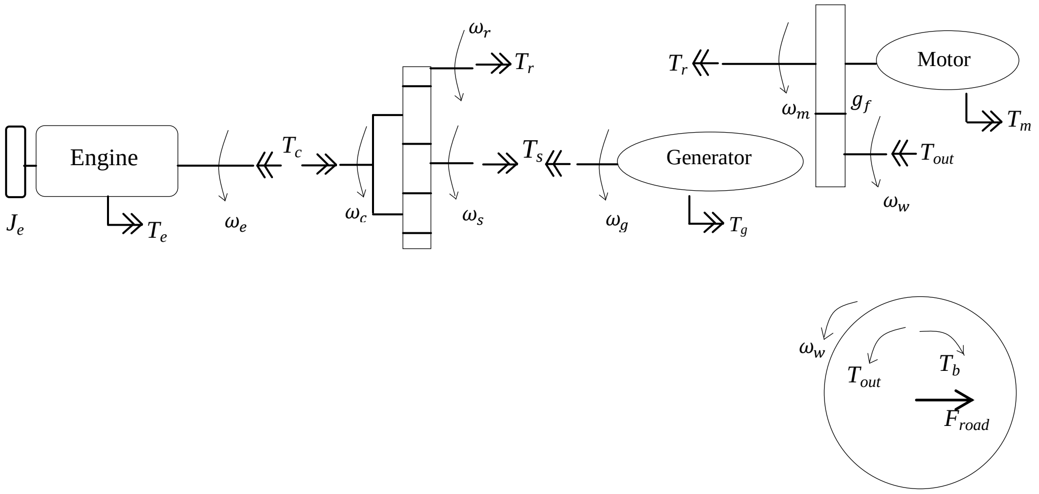
ω_r
T_r
T_r
Motor
ω_m
g_f
T_m
Engine
T_c
T_s
Generator
T_{out}
ω_w
J_e
T_e
ω_e
ω_c
ω_s
ω_g
T_g
ω_w
T_{out}
T_b
F_{road}

Figure 4.3: Simplified scheme of the mechanical side of the powertrain

According to the sign convention both engine and generator and motor act as prime movers. It is stressed here that the braking torque T_b only represents the braking torque provided by the service braking system and it does not take into account the braking torque obtained from regenerative braking. Considering the mechanical connections represented in Figure 4.3, the dynamics of the crankshaft, the generator rotor and the ring gear are described as follows.

$$\begin{cases} J_e \dot{\omega}_e = T_e - T_c \\ T_g - T_s = 0 \\ T_m - T_r - \dfrac{T_{out}}{g_f} = 0 \\ \omega_e = \omega_c \\ \omega_g = \omega_s \\ \omega_m = \omega_r \\ \omega_m = g_f \omega_w \end{cases} \tag{4.7}$$

Subsequently by neglecting any rotary inertia and friction loss inside the power split drive, by combining the governing equations (3.4) with equations (4.7) the following relations are determined.

$$\begin{cases} \omega_g = \left(\dfrac{Z_r}{Z_s} + 1\right)\omega_e - \dfrac{Z_r}{Z_s}\omega_m \\ T_c = -\dfrac{Z_s + Z_r}{Z_s} T_g \\ T_r = \dfrac{Z_r}{Z_s} T_g \\ J_e \dot{\omega}_e = T_e + \dfrac{Z_s + Z_r}{Z_s} T_g \\ T_{out} = g_f \left(T_m - \dfrac{Z_r}{Z_s} T_g\right) \end{cases} \tag{4.8}$$

Applying the longitudinal force equilibrium at the driven wheels, the governing differential equation of the vehicle longitudinal motion can be written as follows:

$$\left(m_v + m_j^w\right)\ddot{x} = \frac{T_{out} - T_b}{r_w} - \frac{1}{2}\rho C_x A(\dot{x})^2 - f_r m_v g \tag{4.9}$$

An important assumption is introduced at this point regarding the torque equilibrium along the driveline. The driveline is assumed to be able to satisfy the torque required by the driver meaning that the torque delivered by the driveline equates the torque required by the driver. As a result the torque required by the driver is treated as an external disturbance which is known at the sampling time and thus the vehicle velocity can be integrated using equation (4.9) once the driveline output torque and the braking torque are replaced by the torque required by the driver as follows.

$$T_{driver} = T_{out} - T_b \tag{4.10}$$

The driver's desired torque and the vehicle longitudinal velocity represent the known external disturbances applied to the system and they can be introduced in equations (4.8) as known variables so that the generator angular velocity, the motor angular velocity and the motor torque can be expressed as follows:

$$\begin{cases} \omega_g = \left(\dfrac{Z_r}{Z_s}+1\right)\omega_e - \dfrac{Z_r}{Z_s}\dfrac{g_f}{r_w}\dot{x} \\[2ex] \omega_m = \dfrac{g_f}{r_w}\dot{x} \\[2ex] T_m = \dfrac{T_{driver}}{g_f} + \dfrac{T_b}{g_f} + T_g\dfrac{Z_r}{Z_s} \end{cases} \tag{4.11}$$

If the battery state of charge and the crankshaft angular velocity represent the states of the system, the engine torque, the generator torque and the total braking torque provided by the service braking system represent the control inputs then the following nonlinear state space form can be defined:

$$\begin{cases} S\dot{O}C = -\dfrac{V_{oc} - \sqrt{(V_{oc})^2 - 4P_{batt}R_{batt}}}{2Q_{batt}R_{batt}} = f_1(x,u,v) \\[2ex] \dot{\omega}_e = \dfrac{T_e + \dfrac{Z_s+Z_r}{Z_s}T_g}{J_e} = f_2(x,u,v) \\[2ex] y = \begin{Bmatrix} SOC \\ \dot{m}_f \\ \omega_g \\ T_m \\ \omega_m \\ P_{batt} \\ \omega_e \end{Bmatrix} = g(x,u,v) \end{cases} \tag{4.12}$$

where:

$$x = \begin{Bmatrix} SOC \\ \omega_e \end{Bmatrix} \quad u = \begin{Bmatrix} T_e \\ T_g \\ T_b \end{Bmatrix} \quad v = \begin{Bmatrix} T_{driver} \\ \dot{x} \end{Bmatrix}$$

The nonlinear state space form in (4.12) provides the description of the time derivatives of the states as function of system states themselves, control inputs and external measured disturbances; however up to this point some variables are related to x, u, v by means of look-up tables.

For example the fuel mass flow rate $\dot{m}_f$ in the output equations is described by a Multi 1D table as function of engine speed and torque, similarly the power loss inside an electric machines is described by a look-up table as function of the operating point of the machine as described in Chapter 3.3.3. In order to overcome this issue each look-up table has been replaced by a regression model because the control strategy can handle a continuous mathematical function better than a look-up table. Four regression surfaces have been obtained to describe respectively fuel mass flow rate, power losses in the electric machines, battery open circuit voltage and internal resistance of a single cell. The post processing of the experimental data and the mathematical procedure that has been followed to compute the regression models is reported below.

Fuel mass flow rate

The available data have been modified due to the fact that:

- 11 curves are provided where each curve reports the fuel mass flow rate as function of a set of values of engine torque and for a specific value of crankshaft angular velocity. 11 different angular velocities have been tested. A problem is represented by the fact that each curve has been obtained for a different number of engine torque samples; moreover the engine torque values that have been tested are different from test to test. While a single vector of angular velocity values is available, there are 11 available vectors of engine torque levels. Therefore a new grid of experimental values of engine speed and torque has been defined starting from the available data.
- Fuel consumption is not given for null and negative values of engine torque
- Torque is expressed as break mean equivalent pressure BMEP [bar] and fuel consumption as g/kWh.

Engine torque can be expressed in [Nm] using the following definition of the BMEP:

$$T = \frac{100 * engineVolume * BMEP}{4\pi} \tag{4.13}$$

where T indicates the engine torque in Nm.

Fuel consumption can be expressed in [g/s] by multiplying the value in g/kWh times the power produced by the engine at a correspondent operating point on a curve:

$$g/_{s} = g/_{kWh} \cdot kW \cdot 1\, h/_{3600\ s} \tag{4.14}$$

After these preliminary transformations the input data have to be manipulated in order to create a grid of couples (ω_e, T_e) which allows the numerical regression to be computed. The grid defines a new domain of values of engine speed and torque for which new correspondent values of fuel mass flow rate are obtained.

Nevertheless since these latter new values have to be calculated from the original ones via numerical interpolation and extrapolation it is advisable to limit the grid within a domain where quite a lot of input values are already available. Among the 11 curves, the one which corresponds to the highest tested value of engine speed is just defined over 7 values of engine torque. This latter number represents the smallest set of engine torque levels among the curves. As a result the grid is limited to the first 7 values of engine torque for each curve. A single vector of levels of engine torque is then created and, together with the original vector of engine speed values, is used to create the grid. The aim is to compute the fuel consumption over the couples (ω_e, T_e) defined by the new vectors of engine torque and speed. In order to clarify the procedure the next figure reports in blue circles the original couples (ω_e, T_e) that have been used to obtain the experimental data of fuel consumption while the red circles represent the new couples.

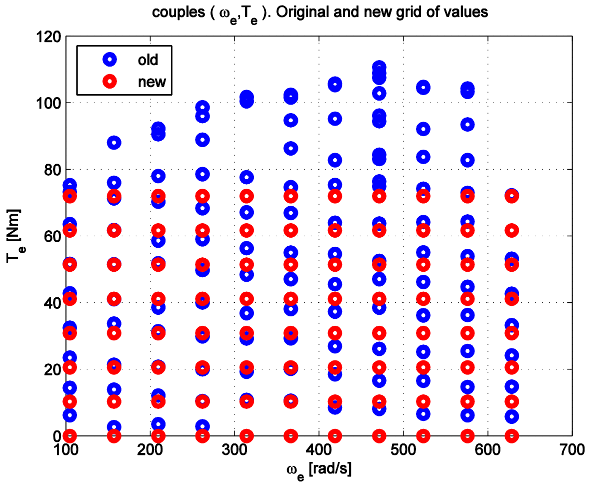

Figure 4.4: Original (blue) and new (red) grid of values of engine torque and speed.

The new vector of engine torque values has actually 8 components where the first one is equal to 0 Nm while the maximum one corresponds to the maximum torque applied among the 11 curves over the first 7 levels of engine torque. The other 6 components are defined in a regular pattern. By prescribing a minimum torque equal to 0 Nm, it is possible to extrapolate the fuel consumption when the engine torque is null.

The new values of fuel consumption have been obtained by interpolation and extrapolation of the original values over the new values of engine torque for each given experimental curve. In order to obtain good results, spline functions have been used for both interpolation and extrapolation. Regarding extrapolation of fuel consumption at null engine torque, spline functions have been used but only the first 4 points of each curve have been considered. This is because a better trend can be obtained close to the null torque when fewer points are considered. The next two figures summarize these steps; Figure 4.5 represents the 11 experimental curves that are provided whereas Figure 4.6 reports an example of interpolation and extrapolation of fuel consumption values over the new values of engine torque and for curve number 8. The blue circles represent the original values while the red circles the new ones. In this latter figure fuel consumption for null torque is still equal to $0\,g/s$; this is because the extrapolation to determine fuel consumption for null engine torque is carried out afterwards.

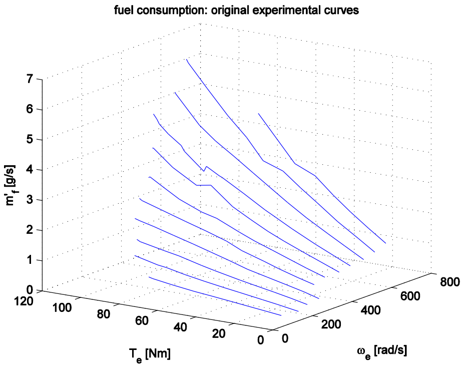

Figure 4.5: 11 Experimental curves which represent fuel mass flow rate as function of engine speed and engine torque.

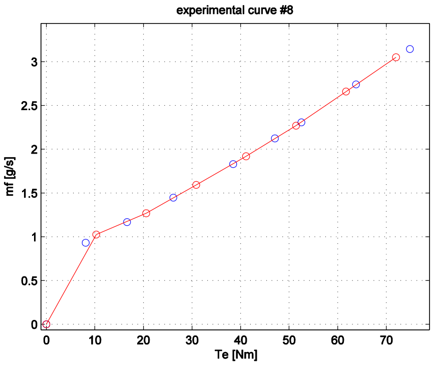

Figure 4.6: An example of interpolation of fuel consumption over the new set of engine torque values for curve number 8.

An analysis of the regression surface obtained after some preliminary trails has shown how assuming a small but not null fuel consumption value for null engine torque improves a lot the quality of the regression over the whole domain (ω_e, T_e). Consequently spline functions extrapolate this value for each curve.

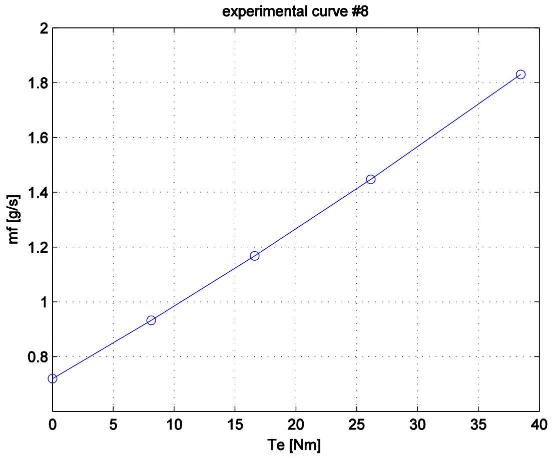

Figure 4.7: Extrapolation to calculate the new value of fuel consumption for a null value of engine torque.

The resulting value is 0.7 g/s which is not negligible but anyway this procedure enables a good fitting of the experimental data over the whole grid. The fuel mass flow rate obtained for the first curve $(\omega_e = 0\,rad/s)$ at the null value of the engine torque is equal to $0\,g/s$. The new domain of values for (ω_e, T_e) and the correspondent resulting observations for $\dot{m}_f$ are hence available and the next figure represents a surface, which connects the new values of $\dot{m}_f$, superimposes to the 11 original curves. This surface is used for the sake of visualization of the dependence of fuel mass flow rate on the engine speed and torque.

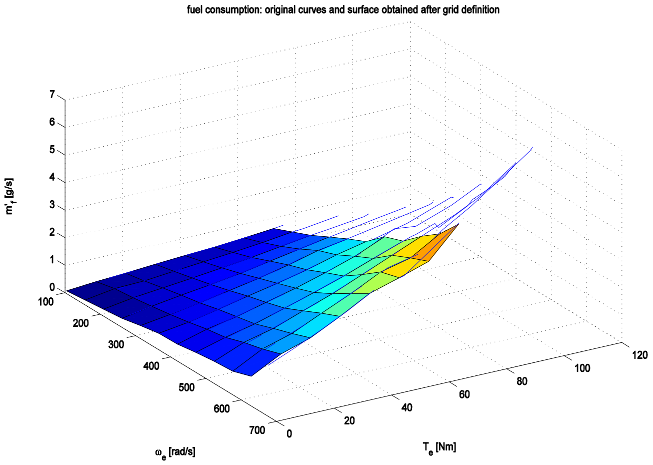

Figure 4.8: The new values of $\dot{m}_f$ are connected to one another by a surface for a better visualization and the surface is superimposed to the original curves.

This surface suggests that fuel flow rate can be related to engine speed through a quadratic function while a higher order relation may explain fuel mass flow rate with respect to engine torque. Regression analysis reveals that the following polynomial expression fits well the new observed values; T_e in [Nm],ω_e in [rad/s] while $\dot{m}_f$ in [g/s]:

$$\begin{aligned}\dot{m}_f = p_1 + p_2\omega_e + p_3T_e + p_4\omega_e^2 + p_5\omega_eT_e + p_6T_e^2 + p_7\omega_e^2T_e \\ + p_8\omega_eT_e^2 + p_9T_e^3\end{aligned} \tag{4.15}$$

In order to assess the quality of the regression model the surface has been extended to those points which lie outside the considered domain, namely for engine torque values higher than 72 Nm, and then it has been compared to those few experimental values that are available at these higher torque levels.
The next figure reports a visual comparison.

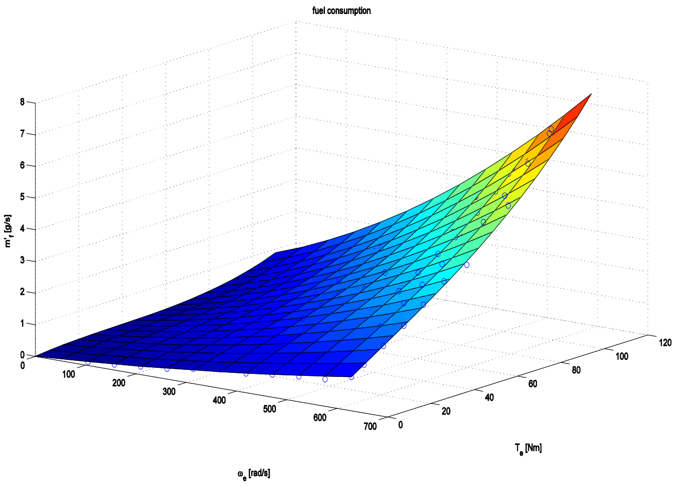

Figure 4.9: Polynomial regression model of fuel flow rate over the entire operating domain of the engine.

The surface fits the experimental data reasonably well even outside the domain used to derive the regression model, thus a new set of regressors has been calculated using an algorithm for global optimization and extending the minimization of the sum of the quadratic residuals over the entire domain defined by the original couples (ω_e, T_e). The regression is poorer when both engine speed and torque assume high values. In this area the surface overestimates the consumption, anyway a higher estimate is conservative so no further changes have been introduced in the regression model of the surface. The final values of the parameters are reported below.

Table 4.1: Regression coefficients of the polynomial regression model for fuel flow rate.

Parameter	Value
p_1	$7.275\ e-3$
p_2	$9.843\ e-4$
p_3	$8.277\ e-3$
p_4	$1.148\ e-6$
p_5	$1.979\ e-5$
p_6	$-1.820\ e-4$
p_7	$6.222\ e-8$
p_8	$2.067\ e-7$
p_9	$1.610\ e-6$

The statistical analysis of the quality of the regression model is meaningful for the latest surface that is determined over the entire domain (ω_e, T_e) since in the region of high power the error is large.

- **Power losses in the electric machines**

Motor and generator are represented by the same machine so just one regression model is necessary; furthermore the data are already given in a way which suits the regression analysis so no further action is needed. Power loss is expressed as function of rotor angular velocity and torque produced at shaft.

A polynomial expression can fit the data reasonably well, where T in [Nm],ω in [rad/s] while P^{loss} in [W].

$$P_m^{loss} = P_g^{loss} = 2.3477\ \omega + 0.00182\ T^2\omega - 4.87^{-8}\ T^4\omega \tag{4.16}$$

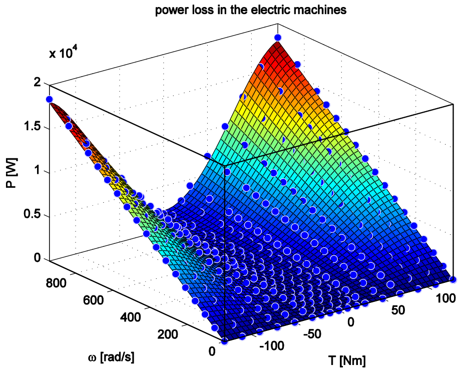

Figure 4.10: Regression surface of power loss in the electric machines.

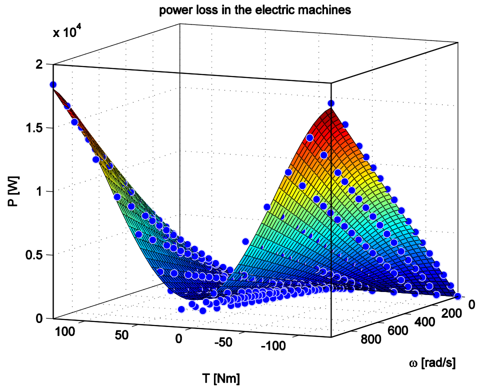

Figure 4.11: Rgression surface of power loss in the electric machines. Second view.

The quality of the regression is poor in the area defined by values of the torque in-between $-25\,Nm \leq T \leq 25Nm$ where power loss is overestimated with respect to the experimental values. This is caused by the fact that Amesim® models the power loss according to static friction and therefore the power loss follows a piecewise linear trend in this area that is difficult to capture with a continuous regression model. There is also an area defined by values of the torque between $\pm 40\,Nm \leq T \leq \pm 70Nm$ where the losses are underestimated. The next figure illustrates these problems for a specific value of the rotor angular velocity.

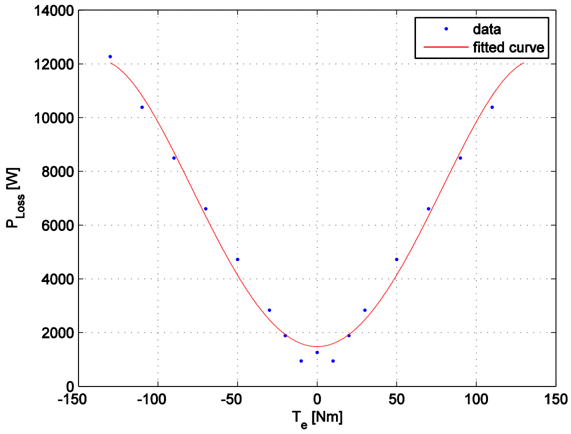

Figure 4.12: Experimental values of power loss (blue circles) and regression model (red curve). Discrepancies between the experimental values and the estimated values using the regression model.

As some simulations show, these differences are not negligible and leads to discrepancies in the results obtained with Matlab and Amesim® as it will be discussed afterwards. However for the sake of MPC implementation according to a receding horizon strategy they can be tolerated. Another problem which some simulations have shown is the fact that this surface is defined only for positive values of angular speed. However the operating point of an electric machine can fall in any of the 4 quadrants therefore the rotor angular velocity can also assume negative values. This problem is easily solved in the nonlinear system by considering the absolute value of the speed when power losses are calculated, however it does create problems in the linearized model as it is explained later on. Lastly the experimental data are limited to a maximum absolute value of the torque equal to $150\,Nm$ consequently none information is available for higher values of the torque even if the electric machines can provide much higher torque levels. The regression model estimates an increasing power loss until almost $180\,Nm$ then the surface decreases. This trend is not coherent with a real application where losses are expected to increase with the torque produced however since no additional information is available no further change has been applied to the regression surface.

Battery internal resistance and open circuit voltage

As illustrated in chapter 3 the cell internal resistance and the cell open circuit voltage are provided as function of the battery internal temperature and the state of discharge. However the dependence on the temperature can be neglected because throughout the analysis the temperature does not change; moreover for a temperature higher than 50 °C the dependency of these two variables on temperature becomes weak and curves tend to follow a plateau. The temperature of the battery is set equal to 80 °C so these variables are expressed only as function of the state of discharge using the values reported for 50 °C which represent the maximum tested temperature. A third order polynomial fits very well the experimental data of the cell internal resistance.

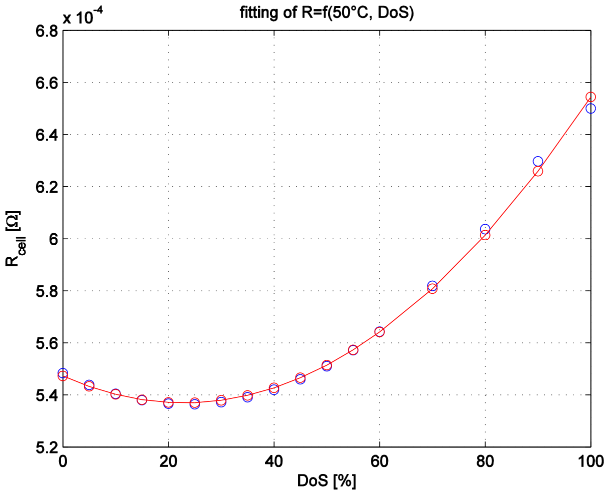

Figure 4.13: Cell internal resistance. Experimental data (blue circles) and correspondent data obtained from the regression model (red circles).

The regression model requires SoD in [%] and returns R_{cell} in [Ω]:

$$R_{cell} = 1.977e-08 * SoD\text{^}2 \;-\; 9.056e-07 * SoD \;+\; 5.47e-04 \quad (4.17)$$

On the other hand since the level of the battery open circuit voltage has a remarkable importance on the dynamics of the battery state of charge and its precise value is measurable from the Amesim® model, a correspondent regression model has not been formulated. This means that when the reference model is used by the MPC strategy to predict the variation of the battery state of charge over the prediction horizon, the open circuit voltage is kept constant to the value measured at the sampling time.

Similarly once the battery internal resistance is calculated at the sampling time, its value is kept constant over the whole prediction horizon. On the opposite the regression models for fuel mass flow rate and power losses are used to dynamically predict the correspondent quantities over the prediction horizon.

Consequently by assuming constant values for R_{batt} and V_{oc} and by substituting equations (4.11) into the analytical expression of the regression surfaces (4.15), (4.16) it is possible to express these latter models as functions of system states, control inputs and external disturbances, hence the nonlinear state space form can be represented by continuous analytical functions.

4.2.2 The operating constraints

A number of constraints prevent the powertrain from assuming any possible operating condition and they should be taken into account by the control strategy in order to define a set of control inputs which are feasible for the powertrain. The list of operating constraints that have been included in the control strategy is reported below.

Outputs:

$$\begin{gathered} SOC_{min} \leq SOC \leq SOC^{max} \\ \omega_g^{min} \leq \omega_g \leq \omega_g^{max} \\ T_m \leq f(V, \omega_m) \\ \omega_m^{min} \leq \omega_g \leq \omega_m^{max} \\ P_{batt}^{min} \leq P_{batt} \leq P_{batt}^{max} \\ \omega_e^{min} \leq \omega_e \leq \omega_e^{max} \end{gathered} \tag{4.18}$$

***Control inputs*:**

$$\begin{gathered} T_e \leq f(\omega_e) \\ T_g \leq f(V, \omega_g) \\ T_b^{min} \leq T_b \leq T_b^{max} \end{gathered} \tag{4.19}$$

The constraints on engine, generator and motor torque are defined by the Amesim® model through look-up tables. For instance the maximum torque that the electric machines can provide is function of the input voltage and the angular velocity of the rotor and the torque values are provided for a finite set of couples (V, ω).

Since the constraints should be formulated as linear inequalities in order to set up the optimization problem as a Quadratic Programming problem and the algorithm should be able to handle them easily, then these look-up tables should be replaced by continuous mathematical functions. Consequently three polynomial regression models have been used to describe some of the constraints as well and the approach that has been applied to the characteristic curves of the engine and the electric machines is reported here below.

Characteristic curve of the engine

The next figure illustrates the experimental data of maximum and minimum torque that the engine can provide as function of the crankshaft angular velocity with blue circles and the lines that have been used to translate these two curves into linear inequalities.

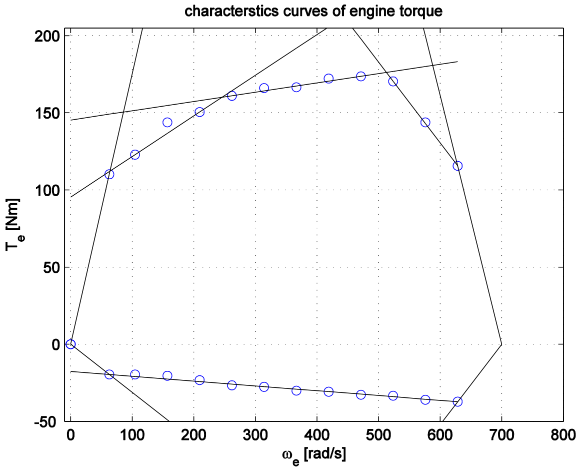

Figure 4.14: Characteristic curves of the engine and correspondent simplification with lines.

For each value of the crankshaft angular velocity, a correspondent engine torque is calculated for each line and the maximum and minimum torque levels that the engine can provide are defined respectively as the lowest one among the positive values and the highest one among the negative values. As Figure 4.14 shows, the description of the engine characteristic curves given by the straight lines is good.

The linear inequalities are thus written according to this form.

$$\begin{array}{rl}
m_5\omega_e \leq T_e(k+i) & \text{for } 0\,rad/s \leq \omega_e \leq 62.83\,rad/s \\
m_6\omega_e + q_6 \leq T_e(k+i) & \text{for } 62.83\,rad/s \leq \omega_e \leq 628.3\,rad/s \\
m_7\omega_e + q_7 \leq T_e(k+i) & \text{for } 628.3rad/s \leq \omega_e \leq 700\,rad/s \\
T_e(k+i) \leq m_8\omega_e & \text{for } 0\,rad/s \leq \omega_e \leq 62.83\,rad/s \\
T_e(k+i) \leq m_9\omega_e + q_9 & \text{for } 62.83rad/s \leq \omega_e \leq 246\,rad/s \\
T_e(k+i) \leq m_{10}\omega_e + q_{10} & \text{for } 246\,rad/s \leq \omega_e \leq 513rad/s \\
T_e(k+i) \leq m_{11}\omega_e + q_{11} & \text{for } 513\,rad/s \leq \omega_e \leq 628.3\,rad/s \\
T_e(k+i) \leq m_{12}\omega_e + q_{12} & \text{for } 628.3rad/s \leq \omega_e \leq 700\,rad/s
\end{array} \tag{4.20}$$

The experimental data do not specify the maximum value of the angular velocity of the crankshaft therefore the lines defined by the parameters m_7, q_7 and m_{12}, q_{12} are used to enclose the operating domain of the engine and to set the maximum value of the angular velocity of the crankshaft to 700 rad/s. This value is chosen considering that the performance of the engine drops significantly once the range of maximum power release is overcome. The values of the coefficients are:

Table 4.2: Coefficients used to define the linear constraints of the engine characteristic curves.

Coefficient	Value		Coefficient	Value
m_5	-0.3119			
m_6	-0.03119		q_6	-17.64
m_7	0.5195		q_7	-363.7
m_8	1.753			
m_9	0.2634		q_9	95.34
m_{10}	0.0602		q_{10}	145.3
m_{11}	-0.5227		q_{11}	444.1
m_{12}	-1.613		q_{12}	1129

Characteristic curve of the electric machines

Figure 3.14 highlights the dependence of the torque produced by an electric machine on the rotor angular velocity and on the input voltage. The experimental data refer to test cases where the maximum input voltage was set equal to 150 V but throughout the analysis the input voltage produced by the battery has always been much higher. The battery produces a nominal output voltage of 271V at a state of charge of the battery equal to 60% and this value is always much higher than 150 V during the whole driving mission. Consequently the dependence on the input voltage can be neglected and the linear constraints can be derived just considering the values defined as function of the rotor angular velocity for an input voltage of 150 V. The following figure represents the points that have been considered to derive the linear constraints; the lines which connect two subsequent blue circles are added just for the sake of visualization.

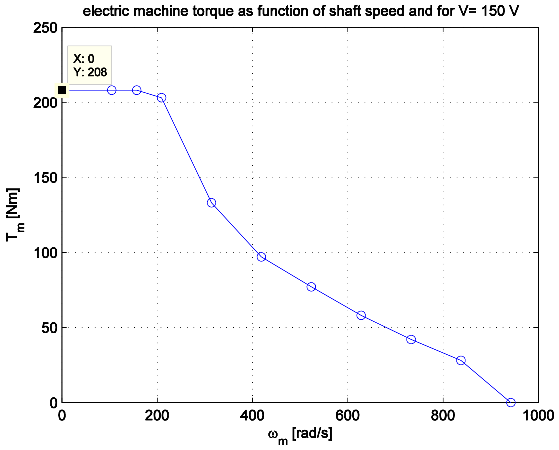

Figure 4.15: Characteristic curve of the electric machines.

The electric generator can operate in any of the four quadrants while it is assumed that the angular velocity of the motor can only be positive.

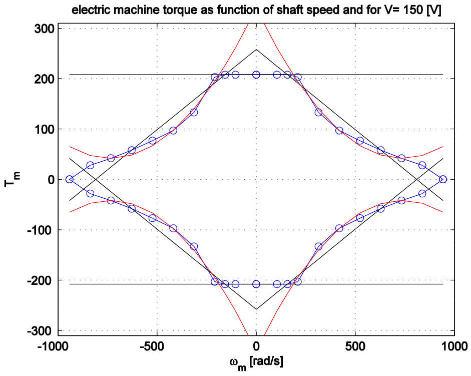

Figure 4.16: Complete operating domain of the electric machines.

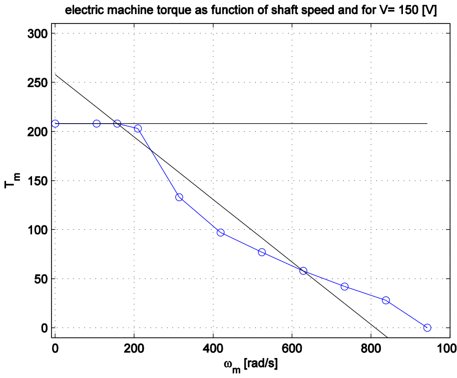

Figure 4.17: Example of linearization of the characteristic curve of the electric machines.

Figure 4.16 reports also two different ways to define the constraints, either as linear (black lines) or quadratic (red curves) constraints. Quadratic constraints enable a much better representation of the torque limit however the optimization problem would lose its convexity due to the curvature of the curve, therefore linear constraints are preferable. Figure 4.17 shows instead a problem that has to be accepted once linear constraints are defined. The straight line which replaces the characteristic curve in the area of constant power release either underestimates or overestimates the actual capabilities of the machine. Moreover the maximum angular velocity of the rotor that is defined by this line is lower than the actual capability of the machine. Considering the linear constraints and their application to the entire operating domain of the machine the following linear inequalities can be defined.

$$\begin{array}{cl}
T_g \le 208\,Nm & \text{for } -157.1\,rad/s \le \omega_g \le 157.1\,rad/s \\
-208\,Nm \le T_g & \text{for } -157.1\,rad/s \le \omega_g \le 157.1\,rad/s \\
m_1\omega_g + q_1 \le T_g & \text{for } 157.1\,rad/s \le \omega_g \le 810\,rad/s \\
m_2\omega_g + q_2 \le T_g & \text{for } -151.7\,rad/s \le \omega_m \le -810\,rad/s \\
T_g \le m_3\omega_g + q_3 & \text{for } 151.7\,rad/s \le \omega_m \le 810\,rad/s \\
T_g \le m_4\omega_g + q_4 & \text{for } -151.7\,rad/s \le \omega_m \le -810\,rad/s \\
T_m \le 208\,Nm & \text{for } -151.7\,rad/s \le \omega_m \le 151.7rad/s \\
-208\,Nm \le T_m & \text{for } -151.7\,rad/s \le \omega_m \le 151.7rad/s \\
T_m \le m_0\omega_m + q_0 & \text{for } 151.7\,rad/s \le \omega_m \le 810\,rad/s \\
-m_0\omega_m - q_0 \le T_m & \text{for } 151.7\,rad/s \le \omega_m \le 810\,rad/s
\end{array} \tag{4.21}$$

The values of the coefficients are reported here below:

Table 4.3: Coefficients used to define the linear constraints of the electric machines on maximum torque.

Coefficient	Value		Coefficient	Value
$m_0 = m_2 = m_3$	-0.3183		$q_0 = q_3 = q_4$	258.01
$m_1 = m_4$	0.3183		$q_1 = q_2$	-258.01

From the linear inequalities, the upper and lower angular velocities of the crankshaft, generator and motor can be calculated.

$$\begin{gathered} 0\,{}^{rad}\!/_{s} \leq \omega_e \leq 700\ {}^{rad}\!/_{s} \\ -810\,{}^{rad}\!/_{s} \leq \omega_m \leq 810\ {}^{rad}\!/_{s} \\ -810\,{}^{rad}\!/_{s} \leq \omega_g \leq 810\ {}^{rad}\!/_{s} \end{gathered} \tag{4.22}$$

The constraints on maximum and minimum level of the battery state of charge have been defined according to the indications reported in [22] and they correspond to:

- $SOC_{min} = 40\%$
- $SOC^{max} = 80\%$

The battery can either release or absorb the maximum power when the output voltage is null; according to the scheme of the equivalent electric circuit represented in fig. XX this battery output power can be written as follows:

$$P_{batt}^{max} = VI = \frac{VV_{oc} - V^2}{R_{batt}} \tag{4.23}$$

This function of battery output voltage has a point of maximum for:

$$V = \frac{V_{oc}}{2} \tag{4.24}$$

Which corresponds to the maximum battery power in absolute value equal to:

$$|P_{batt}^{max}| = |P_{batt}^{min}| = \frac{V_{oc}^2}{4R_{batt}} \tag{4.25}$$

This limit changes according to the state of charge since both the battery open circuit voltage and the battery internal resistance depend on the state of discharge of the battery.

4.2.3 The cost function

The energy management of a hybrid electric vehicle is usually characterized by numerous objectives which are usually in contrast with one another. The main targets of the MPC control strategy are the reduction of total fuel consumption and charge sustenance of the hybrid electric vehicle.

Consequently these two performance indices are included in the cost function by means of two quadratic terms which represent the instantaneous fuel mass flow rate and the deviation of the battery state of charge with respect to its reference value. The reference value is 60% and it has been selected according to the suggestion given in [22]; this value is kept constant throughout the driving mission for any drive cycle. The cost function includes other terms that stabilize the control action like the penalty weights on the levels and variations of the control inputs.

$$\begin{aligned} J(U) = \sum_{i=1}^{H_p-1} \Big[&(SOC(k+i) - SOC^{ref})^2_{w_{SOC}} + \left(\dot{m}_f(k+i)\right)^2_{w_{\dot{m}_f}} \\ &+ \left(\omega_g(k+i) - \omega_g^{ref}\right)^2_{w_{\omega_g}} + \left(\omega_e(k+i)\right)^2_{w_{\omega_e}} \Big] \\ &+ \sum_{i=0}^{H_c-1} \left[\left(u(k+i)\right)^2_{w_u} + \left(\Delta u(k+i)\right)^2_{w_{\Delta u}} \right] \end{aligned} \tag{4.26}$$

The second power of each term appear in the cost function in order to define a quadratic objective and thus retain the standard formulation of a quadratic programming problem.

4.2.4 The linearized state space form

A MPC based control strategy can even exploit a nonlinear reference model to predict system outputs and calculate an optimal control action. In this case the approach is called Nonlinear MPC (NLMPC) and it requires generally a high computational effort and some doubt that a NLMPC can be practically implemented as control strategy for the energy management [14]. For this reason a linear time varying model predictive control strategy (LTV-MPC) has been developed in this thesis. A LTV-MPC follows the standard approach reported in the reference literature [23] where a discretized linear state space form is used as reference model to develop an optimal control strategy. From the nonlinear state space form a linearized state space form is obtained as a truncated Taylor series around a specific operating condition. At each sampling time the values of the states, control inputs, measured disturbances are sampled and stored in the correspondent vectors X_o, U_o, V_o. The small variations about the linearization point of these vectors can be approximated through linear functions according to a Taylor series which is truncated at the linear terms. Then the system is discretized applying Euler forward with a constant discretization period. The partial derivatives of the state and output equations are evaluated at the linearization point and the final outcome is a set of matrices which relates the system outputs and the time derivatives of the states to the variations of the states themselves, the control inputs and the external measured disturbances.

$$\begin{cases} \dot{x}(x_o+\delta x, u_o+\delta u, v_o+\delta v) \approx \\ f(x_o,u_o,v_o) + \left.\dfrac{\partial f(x,u,v)}{\partial x}\right|_o (x-x_o) + \left.\dfrac{\partial f(x,u,v)}{\partial u}\right|_o (u-u_o) + \left.\dfrac{\partial f(x,u,v)}{\partial v}\right|_o (v-v_o) \\ \\ y(x_o+\delta x, u_o+\delta u, v_o+\delta v) \approx \\ g(x_o,u_o,v_o) + \left.\dfrac{\partial g(x,u,v)}{\partial x}\right|_o (x-x_o) + \left.\dfrac{\partial g(x,u,v)}{\partial u}\right|_o (u-u_o) + \left.\dfrac{\partial g(x,u,v)}{\partial v}\right|_o (v-v_o) \end{cases}$$

The system can be written in matrix form as follows:

$$\begin{cases} \dot{x} \approx f(x_o,u_o,v_o) + A(x-x_o) + B_u(u-u_o) + B_v(v-v_o) \\ y \approx g(x_o,u_o,v_o) + C(x-x_o) + D_u(u-u_o) + D_v(v-v_o) \end{cases} \tag{4.27}$$

with a further substitution, it can be simplified to:

$$\begin{cases} \dot{x} \approx F + Ax + B_u u + B_v v \\ y \approx G + Cx + D_u u + D_v v \end{cases} \tag{4.28}$$

where:

$$A = \left.\frac{\partial f}{\partial x}\right|_0 \quad B_u = \left.\frac{\partial f}{\partial u}\right|_0 \quad B_v = \left.\frac{\partial f}{\partial v}\right|_0 \quad C = \left.\frac{\partial g}{\partial x}\right|_0 \quad D_u = \left.\frac{\partial g}{\partial u}\right|_0 \quad D_v = \left.\frac{\partial g}{\partial v}\right|_0$$

$$F = f(x_o,u_o,v_o) - Ax_o - B_u u_o - B_v v_o$$

$$G = g(x_o,u_o,v_o) - Ax_o - B_u u_o - B_v v_o$$

Euler forward is applied to discretize the linearized state space form. According to this approach a continuous time derivative evaluated at time *t* is approximated by a forward finite difference as follows:

$$\dot{x}(t) \approx \frac{x(t+\delta) - x(t)}{\delta} \tag{4.29}$$

Suppose that the independent variable t can only assume discrete levels t_k with $k = 0, \dots, N-1$, then the variation δ is finite. Consider now that the variation δ corresponds to the discretization period T_s, thus the linearized state space form can be discretized as follows:

$$\begin{cases} x(k+1) = (I + AT_s)x(k) + T_sB_uu(k) + T_sB_vv(k) + T_sF \\ \qquad y(k) = Cx(k) + D_uu(k) + D_vv(k) + G \end{cases} \tag{4.30}$$

By rearranging the terms in (4.30) the following final matrix formulation is found:

$$\begin{cases} x(k+1) = A_dx(k) + B^u{}_du(k) + B^v{}_dv(k) + F_d \\ \quad y(k) = C_dx(k) + D_{d_u}u(k) + D_{d_v}v(k) + g \end{cases} \tag{4.31}$$

where the pedix d stands for discrete. The matrices which appear in the output equations are actually equal to those of the continuous linearized state space form since the discretization only introduces some changes in the discrete time derivatives of the state equations. The discrete state space form (4.31) represents the basis of the MPC approach. The approach takes the title “time varying” since at each sampling time the new available information on system states, control inputs and measured disturbances are used to compute the new matrices of the linearized system. In Appendix A it is described how this state space form is used to predict the sequence of system outputs, to build the matrix form of the constraints and the matrix form of the cost function in order to set up the optimization problem. As previously remarked the regression model of the generator power loss introduces a problem to calculate the partial derivatives since the angular velocity of the rotor appears with the absolute value. In practice even the linearized state space form contains still a nonlinear term given by the derivative of the absolute value of the angular velocity of the rotor of the generator. In order to solve this issue and retain a linear formulation of the partial derivatives of the generator power loss, two different expressions of the matrices of the linearized state space form have been defined. In particular the sign of the coefficients of the regression model is changed according to the sign of the generator angular velocity; in this way the components of the matrices have two possible expressions. The sign of the generator angular velocity is determined at the sampling time through equations (4.11) and it is assumed that it does not change over the prediction horizon. Depending on the sign the following regression model is assumed to calculate the partial derivatives of the battery power.

$$\begin{aligned} &\text{if } \omega_g \geq 0 \quad \rightarrow \quad P_{loss} = 2.3477\,\omega + 0.00182\,T^2\omega - 4.87^{-8}\,T^4\omega \\ &\text{if } \omega_g < 0 \quad \rightarrow \quad P_{loss} = -2.3477\,\omega - 0.00182\,T^2\omega + 4.87^{-8}\,T^4\omega \end{aligned} \tag{4.32}$$

Important problems related to linearization of the state space form and this latter approximation are treated afterwards.

4.2.5 Quadratic Programming and Active set method

According to the matrix formulation provided in Appendix A, the optimization problem is formulated as a Quadratic Programming problem meaning that the cost function is a quadratic function of the control variables and the constraints are expressed as linear inequalities in the control variables as well. Consequently the Quadratic Programming problem which strives to find the optimal control action U^* can be formulated as follows:

$$\begin{aligned} &\min_U \{\, J(U) = U^t H U + 2q^t U + b_o \} \\ s.t.& \\ &AU \leq b \end{aligned} \tag{4.33}$$

where b_o is vector of constant terms which is neglected in the following.
The number of inequality constraints is generally higher than the number of optimization variables, however these constraints comprise active and inactive constraints. An inequality constraint is said to be active when the strict equality holds:

$$A_i U = b_i \tag{4.34}$$

where *bi* stands for the i-th constraint, A_i is the i-th row of matrix *A*.
An active constraint influences the optimal solution since the objective function is forced to move along this constraint, hence if this constraint were removed from the problem the optimal solution would be different. On the other hand an inactive constraint does not influence the optimal solution and thus it can be neglected in the optimization problem. In order to find a solution to problem (4.33) it is necessary that the number of active constraints is lower than the number of variables to be optimized. In order to assure the convexity of the Quadratic Programming problem the matrix H has to be positive definite or at least semi-positive definite. This property is guaranteed by a proper definition of the penalty weights in the cost function; in particular, using the same notation as Appendix A, the matrices $W_y, W_u, W_{\Delta u}$ which contain the penalty weights on outputs and on levels and variations of control inputs should be semi-positive definite. Being H semi-positive definite assures that the cost function is convex and convexity of the whole optimization problem is guaranteed when the

constraints are linear because they identify flat faces on the convex objective surface thus the feasible domain of the design variables is still convex [23]. The optimization problem is solved numerically with a refined active-set method. Active-set is a primal method, thus it works directly on the given objective and constraint functions to find an optimal solution. The active set method defines at each step a group which is supposed to contain the constraints which are active at a given point U_k. This set is termed *working set* and the optimization is limited to the resulting *working surface* in the feasible domain of the variables to be optimized. The numeric routine starts by guessing a working set of the problem and by looking for a feasible optimum inside the working surface however since the composition of the working set is not known in advance and any point defined by the algorithm has to be feasible, the algorithm checks at any new iteration that any other constraint which is outside the working set is satisfied otherwise it is added to a new working set and the optimization is repeated. Regarding model predictive control, active set and interior point methods are applied the most and the issue to determine which algorithm suits better for MPC applications is still unsolved. In this thesis active set method has been used since interior point method tends to find an optimum far from the constraints due to the barrier functions. For this kind of problem it is likely that the optimal solution lies on the constraints rather than inside the working surface. Moreover a high efficient algorithm for convex quadratic programming problem was available [24] and the time required to solve a single optimization problem was much shorter in comparison to Matlab® built-in functions.

4.3 How the strategy works

The code of the strategy has been implemented in Simulink® and run in cosimulation with Amesim®. The high fidelity model of the hybrid powertrain is implemented in Amesim® thus these two software communicates at each sampling time. The communication is organised in two steps, in the first part the control strategy samples the values of the inputs from the Amesim® model and uses this values to elaborate the optimal control actions. Subsequently the control inputs are sent to the vehicle model and kept with zero order hold along the following sampling period. The inputs and outputs of the control strategy are:

Inputs:

- Driver’s torque request at driven wheels
- Vehicle longitudinal speed
- Battery state of charge
- Crankshaft angular velocity
- Engine torque
- Generator torque

- Total braking torque
- Battery open circuit voltage
- Vehicle position (when GPS is implemented in the control strategy)

Outputs:

- Optimal value of engine torque
- Optimal value of generator torque
- Optimal value of total braking torque
- Vector of command signals to the low level controller of the engine

The control strategy is roughly structured into three blocks.
The first block predicts the measured disturbances along the prediction horizon by making use of the information available at the sampling time. In particular the driver's torque request is predicted according to an exponential decay where the first value coincides with the modified sampled torque while the rate of decay is adjusted depending on the level of torque request. The higher the initial torque the quicker its prediction diminishes; this approach comes from the assumption that high levels of torque request are likely to be short in time while low levels of torque request are supposed to last longer in time. The sampled torque request is modified to take into account the actual capability of the powertrain, in fact the fundamental hypothesis that the driveline output torque can instantaneously match the driver's torque request cannot hold when this latter variable exceeds the maximum torque that the driveline can develop at a specific vehicle speed. Eventually the optimization algorithm can successfully compute an optimal solution if the input torque is saturated by the characteristic curve of the electric motor. From the sampled vehicle velocity the motor angular velocity is estimated using (4.11); the limited input torque is obtained as follows:

$$\begin{gathered} if\ T_{sample} > 0 \quad \rightarrow \quad T^{*}_{sample} = min\{T_{sample}, (208, m_o\omega_m + q_o)\} \\ if\ T_{sample} < 0 \quad \rightarrow \quad T^{*}_{sample} = max\{T_{sample}, (-208, -m_o\omega_m - q_o)\} \end{gathered} \tag{4.35}$$

The following values for the rate of decay are used:

$$\begin{gathered} if\ T^{*}_{sample} \geq 600\ Nm \quad \rightarrow \quad \tau_{decay} = 0.5s \\ if\ 200\ Nm \ \leq\ T^{*}_{sample} < 600\ Nm\ \rightarrow\ \tau_{decay} = 1s \\ if\ 0\ Nm \ \leq\ T^{*}_{sample} < 200\ Nm\ \rightarrow\ \tau_{decay} = 2s \\ if\ \ T^{*}_{sample} < 0\ Nm\ \rightarrow\ \tau_{decay} = 2s \end{gathered} \tag{4.36}$$

Then equation (4.9) is used to obtain the prediction of vehicle velocity along the prediction horizon. The second block computes the matrices of the linearized state space form using the inputs acquired at the sampling time; moreover it uses the predictions of the external disturbances to compute the matrices which define the constraints and the cost function. The expressions of these matrices is reported in Appendix A. Note that the sampling period is different than the prediction period used to discretize the system, this latter is longer in order to have a sufficient long prediction horizon with a limited number of variables to be optimized.

$$T_s = 0.1s$$
$$T_{predict} = 0.5s$$

The penalty weights applied to the outputs are assigned according to an exponential decay along the prediction horizon in order to reduce the influence of the last samples which are far from the linearization point. The values of these outputs are predicted using the linearized state space form, hence they are likely to be not correct and thus not important for the optimization problem. The values of the penalty weights are assigned as function either of the input power request or the torque request; the following table is used:

Table 4.4: Penalty weights defined in the cost function.

Input level	$\boldsymbol{w_{SOC}}$	$\boldsymbol{w_{\dot{m}_f}}$	$\boldsymbol{w_{\omega_e}}$	$\boldsymbol{w_{T_e}}$	$\boldsymbol{w_{T_g}}$	$\boldsymbol{w_{T_b}}$	$\boldsymbol{w_{\Delta T_e}}$	$\boldsymbol{w_{\Delta T_g}}$
$-600Nm < T_{sample} < 0Nm$	0	10	0.1	1	0.1	2	0.01	0.01
$T_{sample} \leq -600Nm$	0	1	0.1	1	0.1	0	0.01	0.01
$0\ kW \leq P_{sample} < 2.5kW$	0	10	0.01	0.01	0.01	2	0.005	0.005
$2.5\ kW \leq P_{sample} < 8kW$ (**)	1	1.8	4e-4	1e-4	0.001	2	0.005	0.005
$8\ kW \leq P_{sample} < 14kW$ (**)	1	1.8	4e-4	1e-4	0.001	2	0.01	0.05
$14kW \leq P_{sample} < 20kW$ (*)	1	1.8	4e-4	1e-4	0.001	2	0.01	0.05
$20\ kW \leq P_{sample} < 30kW$ (*)	1	1.8	3e-4	1e-4	0.001	2	0.01	0.05
$30kW \leq P_{sample}$	1	1.6	1e-4	1e-4	0.001	2	0.01	0.05

Considering the power levels denoted with (**) when either the vehicle velocity is lower than 4.7 m/s or the battery state of charge is above the reference level, w_{SOC} is set equal to 0 while $w_{\dot{m}_f}$ is set equal to 7 or 2 in order to encourage MPC to exploit electric traction. For power levels denoted with (*) w_{SOC} is set equal to 0 when the battery is overcharged. Moreover every time the vehicle velocity is below 0.1 m/s, then w_{ω_e} is set equal to 10 in order to encourage MPC to switch off the engine. The penalty weight ω_g is set equal to 0.1.

The last block solves the quadratic programming problem using the sequence of optimal control actions defined at the previous sampling time as initial guess.

5 Results

In this chapter all relevant results are shown and discussed. Firstly the nonlinear and the linearized state space models are validated, thus some figures are used to underline the remarkable considerations about modeling then the MPC-based control strategy is compared to the rule based strategy regarding fuel economy and drivability. Fuel economy is addressed firstly while velocity tracking error and passengers on board comfort during engine starting and stopping is treated afterwards. In the first part of the chapter it is clarified how the comparative simulations have been carried out, then the most important results are provided. It is important to understand how MPC can achieve better fuel economy with respect to the heuristic control strategy. For this purpose the time history of some important outputs is displayed e.g. engine operating points, power split in the powertrain, battery state of charge level. The post processing of the results permits to conclude that the MPC-based strategy performs better extra urban driving rather than urban driving moreover it uses engine power to provide the mean power request while battery power is exploited to deal with acceleration onset and power fluctuations. A simplified analysis of on board passengers comfort is then shown following the specifications provided in [25]. Engine starting and engine stopping have been considered as the input events for comfort evaluation.

5.1 Validation of the models

The nonlinear and the linearized state space forms have been validated by assigning the time history of the control inputs and external disturbances and comparing the outputs with those obtained in Amesim® for the same drive cycle. The trends of the inputs have been obtained by a reference simulation on NEDC that has been run in Amesim® using the rule based strategy. The nonlinear state space form has been integrated using Euler forward with a fixed integration period of 1ms. The nonlinear model provides an acceptable description of the dynamics of the battery state of charge and of the angular velocity of the crankshaft as the next two figure illustrate. The nonlinear model can therefore capture the most important events of the system even if the compliances of the vehicle are not taken into account.

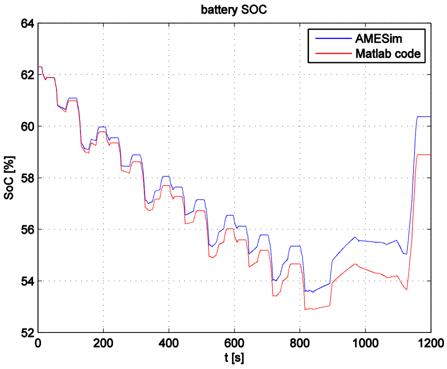

Figure 5.1: Battery SOC as obtained with Amesim® and the nonlinear model.

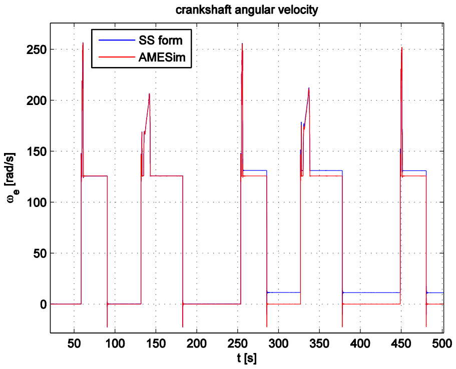

Figure 5.2: Crankshaft angular velocity as obtained with Amesim® and the nonlinear model.

The nonlinear model predicts a higher battery discharge and a higher total fuel consumption; this is due to the fact that both regression surfaces of power losses and fuel mass flow rate overestimate the experimental data. This is not a problem since the MPC strategy will be implemented according to the receding horizon approach and moreover these discrepancies are conservative. The next two figure compare the time history of power loss in the motor and fuel mass flow rate obtained with the two models.

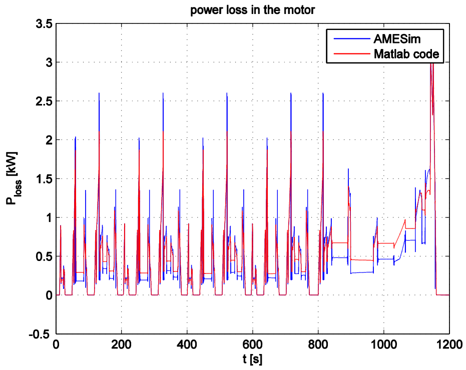

Figure 5.3: Comparison of power loss in the motor.

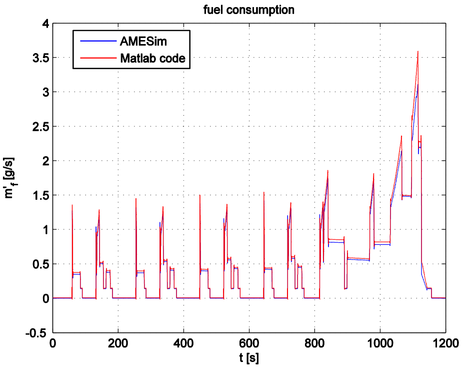

Figure 5.4: Comparison of fuel mass flow rate.

The validation of the linearized state space form is however more important because the optimization routine depends on it. For the validation of this latter model the time trends of control inputs, external disturbances have been assigned along the prediction horizon starting from a given time t_k. The validation highlights that the quality of the prediction is strongly dependent on the conditions of the system at the linearization point, in particular the more the operating conditions along the prediction horizon vary with respect to the conditions at the linearization point, the less accurate the prediction is. The most important problem is related to the poor description of the power loss in the electric machine when the operating conditions change a lot. The next figure represents the power loss in the electric generator; the vehicle is accelerating and the engine is started from rest. The operating conditions that are valid at the linearization point are completely different from the operating conditions that the system experiences throughout the prediction horizon, for instance the engine torque increases from 0 Nm at the linearization point to a maximum level of 50 Nm. The matrices defined at the linearization point are thus unsuitable to provide a reliable description of system outputs over this time interval. This is the main error related to the discretization, in the following a negative consequence of it is analyzed.

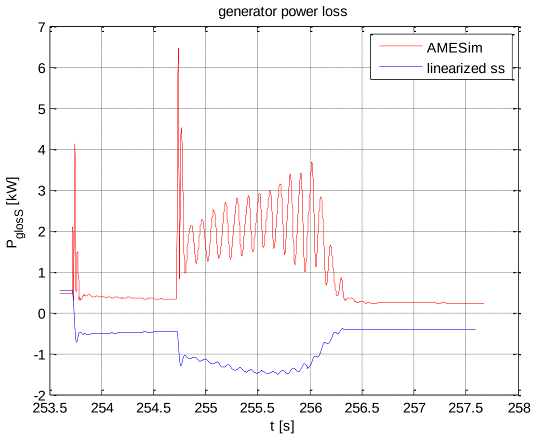

Figure 5.5: Power loss in the generator. Comparison between Amesim® and the linearized SS form.

5.2 Fuel economy

5.2.1 Drive cycles and charge sustenance

Fuel consumption of a vehicle depends on both road conditions (e.g. road slope, wind velocity) and vehicle parameters (e.g. total mass, coefficient of aerodynamic resistance). In order to provide a ranking of different vehicles regarding fuel economy performance which is independent on road conditions, standardized drive cycles have been developed for the sake of testing different vehicles under the same driving conditions. A drive cycle defines the reference velocity and road slope profiles that the vehicle will follow during a specific driving mission. The absolute wind velocity is usually set equal to 0 m/s and the gear shifting schedule is also specified for those vehicles equipped with a manual transmission. The United States, Europe and Japan have correspondent standardized drive cycles which strive to replicate urban and extra-urban driving conditions. The characteristics of these cycles are regularly updated in order to match the actual performance of vehicles on the market. Anyway each cycle underestimates the real road load that a vehicle would encounter in actual driving and therefore they should be used merely as a basis for direct comparison among different vehicles rather than as a way to predict fuel consumption. Five reference drive cycles have been used in this thesis work to compare the achievable fuel economy between a rule based strategy and the MPC-based control strategy. In appendix C the reference velocity profile of these cycles is provided. The results that are reported here refer to a flat road otherwise specified. The hybrid electric vehicle that is analyzed is of charge sustaining type as a consequence a correct evaluation of fuel economy over a specific drive cycle can be done provided that energetic equilibrium is achieved, namely the battery state of charge level at the end of the simulation equates the initial value. This equal level is called *state of charge equilibrium level* in the following. In order to achieve this condition the same cycle has been repeated several times until energetic equilibrium has been obtained.

Amesim® provides as output the total mass of the fuel in grams that has been burnt during the driving mission; from this output result it is possible to calculate the fuel economy according to the following equations and by assuming a fuel density equal to $780\ g/dm^3$.

$$\left({}^{l}\!/_{100km}\right) = \frac{m_{fuel}[g]}{\rho_{fuel}[\frac{g}{dm^3}]} * \frac{100km}{distance\ [km]} \tag{5.1}$$

$$(\text{"}mpg\text{"}\ mile\ pergallon) = \frac{100\ km * 1l}{\left({}^{l}/_{100km}\right) * \frac{1.609\ {}^{km}/_{mile}}{4.54609\ {}^{gallon}/_{l}}} \tag{5.2}$$

5.2.2 Comparison of the results

The following table and the following histogram summarize the total fuel consumption and equilibrium level of the battery state of charge as obtained when the two control strategies are applied to the 5 reference drive cycles.

Table 5.1: Comparison of fuel economy. Final results.

	Rule based				MPC		
Cycle	$SOC_{level}[\%]$	$M_{fuel}[g]$	${}^{l}/_{100km}$		$SOC_{level}[\%]$	$M_{fuel}[g]$	${}^{l}/_{100km}$
NEDC	59.86	509.03	5.927		59.49	493.6	5.742
HWFET	59.65	751.25	5.837		59.73	741.62	5.762
SC03	47.97	286.47	6.378		57.34	261.16	5.815
UDDS	58.14	546.0	5.840		57.46	541.59	5.793
US06	42.00	901.59	8.973		56.17	741.53	7.380

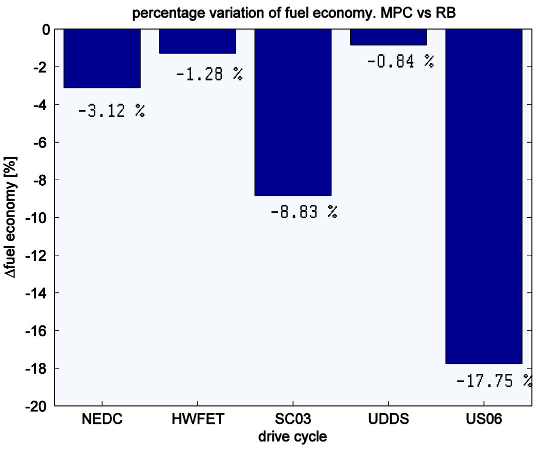

Figure 5.6: Percentage reduction of fuel consumption given by MPC with respect to the rule based strategy.

Table 5.1 reports the fuel economy in absolute value while the histogram in Figure 5.6 reports the fuel economy achievable with MPC in terms of percentage reduction with respect to the baseline represented by the rule based strategy.

The MPC-based energy management strategy succeeds in reducing fuel consumption over all standard driving cycles with respect to the rule based strategy. Charge sustainability is achieved by both strategies. Regarding the battery state of charge level it is important that it never exceeds the minimum and maximum thresholds imposed by the operating constraints and its equilibrium level should be reasonably close to the reference one. From the table it is possible to see that the proposed optimal control strategy can keep the equilibrium level close to the reference value (60%) and in some situations (US06, SC03) it performs better than the rule based strategy. The next figures illustrate the time history of the battery state of charge level as obtained over the five reference drive cycles. It can be concluded that the MPC-based control strategy manages to maintain the battery state of charge level within the operating constraints; on the opposite the rule based strategy violates the minimum threshold in US06. It is stressed here that the heuristic control strategy samples the input information at each simulation step while the MPC-based strategy samples with a fixed sampling period. This is a remarkable piece of advantage for the rule based strategy because the control inputs are updated at each simulation step.

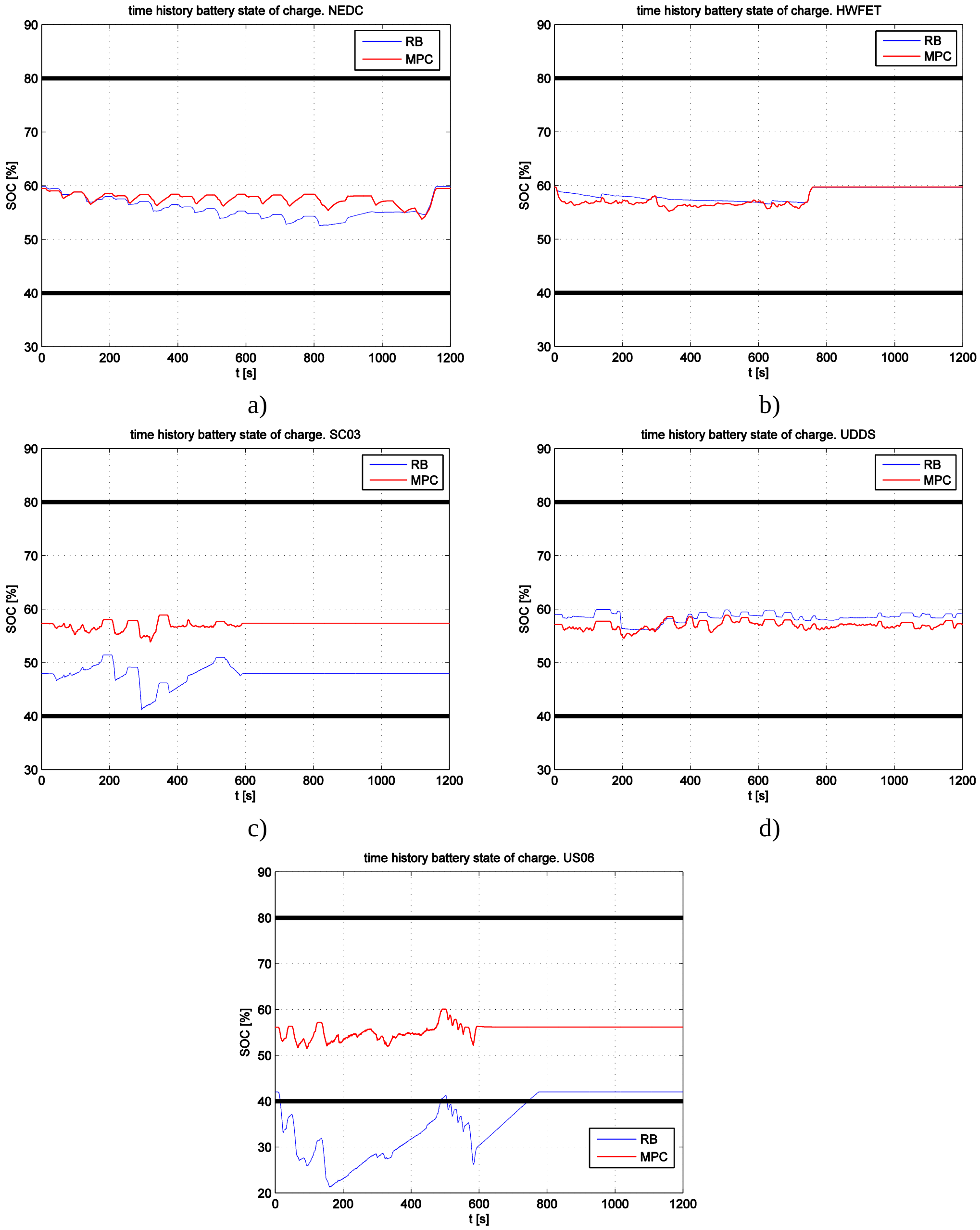

a)

b)

c)

d)

Figure 5.7: Comparison of battery state of charge level over the 5 considered drive cycles as obtained with the rule based strategy (blue curves) and the MPC-based strategy (red curves). a) top left NEDC, b) top right HWFET, c) mid left SC03, d) mid right UDDS, e) low US06

The results are nice however it is clear that the improvement brought by MPC in terms of fuel consumption reduction is sensitive to the driving conditions specified by a drive cycle. In fact MPC performs much better than the heuristic control strategy over SC03 and US06 while the performance is comparable over NEDC and UDDS. This conclusion is linked to the different operating principles of the two strategies consequently it is worth to analyze them in details. Firstly the MPC-based energy management strategy is analyzed on its own to highlight its main operating principle then it is compared against the rule based strategy.

5.2.3 The operating principles of the two control strategies

The European drive cycle NEDC is the basis to illustrate the basic operating principle of the optimal control strategy since the urban part of this cycle involves the repetition of a basic velocity profile four times and hence comparisons can be made between two repetitions. The next figure reports the velocity profile of the portion of the cycle that is used here to analyze the operating principle of the MPC strategy.

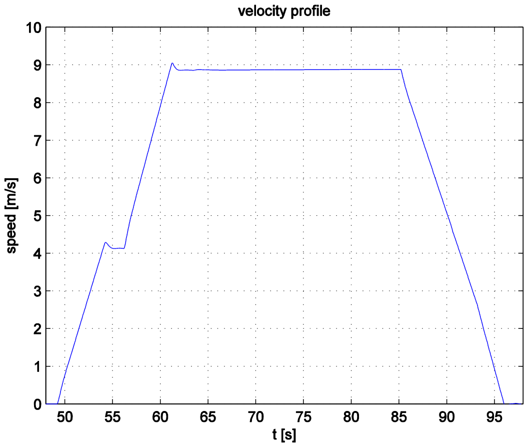

Figure 5.8: Velocity profile of the driving situation used to analyze the operating principle of the MPC strategy.

This portion of the cycle involves a rather long acceleration followed by a pretty short phase of constant vehicle speed; then a long braking brings the vehicle to complete stop. The power flow among the powertrain components that corresponds to this driving situation is represented in the following figure.

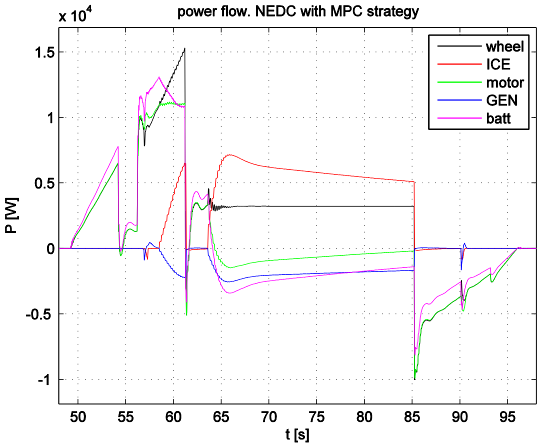

Figure 5.9: Correspondent power flow in the powertrain.

This portion of the cycle highlights how MPC exploits all available driving modes, for instance it employs firstly full electric driving from 50s to almost 57s when vehicle speed is low and during the initial part of the acceleration. Once power request increases more the engine is activated. The generator is used as engine starter and the battery provides additional power to start the engine. The final part of the acceleration is supported by the engine and the battery together; this is the positive split mode since part of the engine power is sent to the motor through the electric side of the powertrain. From 61s to 85s the vehicle is cruising at low speed and power request reduces significantly. Initially the electric mode is still exploited and the engine runs in idle, however as the battery state of charge diminishes the engine torque is increased once more and positive split mode is used to run the vehicle and charge the battery simultaneously. Contrary to the previous case the portion of the engine power that is sent to the electric side of the powertrain is fully used to charge the battery. In this situation the engine provides the whole traction power. At 85s regenerative braking is applied to recover the vehicle’s kinetic energy; however part of the upstream flowing power cannot can be stored in the battery due to power loss. At 90s the generator torque is used to stop the engine.

The same velocity profile is followed between 240s and 300s but the battery state of charge is lower in this second case, thus MPC uses a higher engine torque to reduce the load on the battery and maintain the state of charge level reasonably close to its reference value. This behavior is displayed in the next group of figures which report a direct comparison of the engine torque level decided by MPC and the correspondent battery state of charge level.

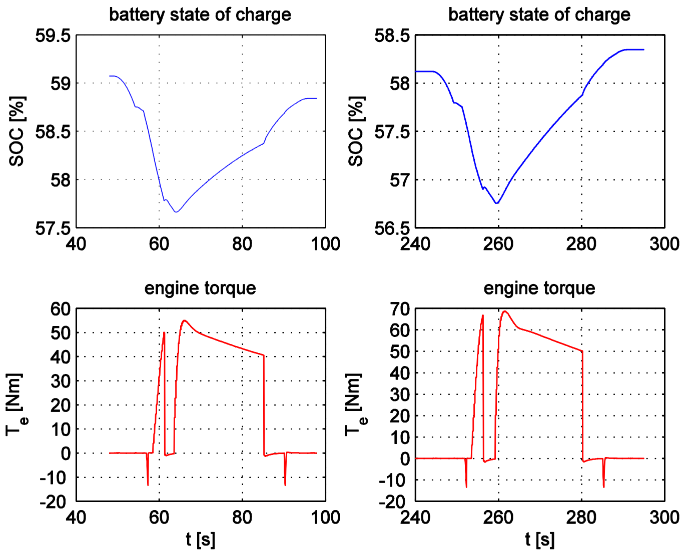

Figure 5.10: Battery state of charge and engine torque for two repetitions of the same velocity profile.

The trend of the engine torque is the same except for the magnitude of the torque which is adjusted in order to provide more power to the electric side of the powertrain. It is important to note that MPC prefers increasing the engine torque rather than the crankshaft angular velocity in order to provide more power to the battery. This solution allows the engine to operate in a region of low fuel consumption. MPC exploits steadily the power split between the engine and the battery where the split ratio depends on the driving situation and on the instantaneous battery state of charge level. The result is a smooth activation of the engine during hard accelerations and a less fluctuating engine operating point during all other driving situations. Moreover MPC takes advantage of regenerative braking to charge the battery and reduce the future power load to the engine; simultaneously the engine torque is quickly reduced to 0 Nm as soon as braking is detected.

The rule based strategy uses the engine as primary power unit either when the power request is high i.e. during acceleration phases, or when the battery state of charge is close to its minimum threshold. Engine power is used to follow the peaks in power request so this control strategy adjusts the engine operating point in accordance to the input level of power request. This behavior has the drawback that the engine is activated brutally as the battery state of charge diminishes below a threshold level or power request exceeds a limit value. The engine operating point moves quickly towards a region in the engine map where high power is generated in order to drive the vehicle and charge the battery.

In order to illustrate the differences in the operating principles of the two strategies, a portion of the urban part of the European drive cycle (NEDC) is used as reference. This driving situation includes a sequence of accelerations followed by a short time interval where vehicle speed is constant as reported in the next figure.

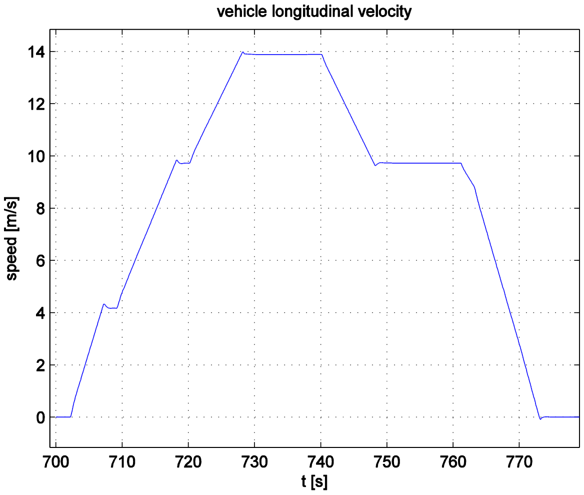

Figure 5.11: Velocity profile which corresponds to the considered driving situation.

The following two figures report the correspondent power flow among the components of the powertrain that is obtained by the application of the two energy management strategies.

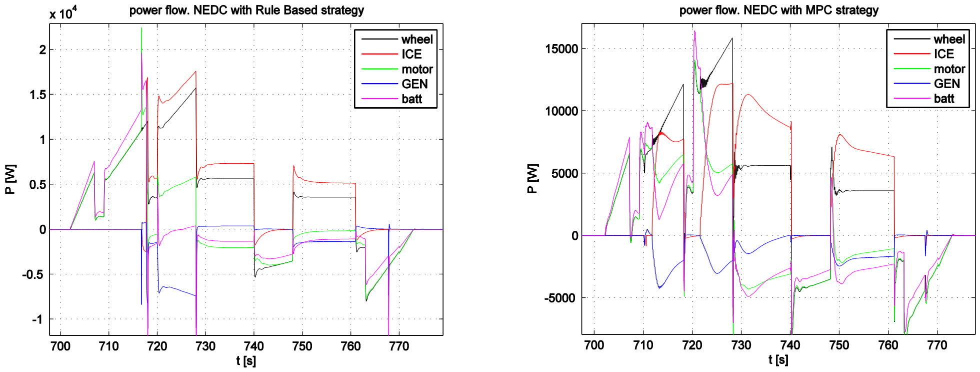

Figure 5.12: Power flow in the powertrain as obtained with the rule based strategy (left)and with MPC (right).

The rule based strategy uses the engine power to balance the highest power request during the acceleration phase; in this situation the crankshaft rotates quicker than the ring gear (if their velocities are referred to the same shaft) and therefore positive split mode is employed. Between 720s and 730s the power released by the battery is almost null; the electric power produced by the generator is sent to the electric motor but eventually this implies that the fuel is the only energy source in this situation. Positive split mode is also applied by MPC which already activates the engine between 712s and 720s; however the battery power is used much more to sustain the load during acceleration in comparison to the rule based strategy. This implies that more engine power has to be used to replenish the battery state of charge level during the subsequent phase where the vehicle is cruising between 730s and 740s. Nonetheless the total load is low in this second driving condition therefore the engine can release a surplus of power to charge the battery while still operating in a region of high efficiency. The following figures report the engine operating points on the engine map which result from the decisions taken by the two energy management control strategies.

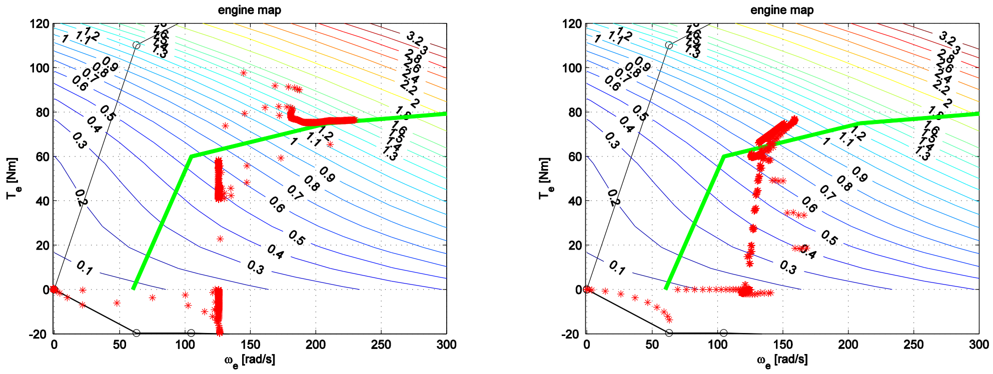

Figure 5.13: Engine operating points as obtained with the rule based strategy (left) and with MPC (right).

MPC can successfully keep the fuel mass flow rate low in comparison to the heuristic control strategy however the engine is used longer in time than with the rule based control strategy and eventually the benefit is negligible over the urban portion of the cycle. In fact if just the urban portion of NEDC were used as a new driving mission the fuel economy obtainable with the two strategies would be the same.

Table 5.2: Fuel economy and battery state of charge equilibrium level over the urban portion of NEDC.

Driving mission limited to the urban portion of NEDC		
Strategy	$SOC_{level}^{equilibrium}$	$^{l}/_{100km}$
Rule based	50.48 %	5.601
MPC	58.42 %	5.613

UDDS is another urban cycle which includes frequent start and stop of the vehicle and the average speed is below 10 m/s, hence the average power request is low. Even in this case the fuel economy achievable with MPC is slightly better than the rule based strategy as it is reported in Table 5.1.

On the other hand when power request increases MPC achieves better results. Considering the following part of the highway cycle (HWFET) where the vehicle accelerates in the initial part then speed remains almost constant.

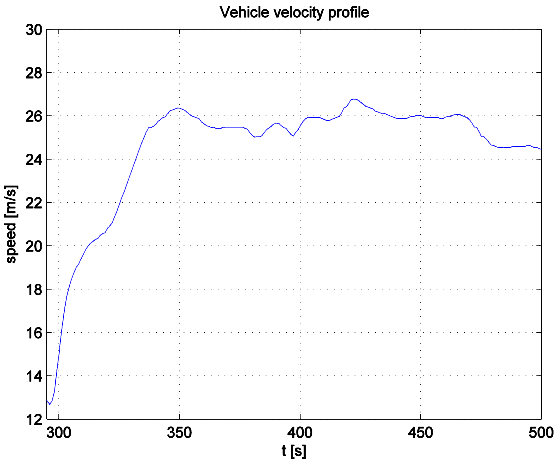

Figure 5.14: Velocity profile of the considered portion of HWFET.

The power flow in the powertrain as obtained with the two strategies is reported in the next two figures.

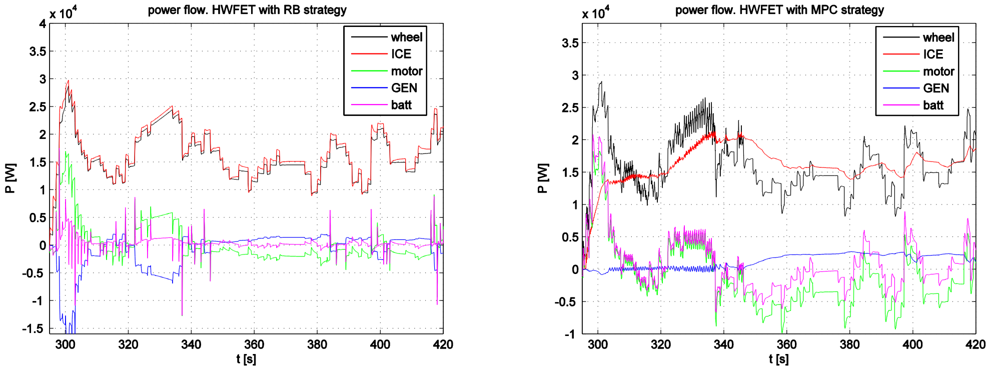

Figure 5.15: Power flow with the rule based strategy in HWFET.

Figure 5.16: Power flow with MPC in HWFET.

MPC manages the engine power in order to provide the mean power request while battery power is used to deal with power fluctuations, thus the battery provides an energy buffer to maintain the engine operating point close to a value of high efficiency.

On the opposite the rule based strategy strives to continuously update the engine operating point to the actual power request. From this point of view this latter strategy does not take advantage of the additional mechanical degree of freedom given by the power-split drive which enables to decouple the engine operating point from the vehicle speed. In fact from Figure 5.15 it can be seen that battery power is kept around the null value, this proves that the rule based strategy mainly uses the engine power to match the input power request. Figure 5.16 shows instead how MPC splits the total power request between the engine and the battery whose power oscillates a lot to deal with fluctuations of power request. This operating principle of MPC comes from the definition of the cost function which penalizes instantaneously the fuel mass flow rate and the deviation of the state of charge. The next two figures represent the engine operating points as defined by the two control strategies.

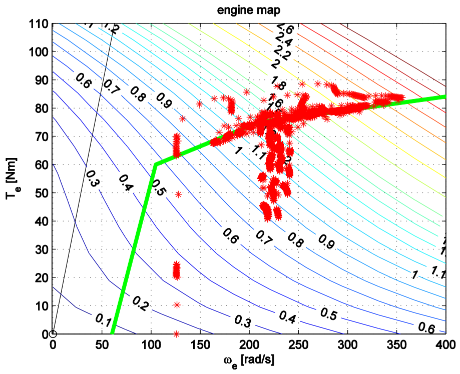

Figure 5.17: Engine operating points defined by the rule based strategy.

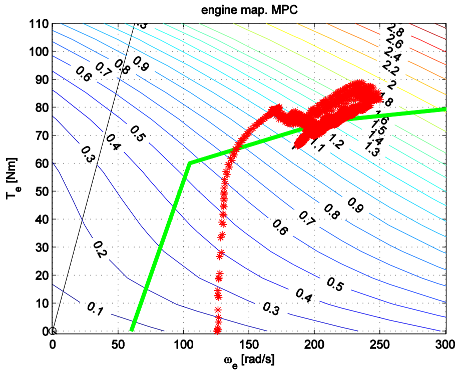

Figure 5.18: Engine operating points obtained with MPC.

The rule based strategy sets the desired engine operating point at high engine speed meaning that although the desired operating point falls on the engine OOL, the fuel mass flow rate is low. On the opposite MPC succeeds in keeping the engine speed low and thus the fuel mass flow rate is always lower than 1.9 g/s. Thanks to the fact that the engine provides only the mean power request, MPC can achieve better engine efficiency than the rule based strategy over this driving situation as the next figure shows; moreover the engine keeps the same operating principle and the efficiency is almost constant.

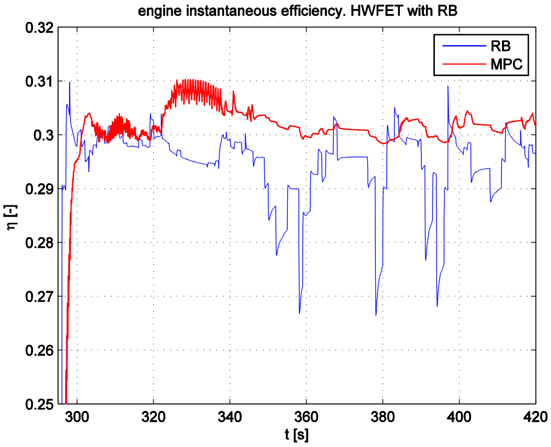

Figure 5.19: Engine efficiency over the analyzed driving situation.

Figure 5.16 is useful to understand the operating principle of MPC when vehicle speed is high, e.g. above 20 m/s. MPC switches from parallel to negative power split mode and vice versa depending on the vehicle velocity; for instance between 310s and 340s the acceleration level reduces consequently MPC decides to exploit the parallel driving mode where the generator angular velocity is almost null so that the entire engine power flows to the driven wheels. This mode is efficient since engine power is not used to charge the battery; from Figure 5.19 it can be seen that engine efficiency reaches the value of 0.31 in this time interval. As vehicle speed increases further MPC shifts to negative split mode meaning that generator angular velocity becomes negative and creates an overdrive ratio to keep the engine speed low while vehicle speed is increasing.

In conclusion the main operating principle of MPC is power split between engine and battery power where the former provides the mean power request while the latter copes with quick fluctuations in power request and driving situations characterized by limited power request. The rule based strategy strives to set the desired engine operating point on the engine optimal operating line for any driving situation; this implies that the engine speed can even assume high values and hence fuel mass flow rate is high. Since urban driving rarely involves high power request, MPC cannot achieve remarkable improvements for this situation while fuel economy is much better for extra-urban routes, SC03 and US06 are two clear examples.

5.2.4 A problem related to linearization

Figure 5.16 and Figure 5.19 show how some high frequency fluctuations appear when the MPC-based control strategy is used between 300s and 340s; in general these fluctuations occur every time parallel driving mode is selected. The reason of this strange behavior is due to the linearization of the generator power loss. In fact as it was illustrated in chapter 4 in order to linearize the power loss associated to the generator it is necessary to consider two different formulations of the partial derivatives of this function with respect to system states, control inputs and measured disturbances depending on the sign of the generator angular velocity at the sampling time. However this can generate unrealistic negative values of power loss associated to electric machines. The next figure reports the generator angular velocity over the same driving condition; it reveals that MPC has few problems as soon as this variable gets closer to the null value.

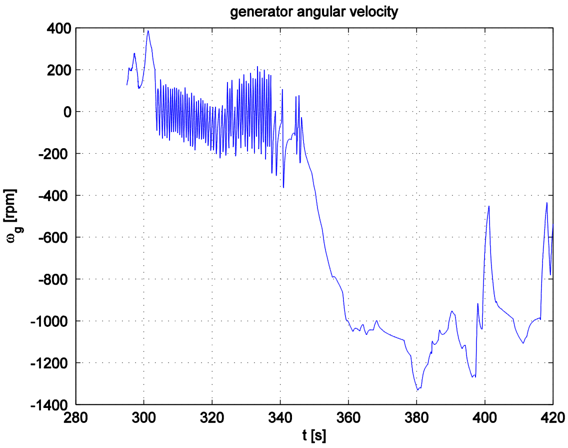

Figure 5.20: Generator angular velocity during parallel driving mode in HWFET.

This issue cannot be completely solved but it can be attenuated using a penalty weight on the deviation of the angular velocity of the generator with respect to a fictitious value in the cost function. This is the reason to include term appears inside the cost function (4.26). When the vehicle is run in parallel driving mode the generator angular velocity should be equal to 0 rad/s therefore a fictitious reference value of 0.1 rad/s is specified in the cost function and MPC is pushed to adjust the generator torque in order to limit the deviation of the generator angular velocity from this reference value. The reference value is fictitious since it is only used to avoid this latter variable from crossing repeatedly the null value and thus creating uncertainty in the optimal control action due to the fact that the operating conditions change a lot from one sampling to the following one.

The penalty weight on this deviation is limited in order to allow MPC to change quickly the driving mode. If this deviation were penalized severely then MPC would be encouraged to keep the parallel driving mode even when it is not the most efficient one. The following figures represent this latter point where the reference on the angular velocity of the generator is introduced in the cost function and the penalty weight is set rather high (20).

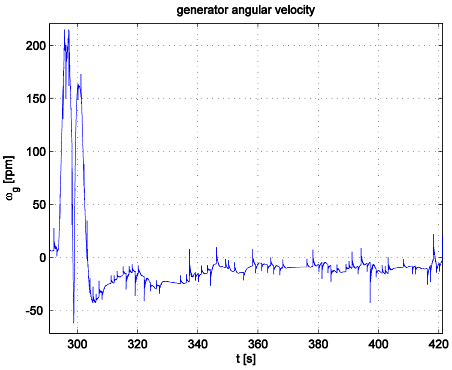

Figure 5.21: Generator angular velocity once its reference value is included in the cost function.

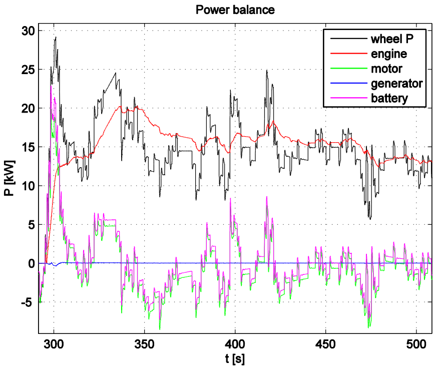

Figure 5.22: Power flow in the powertrain once the reference value of generator angular velocity is introduced.

It can be seen that fluctuations have disappeared nonetheless MPC maintains the parallel driving mode even after 340s. This means that the engine speed is higher than in Figure 5.16 and thus the fuel mass flow rate is slightly higher too.

5.3 Drivability

5.3.1 Velocity tracking error

A energy management control strategy should satisfy the requests coming from the driver in particular the reference velocity profile should be tracked correctly. For each strategy and for each drive cycle the instantaneous error has been calculated and the resulting mean error and standard deviation are reported in the following table.

Table 5.3: Velocity tracking error. Mean value and standard deviation.

	Rule based		**MPC**	
Cycle	μ_{err}	σ_{err}	μ_{err}	σ_{err}
NEDC	0.0016	0.0192	0.0016	0.0296
HWFET	0.0022	0.0201	0.0022	0.0226
SC03	0.0028	0.2669	0.0026	0.206
UDDS	0.0013	0.0237	0.0013	0.0376
US06	0.001	1.302	0.0006	1.0029

The tracking error has a slightly higher standard deviation with MPC since both the control strategy and the low level controller of the electric machines are implemented as discrete time controllers and hence there is a delay between the driver's request and the actual torque produced at the driven wheels. On the other hand the controllers of the rule based strategy update the control actions at each sampling time so it can immediately match the driver's torque request.

5.3.2 Passengers discomfort related to engine starting and stopping

The angular velocity of the crankshaft is controlled by the generator torque. Once the vehicle supervisory controller decides to activate or to switch off the engine, the generator torque level is changed rapidly in order to achieve as quick as possible the new desired set point of the crankshaft angular velocity. However it is important to verify that the change in generator torque does not produce undesired oscillations along the driveline which eventually affects passengers comfort and quality perception of the vehicle. The readiness in the response of the generator torque can be tuned with the proportional gain of the PI control on the instantaneous error between current and desired crankshaft angular velocity. This PI feedback control is implemented in the low level controller of the electric machines. In the next figures the results obtained with the rule based strategy over NEDC are displayed when the proportional gain of the low level controller of the electric machines is set equal to 1. The same driving situation considered in Figure 5.8 is analyzed and the correspondent carbody accelerations and jerks along the longitudinal and the vertical axes are plotted.

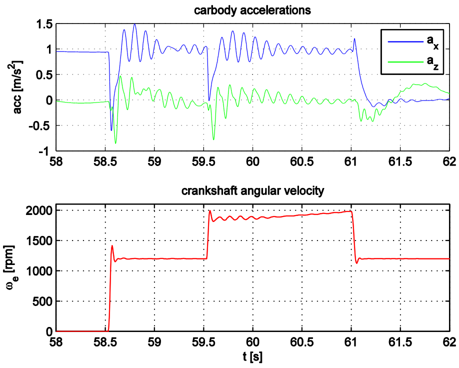

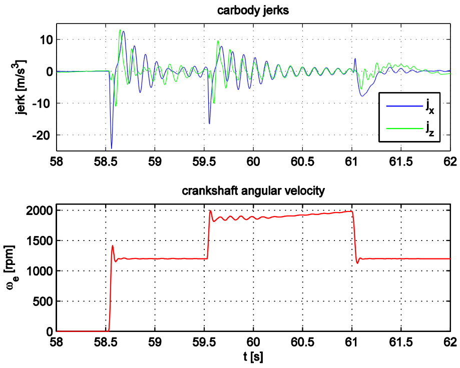

Figure 5.23: Carbody accelerations during engine starting.

Figure 5.24: Carbody jerks during engine starting.

Engine is activated at 58.5s and this event is clearly recognizable in the oscillations of the carbody accelerations and jerks. It is impossible to give an objective evaluation of discomfort, anyway it is necessary to reduce the effect of these oscillations on passengers comfort. In [26] it is claimed that a magnitude of jerk above $10\, m/s^3$ should be avoided while [25] provides an engineering tool to evaluate the effect of vibrations on people even if the equations provided in the standard norm refer to continuous vibrations and not transient events like engine starting and stopping.As these figures show, the variations in carbody longitudinal and vertical accelerations are severe when the crankshaft starts rotating. Both longitudinal and vertical carbody jerks are outside the threshold of $10\, m/s^3$ as a result the decisions taken by the energy management strategy are likely to degrade the on board comfort.

The solution that is implemented by the rule based strategy provides for reducing the proportional gain of the low level controller of the electric machines to 0.1. The change is therefore applied outside the strategy itself.
The improvement is remarkable as the next figures show.

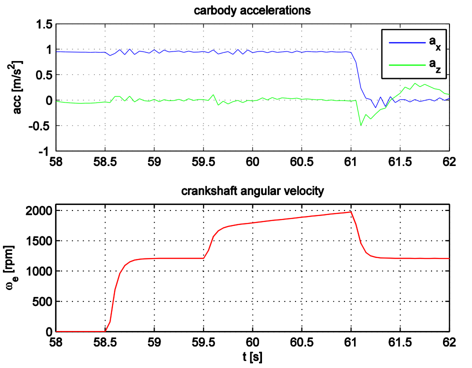

Figure 5.25: Carbody accelerations with a lower proportional gain.

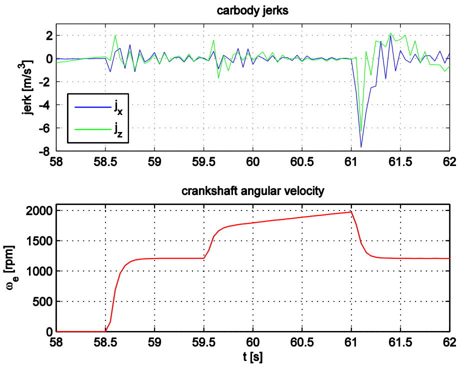

Figure 5.26: Carbody jerks with a lower proportional gain.

At 61s the longitudinal accelerations still varies consistently but this is related to the fact that the vehicle stops accelerating and enters a part of constant speed. The resulting oscillations from the quick drop in torque which occurs at 61s are not an issue in this case since both drivers and passengers expect to feel them.
Regarding the engine starting, this event is no more clearly recognizable in the carbody accelerations thanks to a smoother action of the generator torque. The next two figures compare the generator torque action with a proportional gain equal to 1 and a proportional gain equal to 0.1.

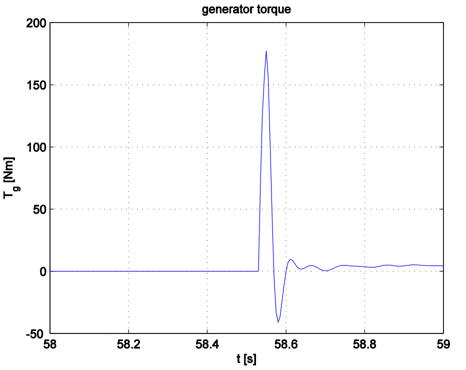

Figure 5.27: Generator torque for a unitary proportional gain.

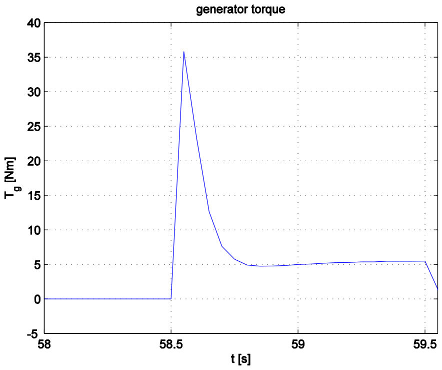

Figure 5.28: Generator torque for a proportional gain equal to 0.1.

Comfort analysis with MPC

The MPC-based control strategy has been developed in order to address the problem of drastic generator torque variation inside the control strategy itself.

Since the generator torque appears among the control input variables and the crankshaft angular velocity is a state of the system, then it is possible to limit the generator torque during engine starting and stopping in order to reach a smooth response of crankshaft angular velocity. The quality of the solution proposed has been evaluated according to the criteria suggested in [25] although they refer to continuous oscillatory events. The purpose is to attenuate the vibrations, not to solve completely the problem which usually involves different methods like small changes in combustion process, stiffness of engine mounts; some further details can be found in [3]. The cycle NEDC is used as reference driving mission because it involves numerous engine start&stop events which are well separated from one another and therefore can be distinguished easily. Variation of motor output torque can also produce remarkable peaks in longitudinal acceleration and jerk however this torque follows the torque requested by the driver as a consequence the driver and the passengers would expect such a variation in torque and the resulting peak acceleration. Furthermore one of the constraints imposed by the drivability refers to the satisfaction at each instant in time of the total torque at wheels requested by the driver. As a result the analysis has been focused on engine starting and stopping events in order to tune the action of the generator torque and reduce the resulting oscillations.

In order to apply the evaluation method proposed in [25] the longitudinal, vertical and pitch accelerations of the carbody are used. Only the part of the acceleration signals which refer to an engine event have been considered, thus the effect of motor torque and engine events on the carbody accelerations should be distinguished. In NEDC the engine start&stop events can be easily identified and decoupled from the variation of motor torque because the engine is activated or stopped when the vehicle is being driven with constant acceleration or deceleration thus the motor torque is almost constant. It also means that the longitudinal acceleration of the vehicle has either a positive or a negative mean value and the oscillations produced by the engine event builds upon this mean value. For this reason the mean value of the longitudinal acceleration is not removed because the passengers' perception of discomfort is related to the overall acceleration value. A set of data is extracted for each acceleration signal in order to consider just the values which correspond to an engine event. The data are sampled using a rectangular-shaped window which does not introduce any signal distortion moreover the time period for this analysis is chosen in such a way that the oscillations damp out significantly so initial and final level of accelerations are similar and the error due to repetition of the measured signal to create a periodic one is limited.

The sampling frequency is chosen equal to 1000HZ. This value respects a constraint given by the norm which prescribes to use a sampling frequency at least equal to:

$$9f_2$$

where f_2 represents a characteristic frequency of the frequency weighting functions provided by the standard ISO norm. It is assumed that all acceleration signals are measured at the driver's seat and the weighting functions W_d, W_k, W_e are used to weigh the longitudinal, vertical and pitch acceleration respectively.

The norm prescribes to weigh the signals in the time domain using proper digital filters having the characteristics defined by the frequency weighting functions.

This operation is carried out by applying recursively a Butterworth digital filter to an acceleration signal, which is divided into bands of octave, and then by applying the weight factor defined by the weighting function for that frequency band. Secondly the signal is reconstructed in time domain by using an inverse Fourier transform. The weighted signal $a_w(t)$ is used to calculate the weighted *rms* value as follows:

$$rms = \sqrt{\frac{1}{T}\int_0^T [a_w(t)]^2 dt} \tag{5.3}$$

The three *rms* values are combined through the comfort factors k_i, which are provided by the norm, to get the overall equivalent acceleration signal a_{tot}.

$$a_{tot} = \sqrt{k_x^2 rms_x^2 + k_z^2 rms_z^2 + k_\theta^2 rms_\theta^2} \tag{5.4}$$

This value is eventually compared to a reference table provided by the norm which describes how a normal human being would judge a certain acceleration level. In order to avoid a feeling of discomfort, the overall equivalent acceleration should be kept below $\mathbf{0.5}\ \boldsymbol{m/s^2}$. These equations hold provided that the crest factor of the weighted acceleration signal is below 9; for this reason this value has always been calculated as follows.

$$CF = \frac{max|a_w(t)|}{rms_a^{weigh}} \tag{5.5}$$

If some peaks are present in the signal the following ratio can become useful.

$$\frac{VDV_a^{weighted}}{rms_a^{weighted}\sqrt[4]{T}} \tag{5.6}$$

T is the observation period of the signal while *VDV* is called vibration dose value and it is calculated as follows:

$$VDV = \sqrt[4]{\int_0^T [a_w(t)]^4 dt} \quad [\frac{m}{s^{1.75}}] \tag{5.7}$$

If the ratio (5.6) exceeds 1.75, the norm suggests that the VDV describes better the acceleration signal rather than its *rms* value. However if no peaks are present in the signal and the signal has a mean value which is not null, then the information given by the VDV is not important because it tends to assume high magnitude due to the fourth power of the average value. For this reason if an acceleration signal has no peak, its *rms* value is assumed to be reliable to provide a good description even if the above mentioned ratio exceeds 1.75.

The NEDC comprises in total 18 engine events, with 9 starting and 9 stopping events. An example of calculation is reported afterwards on the basis of the two first engine events in the cycle NEDC, a starting at 56s and a stopping at 90s.
Firstly consider the engine starting event which is depicted in the following figure.

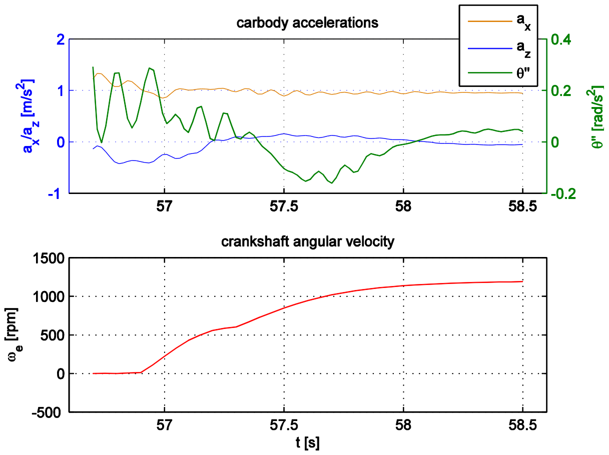

Figure 5.29: Carbody accelerations due to engine starting obtained with MPC.

The trend of crankshaft angular velocity with time is similar to that reported in Figure 5.25 and obtained by the rule based strategy in collaboration with the low level controller of the electric machines. This is because the generator torque is applied gradually by the vehicle supervisory controller in order to achieve the desired set point of the crankshaft angular velocity without remarkable oscillations of the carbody.

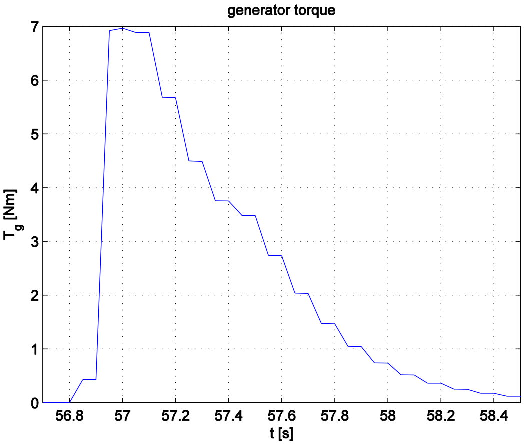

Figure 5.30: Generator torque defined by MPC to start the engine.

Comparing this latter figure to Figure 5.28 it emerges that it takes MPC slightly longer time to bring the engine to the reference idle speed, thus to activate the engine. The trends of longitudinal and vertical accelerations are rather smooth while pitch acceleration shows larger oscillations which however are already present when the engine is started. The three considered acceleration signals are reported below once more together with the results obtained by applying equations (5.3) to (5.4).

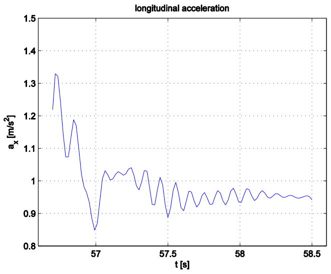

Figure 5.31:Longitudinal acceleration

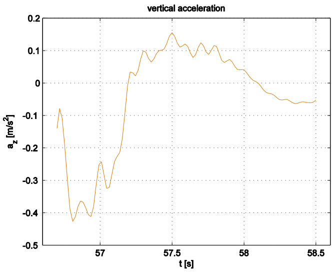

Figure 5.32: Vertical acceleration.

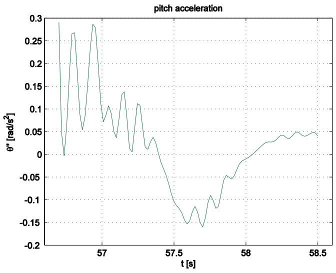

Figure 5.33: Pitch acceleration.

$$rms_{a_x}^{weighted} = 0.3671\, m/s^2 \qquad rms_{a_z}^{weighted} = 0.0341\, m/s^2 \qquad rms_{\theta}^{weighted} = 0.028\, m/s^2$$

$$VDV_{a_x}^{weighted} = 0.7484\, m/s^{1.75} \qquad VDV_{a_z}^{weighted} = 0.0607\, m/s^{1.75} \qquad VDV_{\theta}^{weighted} = 0.044\, m/s^{1.75}$$

$$\frac{VDV_{a_x}^{weighted}}{rms_{a_x}^{weighted}\sqrt[4]{T}} = 1.87 \qquad \frac{VDV_{a_z}^{weighted}}{rms_{a_z}^{weighted}\sqrt[4]{T}} = 1.63 \qquad \frac{VDV_{\theta}^{weighted}}{rms_{\theta}^{weighted}\sqrt[4]{T}} = 1.44$$

The equivalent total acceleration is equal to:

$$a_{tot} = 0.3688\, m/s^2$$

The ratio defined in (5.6) is bigger than 1.75 for the longitudinal acceleration signal which however does not show any spike, thus the high value of the VDV is due to the mean value of this signal. The crest factor of the weighted acceleration signal is far from 9 as a result the VDV value is not used to describe the discomfort felt by the passenger.

At 85s the driver starts braking and the electric motor torque switches quickly to negative values to accomplish a regenerative braking. The engine torque drops rapidly to 0 Nm and this produces a small variation on the crankshaft angular velocity which goes below the idle speed for a while, then MPC decides to use the generator torque to bring the flywheel angular velocity back to the idle speed. The oscillations in the acceleration signals produced by engine stopping can be recognized easily since motor torque remains almost constant in this phase[5]. The next figure represents these output variables.

---

[5] The variation of generator torque affects the motor torque too because a negative generator torque is needed to slow down the crankshaft rotation and this corresponds to a positive torque applied to the driveline output shaft. Consequently in order to satisfy the equilibrium equation and produce the same output torque, the motor should produce a higher negative torque. All these events are related to engine stopping as a result they are treated all together.

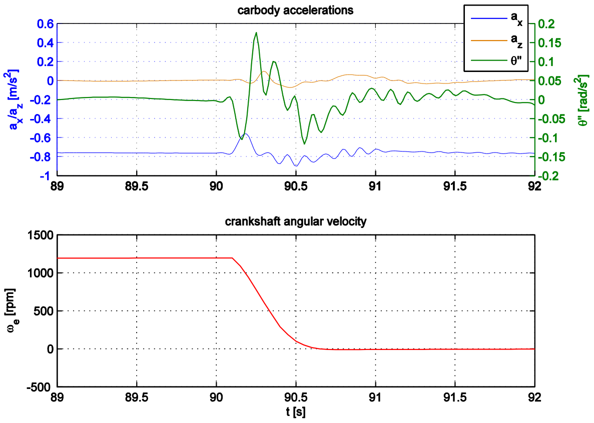

Figure 5.34: Carbody accelerations during engine stopping.

The following results are obtained:

$$rms_{a_x}^{weighted} = 0.2931\ m/s^2 \qquad rms_{a_z}^{weighted} = 0.0197\ m/s^2 \qquad rms_{\theta}^{weighted} = 0.0205\ m/s^2$$

$$VDV_{a_x}^{weighted} = 0.7671\ m/s^{1.75} \qquad VDV_{a_z}^{weighted} = 0.0433\ m/s^{1.75} \qquad VDV_{\theta}^{weighted} = 0.041\ m/s^{1.75}$$

$$\frac{VDV_{a_x}^{weighted}}{rms_{a_x}^{weighted}\ \sqrt[4]{T}} = 1.99 \qquad \frac{VDV_{a_z}^{weighted}}{rms_{a_z}^{weighted}\ \sqrt[4]{T}} = 1.67 \qquad \frac{VDV_{\theta}^{weighted}}{rms_{\theta}^{weighted}\ \sqrt[4]{T}} = 1.52$$

The results computed for the other 16 events are reported in the next table.

Table 5.4: Equivalent accelerations related to engine start&stop events.

starting		**stopping**	
$t_1 \div t_2$ $[s]$	a_{tot} $[m/s^2]$	$t_1 \div t_2$ $[s]$	a_{tot} $[m/s^2]$
125.1 s ÷ 126.8s	0.2544	182.5s ÷ 184s	0.3392
251.8 s ÷ 253.4s	0.3853	285.1s ÷ 286.8s	0.3017
320.1 s ÷ 321.8s	0.2578	377.5s ÷ 378.8s	0.3281
446.8 s ÷ 448.4s	0.3858	480.1s ÷ 481.2s	0.2701
515.1 s ÷ 516.8s	0.2582	572.5s ÷ 573.6s	0.3088
614.8 s ÷ 643.4s	03858	675.1s ÷ 676.4s	0.2876
710.1 s ÷ 711.8s	0.2583	767.5s ÷ 768.4s	0.2852
808.1 s ÷ 809.7s	0.2501	1156.3 ÷ 1157.4s	0.4941

All values are below 0.5 m/s^2.

6 Additional analyses

In this chapter some additional investigations on the performance of the MPC-based control strategy are presented. In the following the terms internal and external parameters are used extensively and the chapter is divided into two main parts where each focuses on one of these two cases. The term external parameters refers to all model parameters which lie outside the strategy itself and contribute to define the vehicle properties. These parameters cannot be tuned by the controller whereas they are imposed by the driving conditions or by the design of the vehicle. On the opposite the internal parameters appear in the script of the strategy and contribute to manipulate the optimization problem, thus they influence the optimal control action defined by MPC. The scope of these further analyses is to assess the robustness of the control strategy against uncertainty of some external parameters of the model and the influence of the internal parameters on the optimization problem. In the latter case the target is to identify a set inside the input space of the internal parameters which allows the energy management control strategy to achieve the best fuel economy. The possibility to flank the optimal control strategy with additional information coming from navigation systems like GPS has also been tested in the latest part of the chapter. The analyses reported in this chapter permits to judge the most important features of the proposed optimal control strategy.

6.1 Robustness of the control strategy

The optimal values of the control inputs are determined as solutions of a constrained optimization problem and the reference state space form changes at each sampling time since it is linearized around the new operating conditions.

Consequently it is not possible to assess stability and robustness of the control strategy towards parameters uncertainty using the mathematical approach of classic control theory. This point is actually very important since some vehicle parameters appear inside the control strategy hence their uncertainty may affect negatively the performance of the strategy. The typical approach is to test the behavior of the strategy against a number of different scenario which involve changing the level of some of the model parameters. As a result some numerical simulations have been run in order to evaluate the behavior of the strategy with respect to the variability of some vehicle parameters. Different driving scenarios have been considered where the value of one parameter at a time has been modified with respect to a base case. The stability of the strategy has been evaluated according to these two principles:

- The time history of control variables as defined by the control strategy do not show unrealistic trends, namely they do not oscillate heavily or quickly switch to a new set point
- The battery state of charge remains within the desired operating band (40% - 80%) and the equilibrium level is reasonably close to the reference value (60%)

Instead the robustness has been evaluated by means of a comparison with the results obtained by the rule based strategy for the same driving conditions. The comparisons have compared the total fuel consumption and the equilibrium level of the battery state of charge achievable with the two strategies. The results that are displayed afterwards refer to a system in energetic equilibrium.

The vehicle model in Amesim® contains several parameters but just a set of them is supposed to have an important influence on fuel economy. In particular the following parameters have been taken into account:

- Carbody mass
- Road slope
- Dimensionless coefficient of aerodynamic drag
- Wheels rotary inertia
- Stiffness of the silent chain in the transaxle
- Adhesion coefficient between tyre and asphalt

The simulations have been carried out according to the one-at-a-time principle (OAT) where the level of one factor is modified at a time while all other factors are kept equal to their base value. The NEDC has been used as reference driving mission since it comprises pieces of both low power and high power request.

6.1.1 Carbody mass

The carbody mass corresponds to the total vehicle mass minus the front and rear unsprung masses. This variable changes in accordance with the number of people on board and the mass of the luggage. The base value is equal to 1280 kg; the following four levels have been tested:

1100 kg, 1400 kg, 1550 kg, 1700 kg

The value 1100 kg is only used to widen the domain of analysis but it is not a realistic condition since the base case corresponds to a situation with a nominal vehicle plus the driver. The following figures and tables compare the rule based strategy to the MPC control strategy in terms of the effect of parameter change on fuel consumption with respect to the base case.

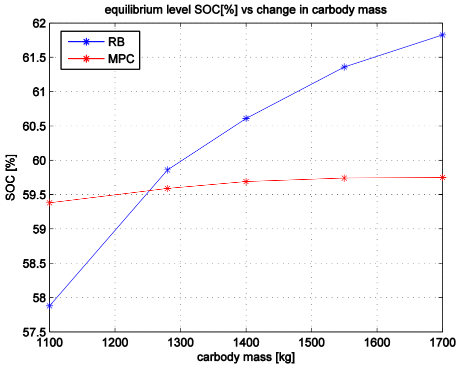

Figure 6.1: Battery SOC equilibrium level as function of carbody mass change.

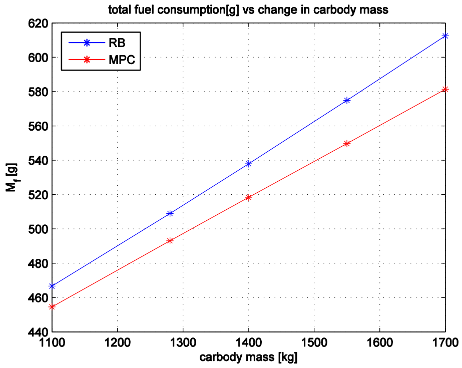

Figure 6.2: Total fuel consumption as function of carbody mass change.

Table 6.1: Performance of the two strategies against carbody mass variation.

rule based	SOC **level**	57.88 %	59.86 %	60.61 %	61.36 %	61.83 %
MPC	SOC **level**	59.38 %	59.49 %	59.69 %	59.74 %	59.75 %
rule based	M_{fuel}	466.7 g	509.0 g	537.9 g	574.9 g	612.5 g
MPC	M_{fuel}	454.6 g	493.6	518.4 g	549.7 g	581.4 g
	Carbody mass	1100 kg	1280 kg	1400 kg	1550 kg	1700 kg

Increasing the carbody mass leads to an increase of the equilibrium level of the battery state of charge because during regenerative braking more energy associated to the inertia of the vehicle can be recovered. Since the strategies strive to maintain the battery state of charge close to its reference value this produces eventually a higher equilibrium level because the strategies do not know that a long braking concludes the cycle. Similarly more power is required to accelerate the vehicle consequently the total fuel consumption increases too.

The percentage variation of fuel economy with respect to the base case is reported in the next table.

Table 6.2: Fuel economy percentage variation with respect to carbody mass.

rule based	$l/100\ km$	5.434	5.927	6.263	6.694	7.132
	$\Delta\%$	-8.31 %	0.0 %	+5.67 %	+12.94 %	+20.33 %
MPC	$l/100\ km$	5.293	5.742	6.036	6.400	6.770
	$\Delta\%$	-7.82 %	0.0 %	+5.12 %	+11.46 %	+17.90 %
	carbody mass	1100 kg	1280 kg	1400 kg	1550 kg	1700 kg

The MPC-based energy management strategy performs better than the rule based strategy in terms of percentage increase of total fuel consumption. Both strategies manage to keep the battery state of charge level in-between the desired operating domain. The MPC-based control strategy seems to be stable as the next figure shows. This figure represents the time history of the engine power in the high speed part of NEDC as function of the base value and higher values of the carbody mass.

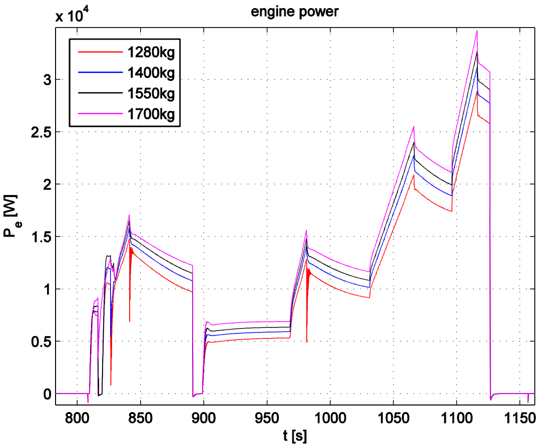

Figure 6.3: Engine power as function of carbody mass levels.

The trends are similar, the magnitude of power release is adjusted according to the increase in carbody mass and the behavior is stable. The next two figures also serve to highlight that MPC only adjust the engine torque and engine angular velocity in order to produce more or less power but the operations of the engine are not modified. This indicates a recurring behavior of MPC despite the change in operating conditions; hence the strategy is stable and robust.

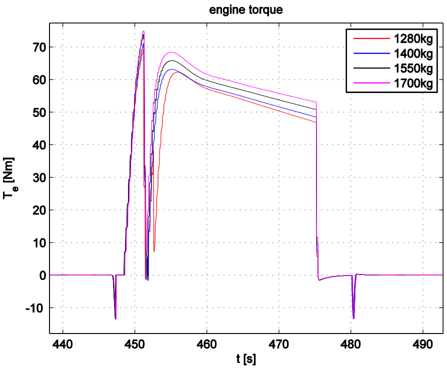

Figure 6.4: Engine torque as function of carbody mass.

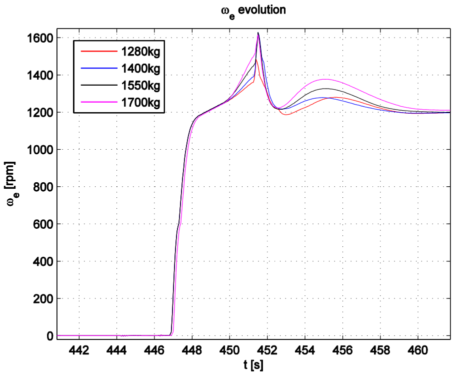

Figure 6.5: Engine speed as function of carbody mass.

6.1.2 Road slope

The road surface has been defined as an inclined plane with constant slope, hence the vehicle moves forward on a road of linear increasing height. However the initial and the final part of the road are flat. The road profile is therefore simple but this approach allows fuel economy to be directly related to a specific road slope. The reference velocity profile has not been modified according to the change in road slope, thus the driver still tries to follow the velocity profile which holds for a flat road. This assumption implies that power request increases significantly in the high speed part of the cycle therefore rather limited slope values have been tested. The base case corresponds to a null road slope value; the following conditions have been considered:

$$slope: 0°(0\%)\,, 0.3°\ (0.52\%)\,, 0.6°\ (1.05\%), 1°\ (1.75\%), 2°\ (3.49\%)$$

The next figure illustrates the road height as function of vehicle position in the absolute frame for the case of 0.6°.

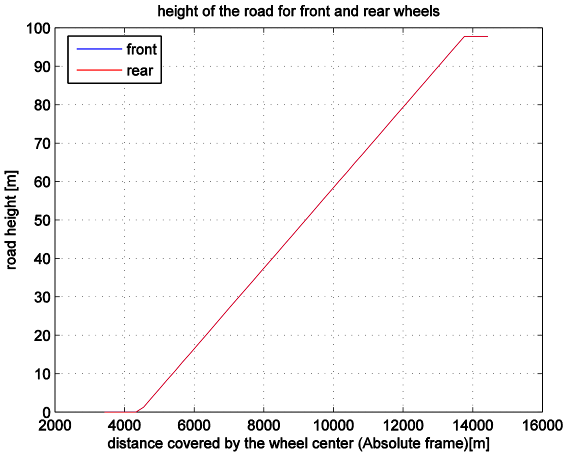

Figure 6.6: Road height as function of vehicle absolute position. Road slope is equal to 0.6° and the absolute position of carbody center of gravity is 3422.85 m.

The following results have been obtained.

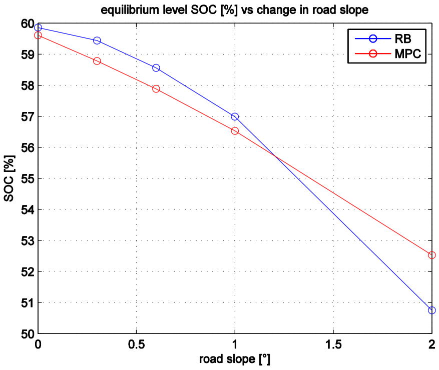

Figure 6.7: SOC equilibrium level as function of road slope.

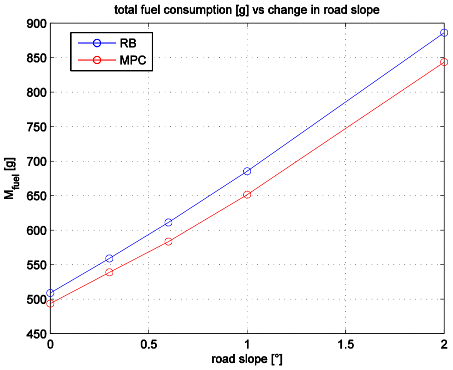

Figure 6.8: Fuel consumption as function of road slope.

Table 6.3: Values of the results displayed in the two figures above.

rule based	$SOC\ level$	59.86 %	59.44 %	58.86 %	56.99 %	50.75 %
MPC	$SOC\ level$	59.60 %	58.78 %	57.88 %	56.53 %	52.53 %
rule based	M_{fuel}	509.0 g	559.0 g	611.2 g	685.4 g	886.2 g
MPC	M_{fuel}	493.6 g	538.8 g	583.5 g	651.5 g	843.6 g
	road slope	0°	0.3 °	0.6 °	1 °	2 °

Table 6.4: Fuel economy and percentage variation with respect to the base case.

rule based	$l/100\ km$	5.927	6.509	7.117	7.981	10.32
	$\Delta\%$	0.0 %	+9.82 %	+20.08 %	+34.65 %	+74.12 %
MPC	$l/100\ km$	5.742	6.376	6.794	7.586	9.823
	$\Delta\%$	0.0 %	+7.58 %	+18.33 %	+32.12 %	+71.08 %
	road slope	0°	0.3 °	0.6 °	1 °	2 °

Even in this case the optimal control strategy is stable; the next figure shows how MPC tends to maintain the battery state of charge inside a band whose limits correspond to 56% and 58% for any value of road slope. This indicates that the strategy keeps the same operating principle and it indicates its capability to cope with modified driving conditions.

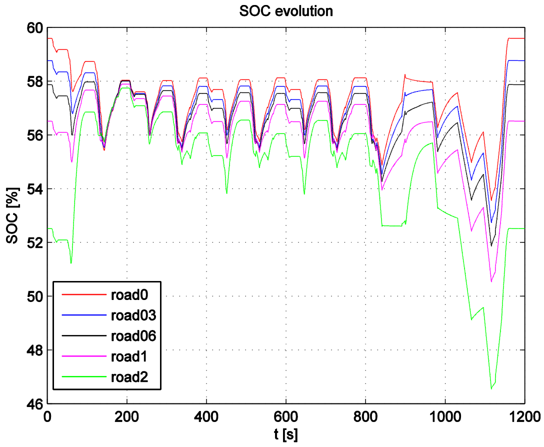

Figure 6.9: Time history of the SOC level as function of road slope.

6.1.3 Dimensionless coefficient of aerodynamic drag

Five different configurations have been analyzed and the base case corresponds to $C_x = 0.3\ [-]$.

$$C_x = 0.2,\ \ 0.25,\ \ 0.3,\ \ 0.35,\ \ 0.4\ .\ [\text{-}]$$

The following results have been obtained.

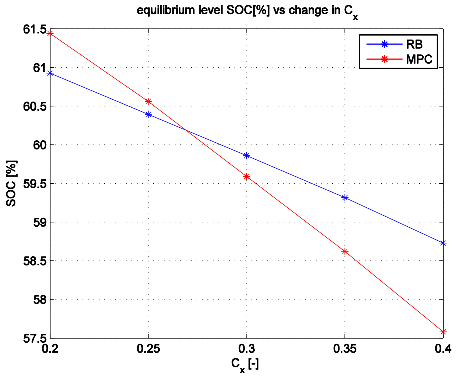

Figure 6.10: SOC equilibrium level as function of Cx

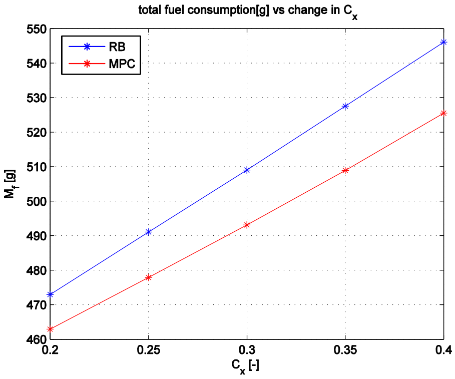

Figure 6.11: Fuel consumption as function of Cx.

Table 6.5: Values of SOC level and fuel consumption shown in the two figures above.

rule based	SOC **level**	60.92 %	60.39 %	59.86 %	59.31 %	58.73 %
MPC	SOC **level**	61.44 %	60.56 %	59.59 %	58.62 %	57.58 %
rule based	M_{fuel}	473.0 g	491.0 g	509.0 g	527.5 g	546.1 g
MPC	M_{fuel}	462.9 g	477.9 g	493.6 g	508.9 g	525.2 g
	C_x	0.2	0.25	0.3	0.35	0.4

Table 6.6: Fuel economy and percentage variation with respect to the base case.

rule based	$l/100\ km$	5.508	5.717	5.927	6.142	6.359
	$\Delta\%$	-7.07 %	-3.54 %	0.0 %	+3.63 %	+7.29 %
MPC	$l/100\ km$	5.390	5.565	5.742	5.926	6.116
	$\Delta\%$	-6.13 %	-3.08 %	0.0 %	+3.20 %	+6.51 %
	C_x	0.2	0.25	0.3	0.35	0.4

In this case the change of this factor seems to have higher influence on the variation of the equilibrium level of the battery state of charge rather than on total fuel consumption. This conclusion can be explained considering that the aerodynamic resistance becomes severe as the vehicle speed increases, roughly above 15 m/s the aerodynamic drag becomes the most important term in overall resistive force. The vehicle drives above this velocity threshold for a limited part of NEDC consequently the change in total fuel consumption is limited among different configurations. On the other hand the equilibrium level of the battery state of charge reduces as C_x increases and this is because less power can be recovered due to regenerative braking. Comparing the results obtained by increasing the carbody mass, where SOC_{level} increases as well, to these latter results it is clear that the MPC strategy maintains the battery state of charge level between 56% and 58% throughout the driving mission. Then if the vehicle has more inertia a higher final state of charge level is reached whereas with higher aerodynamic resistance regenerative braking is less efficient.

6.1.4 Parameters with low influence

The rotary inertia of the wheels, the stiffness of the silent chain and the adhesion coefficient between tyre and road have proved to have a very limited influence on fuel economy. The following cases have been tested:, the base case is written with red color.

$$J_{wheel}: \quad 1\,kgm^2\,, \qquad 2\,kgm^2\,, \qquad 3\,kgm^2\,, \qquad 4kgm^2$$

$$k_{chain}: \quad 50\frac{kN}{m}\,, \qquad 100\frac{kN}{m}\,, \qquad 300\frac{kN}{m}\,, \qquad 500\frac{kN}{m}$$

$$\mu_{adhesion}: \quad 0.8\,[-], \quad 0.9\,\,[-], \quad 1.0\,[-]$$

The results are only given for the MPC strategy.

Table 6.7: SOC equilibrium level and total fuel consumption as function of wheels rotary inertia.

$SOC\ level$	59.46 %	59.59 %	59.72 %	59.85 %
M_{fuel}	492.9 g	493.6 g	494.2 g	494.9 g
J_{wheel}	1 kgm^2	2 kgm^2	3 kgm^2	4 kgm^2

Table 6.8: SOC equilibrium level and total fuel consumption as function of silent chain stiffness.

$SOC\ level$	59.5907 %	59.5910 %	59.5912 %	59.5912 %
M_{fuel}	493.587 g	493.589 g	493.607 g	493.640 g
k	50 kN/m	100 kN/m	300 kN/m	500 kN/m

Table 6.9: SOC equilibrium level and total fuel consumption as function of adhesion coefficient tyre-road.

$SOC\ level$	59.5911 %	59.5911 %	59.5912 %
M_{fuel}	493.5870 g	493.5876 g	493.5876 g
$\mu_{adhesion}$	0.8	0.9	1.0

Some of the vehicle parameters that have been tested here appear inside the strategy too. They are used to predict the vehicle velocity over the prediction horizon from the prediction of torque request by integrating the discrete differential equation (4.9). The nominal values are implemented in the strategy and have been used to tune the MPC-based control strategy. In particular the total vehicle mass $m_{vehicle}$, the dimensionless coefficient of aerodynamic drag C_x, the rolling resistance coefficient f_r and the rotary inertia of the wheels J_{wheels} have been analyzed.

This analysis assumes that the value of a vehicle parameter specified inside the strategy does not correspond to the actual value hence it may influence the performance and the stability of the strategy. For this purpose the actual vehicle parameters have been kept fixed to their nominal values while the correspondent values inside the strategy have been varied one at a time. The following cases have been considered and 11 simulations have been run on NEDC; the first case is the base case.

Table 6.10: The 11 configurations that have been tested in this analysis.

test	$m_{vehicle}[kg]$	C_x [−]	f_r [−]	J_{wheel} [kgm^2]
1	1360	0.3	0.025	2
2	1500	0.3	0.025	2
3	1730	0.3	0.025	2
4	1360	0.15	0.025	2
5	1360	0.4	0.025	2
6	1360	0.55	0.025	2
7	1360	0.3	0.01	2
8	1360	0.3	0.04	2
9	1360	0.3	0.1	2
10	1360	0.3	0.025	1
11	1360	0.3	0.025	4

The results are reported in the next two figures in terms of state of charge equilibrium level and total fuel consumption.

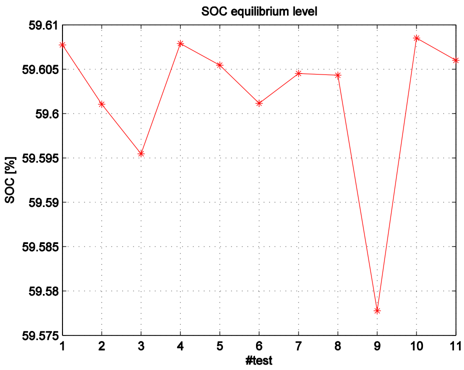

Figure 6.12: SOC equilibrium level correspondent to the 11 configurations listed above.

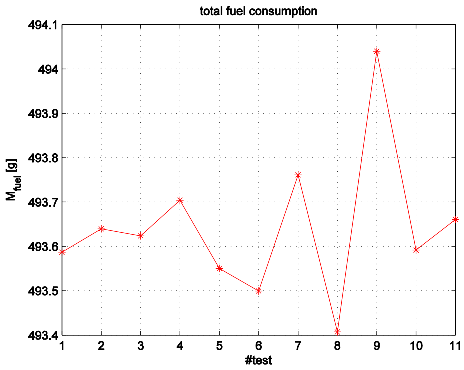

Figure 6.13: Total fuel consumption correspondent to the 11 configurations listed above.

The results reveal that the variability of these parameters do not cause major changes in the final outcomes of the system. Consequently MPC shows good robustness towards this type of uncertainty, in other words it can be stated that small errors in the prediction of the vehicle velocity over the prediction horizon do not affect the outcome of the strategy.

6.2 Analysis of internal parameters

The values of the control inputs are the solutions of a constrained optimization problem which depends on the objective function and the constraints but also on some internal parameters which are commonly use to manipulate the numerical research of an optimal solution. It is therefore worth to understand which internal parameters have the highest influence on the optimization problem because this may improve the performance of the control strategy by identifying a proper tuning procedure.

Two main ideas have inspired this analysis:

1) The OAT analysis carried out on some vehicle and road parameters has revealed that the carbody mass, the road slope and the coefficient of aerodynamic resistance have the highest influence on fuel economy. It is not possible to known the variation of C_x for instance when a luggage is put on the roof of a vehicle but it is possible to estimate the variation of carbody mass and road slope on real time nowadays.

   The former data can be for example estimated through load sensing valves while the latter data can be obtained using information provided by navigation systems like GPS/GIS.
2) The values of the internal parameters have been tuned manually on the basis of several simulations carried out on 5 reference drive cycles, it is important to analyze if another set of values may improve the performance of the strategy particularly when this set is obtained from an optimization procedure.

The application of navigation systems to the energy management control strategy to detect road slope variation is treated in the next part, while the problem of dealing with a variable carbody mass is treated here below.

6.2.1 Sensitivity analysis

The assessment of the effect of changing the values of the internal parameters has been accomplished together with an investigation of the possibility to improve fuel economy if the change in carbody mass were known. In practice different configurations of the internal parameters have been tested and the outcomes of the system (total fuel consumption and state of charge equilibrium level) have been stored. All configurations have been tested against two values of the carbody mass in order to understand if fuel economy could be improve by changing the values of the internal parameters coherently to the change in carbody mass. Sensitivity analysis is a powerful tool for this kind of numerical investigation since it provides a structured method to evaluate the response of the system to a number of input configurations and thus infer the connections between inputs and outputs. Appendix B provides more insight into this mathematical technique and into the procedure adopted in this thesis work. Design Of Experiment (DOE) analysis has been used extensively to define a list of suitable configurations of internal parameters to be tested. The experimental design has been structured in two main steps:

- 2-level design of experiment in order to determine the parameters having the highest influence on fuel economy.
- A refined DOE analysis based on Central Composite Design (CCD) in order to explore a wider input space of the internal parameters and calculate an optimal set.

Firstly the procedure is briefly described; secondly the results are reported and commented. Further details concerning DOE and CCD are available in Appendix B.

Description of the analysis

a) Full factorial 2-level DOE analysis

Initially the internal parameters have been sifted out in order to select a small subset of parameters which are likely to influence heavily the optimization algorithm. For example the penalty weights on the level and variation of the control inputs have the target to stabilize the control action but they do not affect fuel economy; similarly the rate of decay used to predict the torque requested by the driver has a minimum influence on the optimization routine. Eventually five parameters have been considered in the experimental design:

- H_p : length of the prediction horizon
- H_c : length of the control horizon
- T_i : defined as $H_i - H_p$, it represents the number of steps in the prediction horizon for which the penalty weights on the outputs are not further weighted by an exponential decay. If w_{SOC} is the weight applied to the deviation of the battery state of charge in the cost function, then for all k-th steps where $1 \leq k \leq H_i$ the weight is not modified, whereas for all k-th steps with $H_i + 1 \leq k \leq H_p$ the penalty weight is defined as $w_{SOC} \cdot e^{-\frac{i\omega t}{\tau}}$ where $\tau = 0.8s$ and $H_i \leq H_p$.

- w_{SOC}: is the weight applied to the deviation of the battery state of charge with respect to its reference level. Actually this analysis has considered the incremental variable Δw_{SOC} defined as $\Delta w_{SOC} = w_{SOC} - w_{SOC}^{base}$ where w_{SOC}^{base} is the base value of this weight.
- $w_{\dot{m}_f}$: is the penalty weight on the fuel mass flow rate. Even in this case the design variable is $\Delta w_{\dot{m}_f} = w_{\dot{m}_f} - w_{\dot{m}_f}^{base}$

The base values of the parameters are reported here below:

$$H_p = 12\ ;\ H_c = 10\ ;\ T_i = -2\ ;\ w_{SOC} = 1\ ;\ w_{\dot{m}_f} = 1.8\,, 1.6$$

Two values are specified for $w_{\dot{m}_f}$ because when the power request exceeds 30kW then $w_{\dot{m}_f} = 1.6$, while $w_{\dot{m}_f} = 1.8$ for all other situations.

The cycles NEDC and HWFET have been chosen as reference cycles since they involve different driving situations. NEDC includes both a typical urban driving and an extra-urban driving while HWFET has a long portion of high speed with medium power request. Moreover since the target is to investigate a possible relation between the value of the carbody mass and the optimal values of the internal parameters, each cycle has been repeated for two values of the *vehicle* mass:

- The base value 1360kg; the driver and no luggage.
- An overloaded vehicle 1730kg; 5 people on board plus the luggage.

Hence 4 driving scenarios have been considered and the correspondent values of carbody mass are 1280kg and 1650 kg. A full factorial 2-level DOE analysis has been carried out according to a L32 design matrix; the main effects are isolated from the cross-correlation effects. The high and low levels of each factor has been taken around the base case except for the length of the control horizon which has to satisfy the condition $H_c \leq H_p$.

Table 6.11: Low and high levels of each factor.

Parameter	Low	Base	High
$\boldsymbol{H_p}$	10	12	14
$\boldsymbol{H_c}$	6	8	10
$\boldsymbol{T_i}$	-4	-2	0
$\boldsymbol{\Delta w_{SOC}}$	-0.2	0	+0.2
$\boldsymbol{\Delta w_{\dot{m}_f}}$	-0.2	0	+0.2

The coefficients of influence, both main effects and cross-correlation effects, have been computed according to the following equations:

$$C_i^{SOC} = \frac{\begin{Bmatrix} +1 \\ -1 \\ \vdots \\ -1 \end{Bmatrix}_i^{t} * \begin{Bmatrix} SOC_1 \\ SOC_2 \\ \vdots \\ SOC_n \end{Bmatrix}}{n^\circ\ of\ observations\ for\ each\ level} \qquad C_i^{M_{fuel}} = \frac{\begin{Bmatrix} +1 \\ -1 \\ \vdots \\ -1 \end{Bmatrix}_i^{t} * \begin{Bmatrix} M_{fuel_1} \\ M_{fuel_2} \\ \vdots \\ M_{fuel_n} \end{Bmatrix}}{n^\circ\ of\ observation\ for\ each\ level}$$

where:

- C_i: coefficient of influence of the i-th column of the design matrix.
- SOC_j , M_{fuel_j} : system outputs correspondent to the j-th configuration of the parameters.
- $\begin{Bmatrix} +1 \\ -1 \\ \vdots \\ -1 \end{Bmatrix}_i$: i-th column of the design matrix.

b) DOE-CCD design

As it is clear from the results of the full factorial 2-level DOE analysis, the length of the prediction horizon has a limited influence on the outputs, thus it has been neglected in the subsequent refined experimental analysis. Its value has been set equal to the base case. The design matrix has been defined according to Central Composite Design since it allows each parameter to be tested on 5 levels with a limited number of simulations. Since the design matrix has been defined having the properties of being circumscribed and rotatable, 25 configurations are tested (See Appendix B for further details about these two properties of the experimental design).

The 5 levels are identified by the numbers:

$$-\alpha\,, -1\,, 0\,, +1\,, +\alpha$$

where α depends on the number of factors and on the desired properties of the design matrix. The properties of being circumscribed and rotatable with 4 factors, lead to $\alpha = 2$. In order to sweep as much as possible the input space of the factors, two configurations have been defined for the 5 levels of the factors. The configurations are reported in the next two tables.

Table 6.12: Levels of each parameter taken for Configuration A.

Configuration A

factor	-2	-1	0	+1	+2
H_p	10	12	14	16	18
T_i	-8	-6	-4	-2	0
Δw_{SOC}	-0.5	-0.25	0	+0.25	+0.5
$\Delta w_{\dot{m}_f}$	-0.5	-0.25	0	+0.25	+0.5

Table 6.13: Levels of each parameter taken for Configuration B.

Configuration B

factor	-2	-1	0	+1	+2
$\boldsymbol{H_p}$	18	19	20	21	22
$\boldsymbol{T_i}$	-8	-6	-4	-2	0
$\Delta\boldsymbol{w_{SOC}}$	-0.5	-0.25	0	+0.25	+0.5
$\Delta\boldsymbol{w_{\dot{m}_f}}$	-0.5	-0.25	0	+0.25	+0.5

The design matrix is defined as follows:

Table 6.14: Design matrix of the DOE-CCD analysis.

run	H_p	T_i	Δw_{SOC}	$\Delta w_{\dot{m}_f}$
#1	-1	-1	-1	-1
#2	-1	-1	-1	1
#3	-1	-1	1	-1
#4	-1	-1	1	1
#5	-1	1	-1	-1
#6	-1	1	-1	1
#7	-1	1	1	-1
#8	-1	1	1	1
#9	1	-1	-1	-1
#10	1	-1	-1	1
#11	1	-1	1	-1
#12	1	-1	1	1
#13	1	1	-1	-1
#14	1	1	-1	1
#15	1	1	1	-1
#16	1	1	1	1
#17	-2	0	0	0
#18	2	0	0	0
#19	0	-2	0	0
#20	0	2	0	0
#21	0	0	-2	0
#22	0	0	2	0
#23	0	0	0	-2
#24	0	0	0	2
#25	0	0	0	0

Total fuel consumption and state of charge equilibrium level are the two important outputs that have been considered in this analysis. The relations between the outputs and the levels of the factors is not clear looking at the 25 observations for this reason the response surface methodology is used to approximate the outputs with a continuous polynomial surface. This surface enables a deeper understanding of the weight of each factor on the outputs since the magnitude of the regression coefficients is used as ranking. For each analysis a regression model of total fuel consumption has been computed and sometimes a regression model of the minimum level of battery state of charge has also been computed.

The quality of the regression model has been assessed through statistical analysis, in particular the normal probability plot of the residuals, the adjusted R^2 coefficient and hypothesis testing of the regression coefficients. If the p-value of the t-test which evaluates the hypothesis that a regression coefficient is null against the hypothesis that it is not null, is greater than 0.05 that coefficient is removed from the regression model and the model is calculated once more.
If the quality of the new model results better than the previous one then that regressor is definitely removed from the model. The ANOVA and the regression fit have been carried out using the Matlab® function “NonLinearFit”.

Results

a) 2-level full factorial DOE

Pareto charts highlight the most important conclusions and the following nomenclature is adopted.

Nomenclature:

$$\begin{aligned} A &= H_p \\ B &= H_c \\ C &= T_i \\ D &= \Delta w_{SOC} \\ E &= \Delta w_{\dot{m}_f} \end{aligned}$$

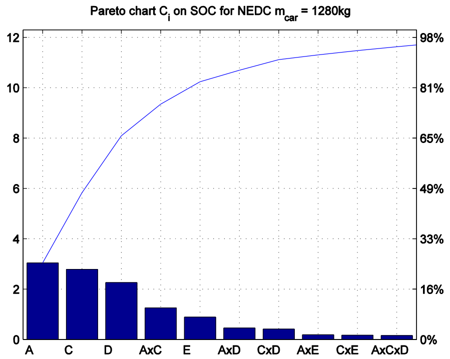

Figure 6.14: Coefficients of influence on SOC. NEDC 1280kg.

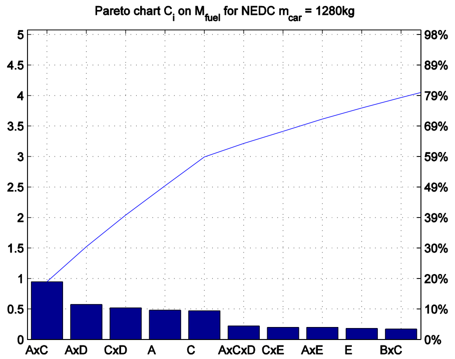

Figure 6.15: Coefficients of influence on fuel consumption. NEDC 1280kg

Table 6.15: Ci on SOC.NEDC 1280kg

Fattore	A	C	D	AxC	E
C_i	3.04	2.79	2.26	-1.3	-0.89

Table 6.16: Ci on fuel. NEDC 1280kg.

Fattore	AxC	AxD	CxD	A	C
C_i	0.94	0.6	0.52	-0.5	-0.5

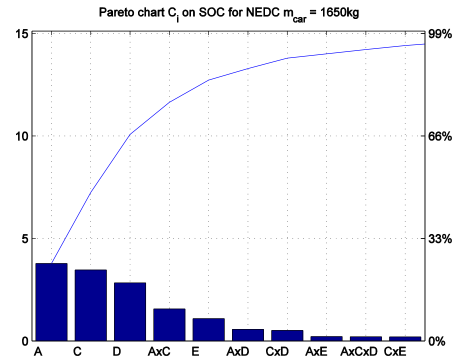

Figure 6.16: Coefficients of influence on SOC. NEDC 1650kg.

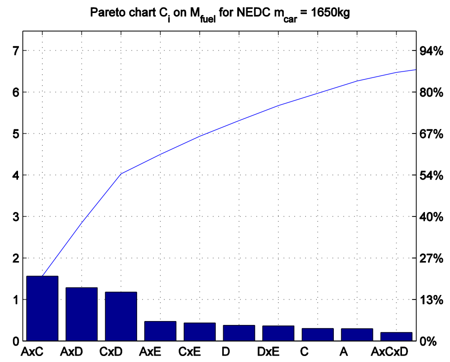

Figure 6.17: Coefficients of influence on fuel consumption. NEDC 1650kg.

Table 6.17: Ci on SOC. NEDC 1650kg.

Fattore	A	C	D	AxC	E
C_i	3.78	3.46	2.83	-1.6	-1.1

Table 6.18: Ci on fuel. NEDC 1650kg.

Fattore	AxC	AxD	CxD	AxE	CxE
C_i	1.56	1.3	1.2	-0.5	-0.4

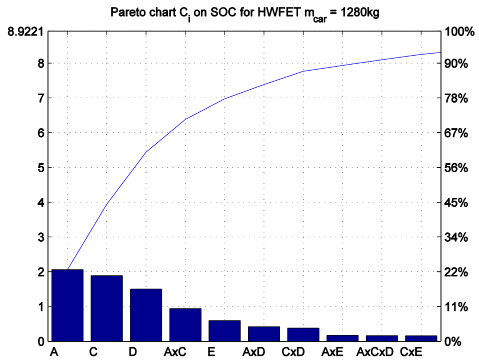

Figure 6.18: Coefficients of influence on SOC. HWFET 1280kg.

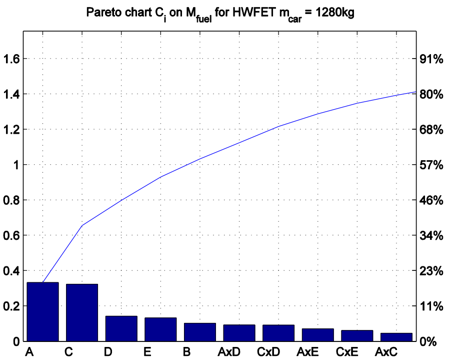

Figure 6.19: Coefficients of influence on fuel consumption. HWFET 1280kg.

Table 6.19: Ci on SOC. HWFET 1280kg.

Fattore	A	C	D	AxC	E
C_i	2.06	1.88	1.50	-0.9	-0.6

Table 6.20: Ci on fuel. HWFET 1280kg.

Fattore	A	C	D	E	B
C_i	-0.3	-0.3	-0.14	-0.13	0.10

Among these five factors, the length of the control horizon is the one which seems to have the lowest influence on the considered system outputs since it does not appear in most of the Pareto charts that are displayed above.

As a result this parameter has not been considered in the CCD experimental design and its value has been set equal to the nominal one (10 step). Regarding the other factors, the ranking of coefficients of influence on the equilibrium level of the state of charge does not change depending on the drive cycle and the vehicle mass. The length of the prediction horizon, the parameters T_i and Δw_{SOC} seem to have the highest importance on both system outputs. Another fundamental consideration is that the magnitude of the coefficients of influence on the equilibrium level of the battery state of charge is high, for instance the length of the prediction horizon has a correspondent coefficient which is always greater than 2. On the other hand the magnitude of the most important coefficients on total fuel consumption is limited and this suggests that it is difficult to produce remarkable variations of this output by tuning the values of the internal parameters of the strategy. Moreover the ranking changes depending on the drive cycle and on the value of the carbody mass.

b) DOE-CCD and regression analysis

Even before starting any complex mathematical post-processing of the results, it is clear from the collected observations that any attempt to reduce significantly the total fuel consumption is going to be unsuccessful. The following figures report the collected 25 observations of state of charge equilibrium level and total fuel consumption obtained over the NEDC with a carbody mass of 1650 kg, configuration A and for HWFET with a carbody mass of 1650 kg, configuration B.

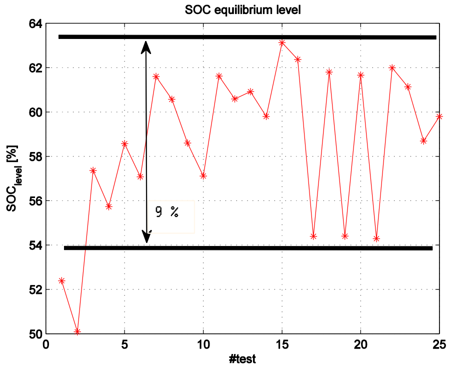

Figure 6.20: 25 values of SOC final level. NEDC 1650kg.

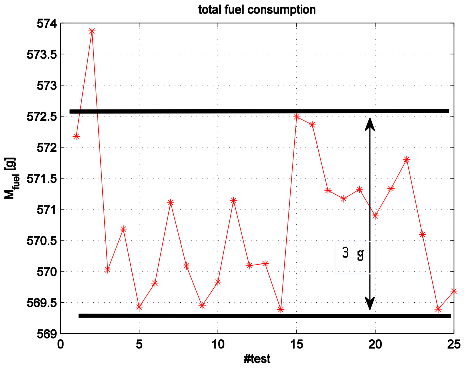

Figure 6.21: 25 values of fuel consumption. NEDC 1650kg.

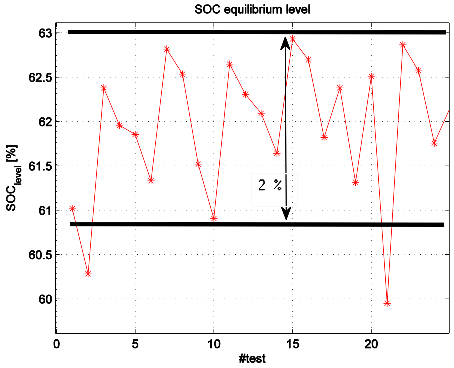

Figure 6.22: 25 values of SOC final level. HWFET 1650kg Conf. B.

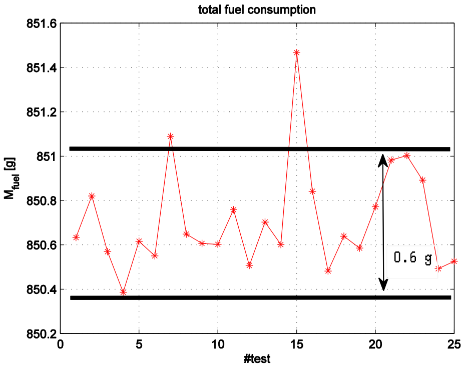

Figure 6.23: 25 values of fuel consumption.HWFET 1650kg Conf B.

The variation of total fuel consumption is limited and the span reduces moving to configuration B; similarly the variation of state of charge equilibrium level reduces too. In Figure 6.21 the observation number 25 corresponds to the result achievable with the nominal configuration of internal parameters. This result is close to the minimum total consumption that has been observed during these 25 observations, hence the nominal set of values would already result in a good fuel economy. In the case of the cycle HWFET with a carbody mass of 1650kg the nominal set of internal parameters brings to a total fuel consumption of 850.6 g hence even in this case the nominal set is close to the minimum observed result.

A polynomial regression model has been computed for each test case over the 25 collected data. The comparison of the models proves that general conclusions can be drawn not regarding the particular drive cycle or the value of the carbody mass, thus the regression model derived for the NEDC with a carbody mass of 1280kg and configuration A is discussed in the following as reference example.

A polynomial regression model has also been computed to describe the minimum level of the battery state of charge as function of the internal parameters in order to highlight the whole effect of these parameters on the energy management problem.

NEDC 1280kg. Configuration A

The regression analysis produces the following results.

Table 6.21: Coefficients of the regression model of fuel consumption and SOC minimum level.

Regression model for M_{fuel}		
NEDC 1280 Configuration A		
Factor	**Estimated Value**	**p-value**
H_p	-1.00	0.01
T_i	-1.21	6.74e-5
Δw_{SOC}	-6.16	0.0015
$\Delta w_{\dot{m}_f}$	/	/
$H_p \cdot T_i$	0.109	2.05e-6
$H_p \cdot \Delta w_{SOC}$	0.65	3.71e-5
$H_p \cdot \Delta w_{\dot{m}_f}$	-0.12	0.0018
$T_i \cdot \Delta w_{SOC}$	0.66	3.62e-5
$T_i \cdot \Delta w_{\dot{m}_f}$	-0.29	0.011
$\Delta w_{\dot{m}_f} \cdot \Delta w_{SOC}$	-1.43	0.108
$(H_p)^2$	0.048	0.0013
$(T_i)^2$	0.049	0.0012
$(\Delta w_{SOC})^2$	2.54	0.0053
$\left(\Delta w_{\dot{m}_f}\right)^2$	/	/

Regression model for $SOC_{level}^{minimum}$		
NEDC 1280kg Configuration A		
Factor	**Estimated Value**	**p-value**
H_p	2.41	8.0e-6
T_i	2.37	7.62e-8
Δw_{SOC}	11.28	6.17e-6
$\Delta w_{\dot{m}_f}$	-4.19	0.012
$H_p \cdot T_i$	-0.17	2.30e-8
$H_p \cdot \Delta w_{SOC}$	-0.58	8.28e-5
$H_p \cdot \Delta w_{\dot{m}_f}$	0.22	0.042
$T_i \cdot \Delta w_{SOC}$	-0.57	8.86e-5
$T_i \cdot \Delta w_{\dot{m}_f}$	0.22	0.044
$\Delta w_{\dot{m}_f} \cdot \Delta w_{SOC}$	1.57	0.064
$(H_p)^2$	-0.084	8.71e-6
$(T_i)^2$	-0.087	6.32e-6
$(\Delta w_{SOC})^2$	-5.23	1.14e-5
$\left(\Delta w_{\dot{m}_f}\right)^2$	/	/

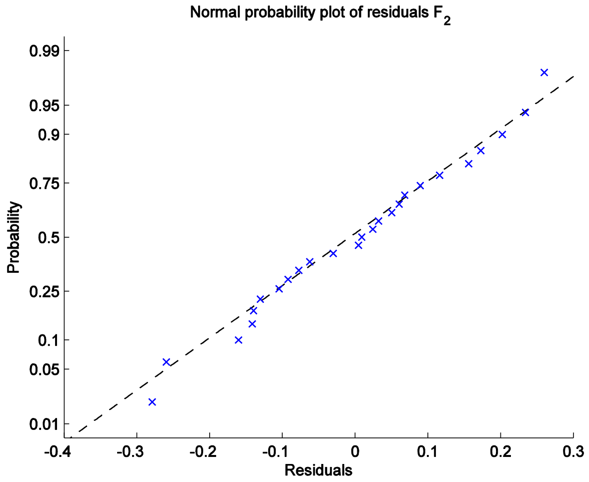

Figure 6.24: Normal probability plot of the residuals.

The adjusted R^2 is equal to 0.902. The normal probability plot, the p-value of the statistical test for goodness of test fit and the value of the adjusted R^2 support the idea that the regression model has a decent quality of regression. Analyzing the regression coefficients it emerges that the influence of $\Delta w_{\dot{m}_f}$ on total fuel consumption is weaker than the other parameters; its linear and quadratic terms have been removed from the regression model in order to achieve a good quality of the regression. On the other hand the quadratic dependence of total fuel consumption with respect to Δw_{SOC} is strong; therefore the regression coefficients seem to confirm the preliminary conclusions that have been achieved from the 2-level full factorial DOE. It is interesting to plot the observed total fuel consumption as function of the length of the prediction horizon solely, thus the outcome of simulations number #17, #18 and #25 are displayed in the following figure.

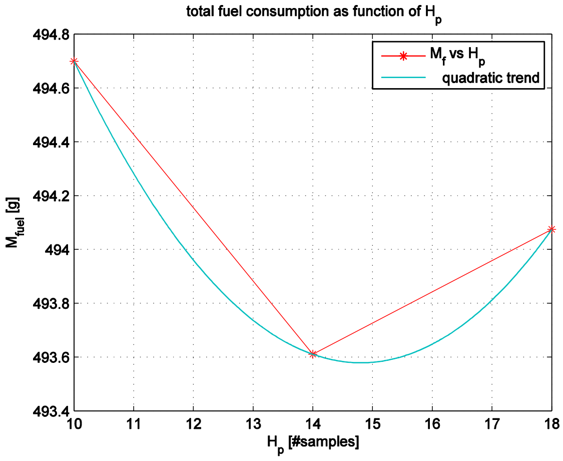

Figure 6.25: Total fuel consumption for low, base and high level of Hp.

There is a length of the prediction horizon which seems to be optimal to achieve the lowest fuel consumption. This conclusion is supported by the optimization procedure which returns the set of internal parameters which minimizes only the total fuel consumption. The genetic algorithm applied to the 25 observations return the following optimal set:

point of minimum F2: 12 ; 0 ; -0.170879 ; 0.499773
minimum value of the object function : 492.6828 (6.1)
exitflag for F2 : 1

The optimal length of the prediction horizon is lower than the optimal value that can be extracted from Figure 6.25 but it is necessary to consider that this figure illustrates the total fuel consumption when the length of the prediction horizon is the only variable which increases its value, whereas the optimization procedure takes into account the cross-correlation terms. For instance the three observations represented in Figure 6.25 refer to configurations where $T_i = -4$ however the optimal set defines an optimal value for $T_i = 0$ this means that these two variables are closely linked to each other and varying them in an opposite way leads to similar final results. If the optimal set defined above is compared to the nominal values of the internal parameters of the MPC strategy it emerges that the main difference is in the optimal value of $\Delta w_{\dot{m}_f}$, thus the penalty weight applied to the fuel mass flow rate increases. This is a reasonable conclusion when the total fuel consumption is the only objective of the genetic algorithm however Table 6.21 illustrates how this latter variable has a strong influence on the minimum level reached by the battery state of charge throughout the driving mission. If the optimal set were implemented in the MPC-based control strategy it would produce a remarkable drop in the equilibrium level of the battery state of charge.

This reasoning is confirmed by a further analysis that has compared directly the nominal set of values to the optimal one in (6.1) over NEDC with a carbody mass of 1280kg.

Table 6.22: Comparison of the nominal against the optimal set of internal parameters.

MPC strategy	M_{fuel}	$SOC_{equilibrium}$	$SOC_{minimum}$
Nominal	493.6 g	59.6	53.6
Optimal	493.0 g	57.2	51.0

Although the minimum level of the battery state of charge is higher than the minimum threshold in both situations, it is important to mitigate the drop of state of charge level in those cycles which involve strong accelerations therefore it is advisable to keep the weight on the fuel mass flow rate equal to its base value.

The analyses carried out with configuration B of the internal parameters prove once more that it is useless to lengthen the prediction horizon more than 14 steps since the total fuel consumption tends to increase. This result is shown in the next two figures both for NEDC and for HWFET.

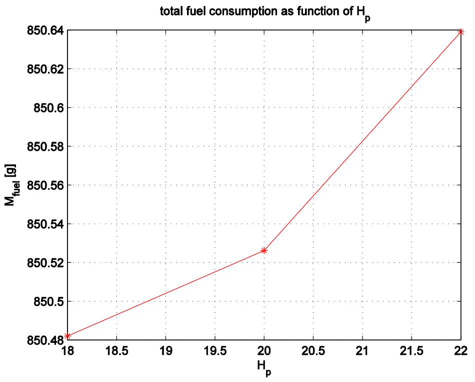

Figure 6.26: Total fuel consumption as function of Hp. HWFET.

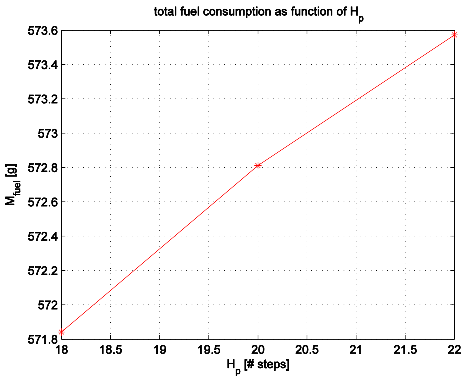

Figure 6.27: Total fuel consumption as function of Hp. NEDC.

Collecting all information, the penalty weight w_{SOC} and the length of the prediction horizon H_p seem to be the internal parameters which have the highest influence on total fuel consumption and battery state of charge. The influence of the parameter T_i is closely related to the value of H_p; in fact both of them tend to increase the importance of the deviation of the battery state of charge in the cost function consequently similar results are achieved by increasing H_p and reducing simultaneously T_i or vice versa. In conclusion the sensitivity analysis on internal parameters reveals that:

- The nominal setting of internal parameters is adequate to achieve good fuel economy over all reference drive cycles. This set manages to keep the battery state of charge level inside the prescribed operating band while reducing total fuel consumption with respect to a rule based strategy.
- It is not possible to find a different set of internal parameters values which allows the control strategy to reduce further the total fuel consumption as function of carbody mass.
- H_p and Δw_{SOC} are the internal parameters which have the highest influence on the performance of the strategy in terms of equilibrium level of the battery state of charge and total fuel consumption.
- The optimal value of H_p is found in-between 11 and 14. It has been observed during the tuning procedure that values lower than 10 produce worse fuel consumption and very small value (i.e. lower than 6 samples) produce an oscillatory behavior of the optimal solution.

6.2.2 Integration of GPS/GIS

Thanks to the information provided by GPS and GIS it is possible to know the instantaneous vehicle position on the earth surface and also map the slope of the road that the vehicle is going to encounter. This information can be used to predict the power request that the driver is likely to require in the near future.
The information on vehicle spatial position can be even more useful in the case of a pubic mean of transportation like a bus which is supposed to repeat the same driving route several times per day and therefore the stochastic properties of future driving conditions can be foreseen with more accuracy than for a passenger vehicle whose path cannot be known in advance. Assuming that the average velocity of the bus and the average driver's torque request have been collected during driving under several repetitions of the same route, it is possible to assign the average power request to each spatial position of the bus along a specific route. If a further simplification is considered, namely the average velocity profile coincides with the reference velocity profile of the considered drive cycle and the average torque request corresponds to the torque request that can be obtained running a simulation on the same drive cycle, then the desired velocity and torque profiles can be provided to the MPC-based control strategy as inputs. This represents undoubtedly an ideal situation but it enables to evaluate the performance of the strategy when it works under the best possible operating conditions. This part of the report deals with such a simplified model and the aim is to investigate the role of the prediction on the numeric solution of the optimization problem. In fact the choice to describe the torque request over the prediction horizon according to an exponential decay is just one of the available approaches, hence by using directly the real envelope of this variable it is possible to judge if an alternative description may bring to a different sequence of control actions.

For this purpose the profiles of the desired vehicle velocity and of the driver's torque request have been stored in look-up tables and used at each sampling time as inputs to the control strategy. The optimization has been limited to a prediction horizon of finite length thus the look-up tables return just a portion of the trends of these two input variables. At sampling time t_k vehicle position and speed, driver's requested torque are measured. In order to be able to predict wheel torque and vehicle speed over the prediction horizon it is necessary to know the correspondent positions of the vehicle center of mass. Vehicle position is calculated after each prediction period by assuming that vehicle speed at one sample remains constant over the following prediction period. Since the prediction period is equal to 0.5s this assumption holds provided that the instantaneous longitudinal acceleration is limited. This is the case for both NEDC and HWFET where longitudinal acceleration exceeds rarely a magnitude level of $0.6m/s^2$. The vehicle velocity and position are updated in parallel, and once the new vehicle position is known a look-up tables is used to determine the torque request at the same sampling time. Eventually the values of vehicle velocity and torque request are stored in two discrete vectors. It is therefore assumed that in a first phase the control strategy communicates with the navigation systems in order to acquire all these information and subsequently the optimization problem is solved. This implies that an ideal situation is considered where communication between MPC and navigation systems can occur in a time period much smaller than the time required to solve the optimization problem and thus the optimal values of the control variables can always be found within a sampling period. All simulations have been carried out testing the nominal control strategy characterized by the following parameters:

$$H_p = 12\,, H_c = 10\,, T_i = -2\,, \Delta w_{SOC} = 0\,, \Delta w_{\dot{m}_f} = 0$$

The vehicle parameters have been set equal to their nominal values. The cycles NEDC and HWFET have been used as reference and a variable road profile has been specified. The reference driving conditions of these two cycles are reported in the next figures.

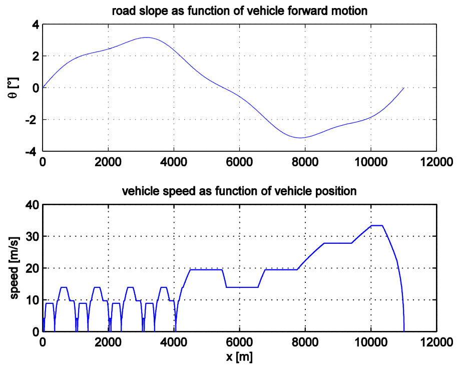

Figure 6.28: Road slope and velocity profile for NEDC.

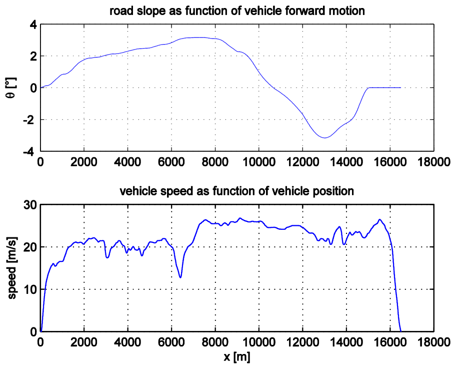

Figure 6.29: Road slope and velocity profile for HWFET.

The simulations have produced the following results.

Table 6.23: Fuel consumption with the nominal MPC strategy and the strategy which knows perfectly the future power request.

	NEDC	**HWFET**
Strategy	$\boldsymbol{M_{fuel}}\ [\boldsymbol{g}]$	$\boldsymbol{M_{fuel}}\ [\boldsymbol{g}]$
Baseline	518.72	761.35
Exact prediction	518.50	761.0

As it is evident from these latter results the influence of the predictions on the solution of the optimization problem and hence on fuel consumption is negligible. The optimization problem does not seem to be severely affected by the predictions of these variables. A piece of evidence which supports this conclusion is shown in the next figure.

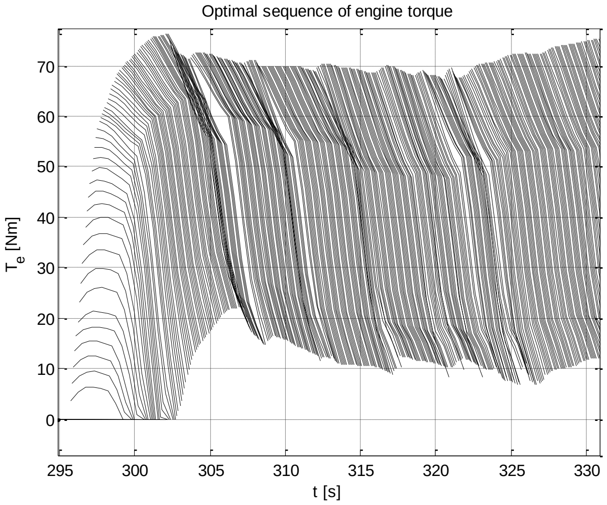

Figure 6.30: Sequence of optimal values of engine torque. HWFET.

This latter figure represents the sequence of optimal values of engine torque over the control horizon obtained as solution of the optimization problem repeated at each sampling time. The engine torque tends to increase in the early stage of the control horizon while it diminishes quickly in the second part. This trend can be seen as the willingness of MPC to restore or keep at high level the battery state of charge in the first part of the prediction while the usage of engine power reduces in the second portion in order to minimize fuel consumption. As a result it seems that the deviation of the battery state of charge with respect to its reference level is the most important term in the first half of the prediction horizon while the fuel mass flow rate becomes more important in the second half. This conclusion can explain why the prediction is not really important in the solution of the optimization problem. The optimization problem is mainly driven by the deviation of the battery state of charge and the level of power request at the sampling time and not by their envelope along the prediction horizon. Nonetheless the prediction is still important to guarantee the stability of the strategy. In fact other simulations have shown how a length of the prediction horizon shorter than 6 samples or a length of the control horizon shorter than 2 samples make the control action irregular and in some cases large fluctuations appear either in the engine or in the generator optimal value.

7 Conclusions and future works

This thesis work has shown the capability of a MPC-based energy management control strategy to achieve better fuel economy than an optimized rule based strategy implemented in Amesim®. The direct comparison with a rule based strategy serves to quantify the performance of the MPC strategy. In particular the improvement of overall efficiency seems to be larger for extra-urban driving, rather than for urban driving. For instance the percentage reduction of fuel consumption in UDDS urban cycle is equal to -0.84% whereas it is equal to $-3.12\ \%, -8.83\ \%, -17.75\ \%$ in cycles NEDC, SC03, US06 respectively which involve urban and extra urban conditions and high speed driving. The key for this step ahead is a more efficient power split between battery and engine. The engine provides the average power request while electric power supports the engine in all driving situations to reduce the overall load and let this power unit work in a region of low fuel consumption. The control action is obtained as the solution of an optimization problem which makes use of a prediction of future power request to decide the power split among the power units. However the results have shown how the optimization problem is mostly driven by the battery state of charge level and the driver's torque request at sampling time. For the same level of power request the engine torque is adjusted depending on the state of discharge of the battery.

The sensitivity analysis focused on internal parameters has shown how the state of charge equilibrium level varies significantly according to the setting of these parameters while total fuel consumption is less influenced. It has been found that the length of the prediction horizon, H_p, and the variation of the penalty weight of the deviation of the state of charge, Δw_{SOC}, have the highest influence on the outcome of the optimization problem. The optimal value of H_p is around 11. By increasing H_p fuel economy degrades. This is a first piece of evidence that prediction is not fundamental but this latter conclusion is mostly supported by the last analysis where additional information coming from GPS/GIS are used to manipulate the control strategy. The correct torque and velocity profiles have been assigned to the strategy but eventually the decisions taken by the controller did not change. In particular, it has been proved that no matter the torque description the optimal values of the control variables remain almost the same; the magnitude of the optimal engine torque depends mainly on the sampled value of the battery state of charge. This is a piece of advantage since future power request is usually unknown. Furthermore it also indicates that the control strategy is quite static and dominated by the deviation of the state of charge level. Prediction is in any case fundamental to solve the optimization problem and stabilize the control strategy however if additional information on traffic, road conditions were available, they should be exploited by another controller which is placed above MPC and can actively modify some parameters of the MPC control strategy like for instance the reference value of the battery state of charge as function of road slope.

In this thesis work the control strategy has been developed in order to take into account few issues related to drivability. In particular a typical problem associated to a HEV is engine starting and stopping which usually occurs when the vehicle is moving and it causes vibrations which degrade the on-board comfort. The amount of vibrations have been reduced by controlling the dynamics of these events through the generator torque. The results have shown how the oscillations related to engine starting and stopping can be significantly reduced when the vehicle supervisory controller can directly adjust this latter control variable. The standard norm ISO 2631-5 prescribes that the equivalent acceleration felt by the passenger should be lower than $0.5\,m/s^2$; the strategy manages to start and stop the engine rotation without causing a total acceleration higher than this threshold value. The comfort analysis has been carried out in the cycle NEDC and it thus shows the capability of the strategy to include objectives defined by different fields.

Another piece of advantage is that the strategy can be applied to any drive cycle and none parameter has been tuned for specific driving conditions. From this point of view this strategy is more robust than, for instance, A-ECMS where the equivalency factor depends on the driving scenario.

Possible drawbacks have been identified in the linear time varying approach which implies to use a linearized state space form at each sampling time. Linearization introduces some errors like for instance the prediction of electric machines power loss. It has been shown how the linearization of the nonlinear function which describes the power loss inside the electric generator can produce an oscillatory behavior of the optimal control action defined by the MPC strategy. This problem has been solved by penalizing the variation of the electric generator output torque when the engine is working and the generator rotor angular velocity approaches the null value. However this idea introduces a penalty weight that is based on the value of the generator angular velocity at the sampling time thus it may suffer from measurement noise in the input data. Moreover the actual implementation of a MPC strategy for energy management of a hybrid vehicle still retains some doubts. In fact the values of the control inputs are determined through numerical solution of an optimization problem and the solver should be fast enough to find an optimal solution within a sampling period. In this thesis a sampling period of 0.1s has been used but similar results can be obtained using a slightly longer sampling period equal to 0.2s. The numerical simulations have shown that the time required to find a suitable optimal solution is shorter than the sampling period, thus the implementation of the strategy on the calculator did not represent an issue. The optimized active set algorithm has been developed to be suitable for real time purposes. Nevertheless it is necessary to investigate more how the strategy should behave when, for any reason, it is not possible to find a solution in view of real time application. Furthermore Model Predictive Control is a model based approach meaning that it is always necessary to define a simple but reliable model of the dynamic system and any modification applied to the powertrain may require to develop a complete new model.

Further improvements may appeal to the extension of the cost function in order to include the emission rates of pollutants and analyze how the operating point of the engine changes when both fuel consumption and pollutant emissions should be minimized. Secondly it would be interesting to refine the analysis of the implementation of navigation systems to improve the optimization problem by designing a high level controller placed above the vehicle supervisory controller in the hierarchical structure of the energy management of a hybrid electric vehicle. Since the solution to the optimization problem seems to be mainly driven by the level of the battery state of charge and power request at the sampling time, it is worth to compare the MPC-based control strategy against A-ECMS which solves an instantaneous optimization problem.

Appendix A - Matrix approach to MPC

Consider the linearized discretized state space form given in (4.31).

$$\begin{cases} x(k+1|k) = A_d x(k|k) + B_d^u u(k|k) + B_d^v v(k|k) + F_d \\ y(k|k) = C_d x(k|k) + D_d^u u(k|k) + D_d^v v(k|k) + G_d \end{cases} \tag{A.1}$$

Once the initial conditions $x(k|k)$, the sequence of control inputs $U = \{u(k|k), \dots, u(k+H_c-1|k)\}$ and the sequence of external disturbances $V = \{v(k|k), \dots, v(k+H_p-1|k)\}$ are assigned, the state space form (A.1) can be used to predict the resulting future values of system states and outputs.
Firstly the states are computed as follows.

$$x(k+1|k) = A_d x(k|k) + B_d^u u(k|k) + B_d^v v(k|k) + F_d$$

$$\begin{aligned} x(k+2|k) = {} & A_d(A_d x(k|k) + B_d^u u(k|k) + B_d^v v(k|k) + F_d) + B_d^u u(k+1|k) \\ & + B_d^v v(k+1|k) + F_d \\ = {} & A_d^2 x(k|k) + [A_d B_d^u \quad B_d^u] \begin{Bmatrix} u(k|k) \\ u(k+1|k) \end{Bmatrix} + [A_d B_d^v \quad B_d^v] \begin{Bmatrix} v(k|k) \\ v(k+1|k) \end{Bmatrix} \\ & + (A_d + I) F_d \end{aligned}$$

$$\begin{aligned} x(k+3|k) = {} & A_d^3 x(k|k) + [A_d^2 B_d^u \quad A_d B_d^u \quad B_d^u] \begin{Bmatrix} u(k|k) \\ u(k+1|k) \\ u(k+2|k) \end{Bmatrix} \\ & + [A_d^2 B_d^v \quad A_d B_d^v \quad B_d^v] \begin{Bmatrix} v(k|k) \\ v(k+1|k) \\ v(k+2|k) \end{Bmatrix} + (A_d^2 + A_d + I) F_d \end{aligned}$$

$$\vdots$$

The predictions of the states are then used to predict the system outputs over the prediction horizon.

$$y(k|k) = C_d x(k|k) + D_d^u u(k|k) + D_d^v v(k|k) + G_d$$

$$\begin{aligned} y(k+1|k) = {} & C_d A_d x(k|k) + [C_d B_d^u \quad D_d^u] \begin{Bmatrix} u(k|k) \\ u(k+1|k) \end{Bmatrix} \\ & + [C_d B_d^v \quad D_d^v] \begin{Bmatrix} v(k|k) \\ v(k+1|k) \end{Bmatrix} + [C_d \quad I] \begin{Bmatrix} F_d \\ G_d \end{Bmatrix} \end{aligned}$$

$$\begin{aligned} y(k+2|k) = {} & C_d A_d^2 x(k|k) + \begin{bmatrix} C_d A_d B_d^u & C_d B_d^u & D_d^u \end{bmatrix} \begin{Bmatrix} u(k|k) \\ u(k+1|k) \\ u(k+2|k) \end{Bmatrix} \\ & + \begin{bmatrix} C_d A_d B_d^v & C_d B_d^v & D_d^v \end{bmatrix} \begin{Bmatrix} v(k|k) \\ v(k+1|k) \\ v(k+2|k) \end{Bmatrix} \\ & + \begin{bmatrix} (C_d A_d + C_d) & I \end{bmatrix} \begin{Bmatrix} F_d \\ G_d \end{Bmatrix} \end{aligned}$$

Using a matrix formulation, the sequence of system outputs over the prediction horizon can be formulated as follows.

$$\text{У} = \Psi\, x(k|k) + \Upsilon U + \Omega V + \Pi \begin{Bmatrix} F \\ g \end{Bmatrix} \tag{A.2}$$

where:

- $V(k+i|k)\ with\ \ i = 0 \ldots . H_p - 1$ sequence of known measured disturbances
- $\hat{X}(k+i|k)\ with\ \ i = 0 \ldots . H_p - 1$ sequence of predicted states
- $\hat{Y}(k+i|k)\ with\ \ i = 0 \ldots . H_p - 1$ sequence of predicted outputs
- $U(k+i|k)\ with\ \ i = 0 \ldots . H_c - 1$ sequence of control inputs to be optimized
- $x(k|k)$ measured system state at the sampling time k
- $y(k+i|k) =$ $\left\{SOC(k+i|k), \dot{m}_f(k+i|k), \omega_g(k+i|k), T_m(k+i|k), \omega_m(k+i|k), P_{batt}(k+i|k), \omega_e(k+i|k)\right\}^t$
- $u(k+i|k) = \left\{T_e(k+i|k), T_g(k+i|k), T_b(k+i|k)\right\}^t$

  $v(k+i|k) = \{T_{drive}(k+i|k), \dot{x}(k+i|k)\}^t$

$$\Psi = \begin{bmatrix} C_d \\ C_d A_d \\ C_d A_d^2 \\ C_d A_d^3 \\ \vdots \\ C_d A_d^{i-1} \\ \vdots \end{bmatrix}$$

$$\Upsilon = \begin{bmatrix} D_{d,u} & [0] & [0] \\ C_d B_{d,u} & D_{d,u} & [0] \\ C_d A_d B_{d,u} & C_d B_{d,u} & D_{d,u} \\ & & \left(C_d B_{d,u} + D_{d,u}\right) \\ C_d A_d^2 B_{d,u} & C_d A_d B_{d,u} & \vdots \\ \vdots & \vdots & \\ C_d A_d^{i-2} B_{d,u} & C_d A_d^{i-c-1} B_{d,u} & \left(\left(\sum_{t=0}^{i-H_c-1} C_d A_d^t B_{d,u}\right) + D_{d,u}\right) \\ \vdots & \vdots & \\ & & \vdots \end{bmatrix}$$

$$\Omega = \begin{bmatrix} D_{d,v} & [0] & & [0] \\ C_d B_{d,v} & D_{d,v} & [0] & [0] \\ C_d A_d B_{d,v} & C_d B_{d,v} & D_{d,v} & \vdots \\ C_d A_d^2 B_{d,v} & C_d A_d B_{d,v} & \cdots & [0] \\ \vdots & \vdots & \vdots & \vdots \\ C_d A_d^{i-2} B_{d,v} & C_d A_d^{i-c-1} B_{d,v} & \cdots & [0] \\ \vdots & \vdots & \vdots & D_{d,v} \end{bmatrix}$$

$$\Pi = \begin{bmatrix} [0] & I \\ \vdots & \vdots \\ \left(\sum_{t=0}^{i-2} C_d A_d^t\right) & \vdots \end{bmatrix}$$

In this formulation it is assumed that $H_c < H_p$ consequently $u(k + H_c + i - 1|k) = u(k + H_c - 1|k)$ for $i = 1, \dots, H_p - H_c$.
In the following it is assumed that:

$$P = \Pi * \begin{Bmatrix} F \\ g \end{Bmatrix}$$

Constraints

Suppose that the constraints for one sample in the prediction and in the control horizon respectively are expressed in matrix form as follows:

$$\left[m_y^{max}\right] y(k+i) \leq \left\{b_y^{max}\right\}$$

$$\left[m_y^{min}\right] y(k+i) \leq \left\{b_y^{min}\right\}$$

$$\left[m_u^{max}\right] u(k+i) \leq \left\{b_u^{max}\right\}$$

$$\left[m_u^{min}\right] u(k+i) \leq \left\{b_u^{min}\right\}$$

The constraints are enforced along the whole prediction and control horizons through the sequences of control inputs and system outputs; block diagonal matrices are created.

$$\begin{bmatrix} \begin{bmatrix} \left[m_y^{max}\right] & & [0] \\ & \ddots & \\ [0] & & \left[m_y^{max}\right] \end{bmatrix} \\ \begin{bmatrix} \left[m_y^{min}\right] & & [0] \\ & \ddots & \\ [0] & & \left[m_y^{min}\right] \end{bmatrix} \end{bmatrix} \mathrm{y} \leq \begin{Bmatrix} \left\{b_y^{max}\right\} \\ \vdots \\ \vdots \\ \left\{b_y^{max}\right\} \\ \left\{b_y^{min}\right\} \\ \vdots \\ \vdots \\ \left\{b_y^{min}\right\} \end{Bmatrix}$$

$$\begin{bmatrix} \begin{bmatrix} \left[m_u^{max}\right] & & [0] \\ & \ddots & \\ [0] & & \left[m_u^{max}\right] \end{bmatrix} \\ \begin{bmatrix} \left[m_u^{min}\right] & & [0] \\ & \ddots & \\ [0] & & \left[m_u^{min}\right] \end{bmatrix} \end{bmatrix} U \leq \begin{Bmatrix} \left\{b_u^{max}\right\} \\ \vdots \\ \vdots \\ \left\{b_u^{max}\right\} \\ \left\{b_u^{min}\right\} \\ \vdots \\ \vdots \\ \left\{b_u^{min}\right\} \end{Bmatrix}$$

A more compact form:

$$\begin{bmatrix} \left[M_y^{max}\right] \\ \left[M_y^{min}\right] \end{bmatrix} \mathrm{y} \leq \begin{Bmatrix} B_y^{max} \\ B_y^{min} \end{Bmatrix}$$

$$\begin{bmatrix} \left[M_u^{max}\right] \\ \left[M_u^{min}\right] \end{bmatrix} U \leq \begin{Bmatrix} B_u^{max} \\ B_u^{min} \end{Bmatrix}$$

By using (A.2) in place of the sequence of system outputs, it is possible to express all constraints with respect to the sequence of control inputs.

$$\left|\begin{matrix}[M_y^{max}]\Upsilon \\ [M_y^{min}]\Upsilon\end{matrix}\right| U \leq \left\{\begin{matrix}B_y^{max} - M_y^{max}\Psi x(k) - M_y^{max}\Omega V - M_y^{max}P \\ B_y^{min} - M_y^{min}\Psi x(k) - M_y^{min}\Omega V - M_y^{min}P\end{matrix}\right\}$$

$$\left|\begin{matrix}[M_u^{max}] \\ [M_u^{min}]\end{matrix}\right| U \leq \left\{\begin{matrix}B_u^{max} \\ B_u^{min}\end{matrix}\right\}$$

Eventually the standard expression of inequalities constraints can be achieved by collecting all matrices and all vectors as follows.

$$[A] = \left|\begin{matrix}[M_y^{max}]\Upsilon \\ [M_y^{min}]\Upsilon \\ [M_u^{max}] \\ [M_u^{min}]\end{matrix}\right| \qquad \{b\} = \left\{\begin{matrix}B_y^{max} - M_y^{max}\Psi x(k) - M_y^{max}\Omega V - M_y^{max}P \\ B_y^{min} - M_y^{min}\Psi x(k) - M_y^{min}\Omega V - M_y^{min}P \\ B_u^{max} \\ B_u^{min}\end{matrix}\right\}$$

Cost function

The discrete expression of the cost function for the energy management problem includes a summation along the control horizon and a summation along the prediction horizon.

$$\begin{aligned}J(U) = \sum_{i=1}^{H_p-1} \Bigg[& (SOC(k+i) - SOC^{ref})^2_{w_{SOC}} + \left(\dot{m}_f(k+i)\right)^2_{w_{\dot{m}_f}} \\ & + \left(\omega_g(k+i) - \omega_g^{ref}\right)^2_{w_{\omega_g}} + \left(\omega_e(k+i)\right)^2_{w_{\omega_e}}\Bigg] \\ & + \sum_{i=0}^{H_c-1}\left[\left(u(k+i)\right)^2_{w_u} + \left(\Delta u(k+i)\right)^2_{w_{\Delta u}}\right]\end{aligned}$$

A more compact expression is achieved by introducing diagonal matrices of the weights and vectors of system outputs and states.

$$\begin{aligned}J(U,k) = & \sum_{i=1}^{H_p-1}\left[(\hat{y}_{cost}(k+i|k) - y^{ref}(k+i|k))^t[Q](\hat{y}_{cost}(k+i|k) - y^{ref}(k+i|k))\right] \\ & + \sum_{i=0}^{H_c-1}\left[u(k+i|k)^t[R]u(k+i|k) + \Delta u(k+i|k)^t[S]\Delta u(k+i|k)\right]\end{aligned}$$

By using the sequences of system outputs and control inputs in place of summations, the following final matrix formulation is obtained.

$$J(U,k) = \left(\hat{y}_{cost} - y^{ref}\right)^t[W_y]\left(\hat{y}_{cost} - y^{ref}\right) + U^t[W_u]U + \Delta U^t[W_{\Delta U}]\Delta U \tag{A.3}$$

where:

$$[W_y] = \begin{bmatrix} [Q] & 0 & 0 \\ 0 & \ddots & 0 \\ 0 & 0 & [Q] \end{bmatrix} \qquad [W_u] = \begin{bmatrix} [R] & 0 & 0 \\ 0 & \ddots & 0 \\ 0 & 0 & [R] \end{bmatrix} \qquad [W_{\Delta u}] = \begin{bmatrix} [S] & 0 & 0 \\ 0 & \ddots & 0 \\ 0 & 0 & [S] \end{bmatrix}$$

$$[Q] = \begin{bmatrix} w_{SOC} & 0 & 0 & 0 \\ 0 & w_{\dot{m}_f} & 0 & 0 \\ 0 & 0 & w_{\omega_g} & 0 \\ 0 & 0 & 0 & w_{\omega_e} \end{bmatrix} \qquad [R] = \begin{bmatrix} w_{T_e} & 0 & 0 \\ 0 & w_{T_g} & 0 \\ 0 & 0 & w_{T_b} \end{bmatrix}$$

$$[S] = \begin{bmatrix} w_{\Delta T_e} & 0 & 0 \\ 0 & w_{\Delta T_g} & 0 \\ 0 & 0 & w_{\Delta T_b} \end{bmatrix} \qquad \eta = \begin{bmatrix} [\xi] & 0 & 0 \\ 0 & \ddots & 0 \\ 0 & 0 & [\xi] \end{bmatrix}$$

$$\xi = \begin{bmatrix} 1 & 0 & 0 & 0 & 0 & 0 & 0 \\ 0 & 1 & 0 & 0 & 0 & 0 & 0 \\ 0 & 0 & 1 & 0 & 0 & 0 & 0 \\ 0 & 0 & 0 & 0 & 0 & 0 & 1 \end{bmatrix}$$

$$\hat{y}_{cost}(k+i|k) = \xi * y(k+i|k)$$

$$y^{ref} = \left\{ SOC^{ref} \; ; \; 0 \; ; \; \omega_g^{ref} \; ; \; 0 \right\}$$

The variation of the control inputs can also be expressed through a matrix approach as follows.

$$\Delta U = \left\{ \begin{matrix} \hat{u}_k - u_{k-1} \\ \hat{u}_{k+1} - \hat{u}_k \\ \vdots \\ \vdots \\ \hat{u}_{k+H_c-1} - \hat{u}_{k+H_c-2} \end{matrix} \right\} = \left\{ \begin{matrix} \hat{u}_k \\ \hat{u}_{k+1} - \hat{u}_k \\ \vdots \\ \vdots \\ \hat{u}_{k+H_c-1} - \hat{u}_{k+H_c-2} \end{matrix} \right\} - \left\{ \begin{matrix} u_{k-1} \\ 0 \\ 0 \\ \vdots \\ 0 \end{matrix} \right\} = [\delta]U - U^{ko}$$

$$[\delta] = \left[\begin{array}{ccccccccccc} 1 & 0 & 0 & & & & & & & & \\ 0 & 1 & 0 & & [0] & & & & \cdots & & \\ 0 & 0 & 1 & & & & & & & & \\ -1 & 0 & 0 & 1 & 0 & 0 & & & & & \\ 0 & -1 & 0 & 0 & 1 & 0 & & [0] & & & \\ 0 & 0 & -1 & 0 & 0 & 1 & & & & & \\ & & & -1 & 0 & 0 & 1 & 0 & 0 & & \\ & [0] & & 0 & -1 & 0 & 0 & 1 & 0 & [0] & \cdots \\ & & & 0 & 0 & -1 & 0 & 0 & 1 & \ddots & \\ & & & & \ddots & & & \ddots & & & \end{array} \right]$$

The vector U^{ko} is known since the vector $u_{k-1} = \left\{ T_e^{k-1}; T_g^{k-1}; T_b^{k-1} \right\}$ contains the values of the control inputs defined at the end of the previous optimization problem and currently applied to the system; it is fully measurable.

The equation (A.3) can be expanded using the definitions given above and eventually the whole expressions of matrix H and vector q are computed as follows.

$$J(U,k) = (\mathrm{y}_{cost} - \mathrm{y}^{ref})^t \left[W_y\right] (\mathrm{y}_{cost} - \mathrm{y}^{ref}) + U^t [W_u] U + \Delta U^t [W_{\Delta U}] \Delta U$$

$$\begin{aligned} J(U,k) = (\eta\Psi\, x(k|k) + \eta\Upsilon U + \eta\Omega V + \eta P - \mathrm{y}^{ref})^t \left[W_y\right] (\eta\Psi\, x(k|k) + \eta\Upsilon U \\ + \eta\Omega V + \eta P - \mathrm{y}^{ref}) + U^t [W_u] U + \Delta U^t [W_{\Delta U}] \Delta U \end{aligned}$$

$$\begin{aligned} = U^t\big(W_u + \Upsilon^t \eta^t W_y \eta\Upsilon + \Delta^t W_{\Delta U} \Delta \big) U \\ + 2\big[x_k^t \Psi^t \eta^t W_y \eta\Upsilon + V^t \Omega^t \eta^t W_y \eta\Upsilon + P^t \eta^t W_y \eta\Upsilon - \mathrm{y}^{ref} W_y \eta\Upsilon \\ - U^{ko} W_{\Delta U} \Delta \big] U + constant \end{aligned}$$

$$= U^t H U + 2 q^t U + constant$$

The constant term includes all terms that do not multiple U.

Appendix B - Sensitivity analysis and RSM

Suppose the relation between inputs and outputs of a system were known in a closed loop form as [27]:

$$y = f(x_1, \dots, x_k) = f(\boldsymbol{X}) \tag{B.1}$$

where y represents in the general case a vector of outputs while $\boldsymbol{X}$ represents generally a vector of inputs, then a sensitivity coefficient would be defined as the rate of change of one system outputs with respect to a variation of one system inputs.

$$C_i \approx \frac{\Delta y}{\Delta x_i} \tag{B.2}$$

In a mathematical form it would correspond to the partial derivative of the function $f(X)$ with respect to the i-th input, evaluated at a specific set point X_o. The function $f(\boldsymbol{X})$ is generally unknown in closed loop form consequently some techniques have been developed in order to rank the influence of each input parameter on each system output on the basis of observations collected during some tests on the system. The mathematical approach which applies one of these techniques is called *Sensitivity Analysis* and it is widely applied in engineering design in order to identify which parameters or independent variables affect the most the response of a system. Once these parameters, variables have been identified their values can be adjusted in order to obtain a desired response of the system. It can also highlight the robustness of the system with respect to parameter uncertainty. Since most of the techniques determine the sensitivity coefficients according to various formulations of (B.2), they rely on the assumption of linear response of the system and therefore the results from a sensitivity analysis are limited to the region of the input domain which was explored during the tests. Furthermore it is likely that the observations may depend on the particular set point X_o that is selected as base configuration so the analysis should be repeated using different initial set points, in particular if the system response is assumed to be nonlinear. Depending on whether the data come from experimental runs or from computer based simulations, the techniques to set up a sensitivity analysis may vary because computer based simulations lack of the variability in the input data. In both cases the available resources (money, time, knowledge of the system etc…) to carry out a set of runs are usually limited and this prevents from running a large set of configurations. For this reason different techniques are available to identify the relations among inputs and outputs ranging from simple procedures to more complex mathematical approaches [27]. The one-at-a-time analysis (OAT) represents the simplest and the least accurate design for sensitivity analysis since it implies to vary one input parameter at a time while all other parameters are kept fixed to their base values; in this way the change in the system response can be undoubtedly related to the change in a parameter level. The main drawback of an OAT analysis is represented by the impossibility to capture any correlation among the input parameters which may affect severely the system response. In fact the effect of a parameter on system response depends generally on the values assumed by the other parameters of the model. For this reason the OAT analysis is regarded to as a Local sensitivity analysis while Global sensitivity analysis involves changing simultaneously the levels of all parameters or at least part of them; the techniques which are presented here below belong to this latter class. Design of experiment (DOE) represents one step ahead towards a better description of the behavior of the system. This technique provides for creating a list of configurations to be tested where each parameter assumes a different level. It is based on a set of principles:

- comparison: all results are compared to a base case.
- randomization: namely the process which determines the parameter configurations to be tested. This process is fundamental because all configurations should be selected in order to be independent on one another.
- replication: in case of a process with a stochastic outcome, a configuration may be analyzed a number of times in order to evaluate the variability associated to random error on the output
- factorial experiment: each parameter can change level independently on the level assumed by the other factors

Thanks to the simultaneous variation of parameters level it is possible to draw some conclusions on main effects and correlation effects of parameters on system response. The list of parameters configurations is created according to different sampling approaches and typical methods are factorial design, CCD and D-design. The list is stored in a proper matrix, called design matrix. Factorial design is usually applied to have a first understanding of input-output relations. Depending on the structure of the list, either a full or a fractional factorial design can be carried out meaning that in the former case all main effects and all interaction effects can be successfully isolated while in the latter case the parameter main effects can be influenced by any correlations among two or more parameters. However since a fractional factorial design requires a smaller number of runs and the influence of high order correlations is usually weak on system response, this analysis is usually preferred. A design matrix is classified according to its resolution, namely the degree to which estimated main effects are confounded with estimated interaction effects.

If the number of parameters is larger than 5, other factorial designs are preferable like for instance central composite design (CCD) and D-design which are optimized sampling techniques to pick the levels of the parameters in such a way that the input space can be reasonably described at a smaller computational cost in comparison to a full/fractional factorial design [28]. In addition the factorial design is based on the assumption of linear relation between inputs and output but if a quadratic relation were assumed a higher number of observations would be required and in this case optimized sampling techniques like CCD are preferable. The next pictures compare a 2-level full factorial design (left) with a circumscribed and routable CCD-design (right). The dots and the stars represent different combinations of parameter levels which are standardized with respect to the base case for the sake of illustration.

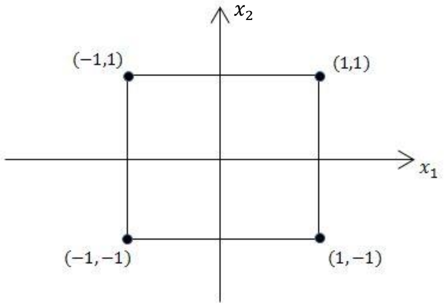

Figure B.1: Full factorial design

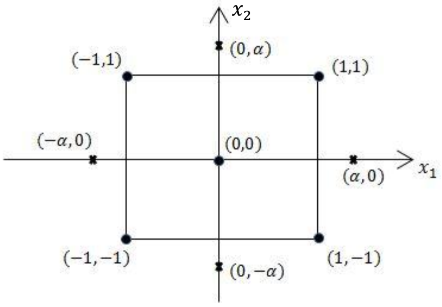

Figure B.2: CCD-design.

Taking for example two parameters x_1, x_2 a positive $\Delta^+_{x_i}$ and a negative $\Delta^-_{x_i}$ variation with respect to their correspondent base level x_i^o, is specified for each of them. A new upper and lower level can be found and standardized as follows, for example, for x_1 [28]:

$$-1 = \frac{x_1^o - \left(x_1^o + \Delta^-_{x_i}\right)}{\Delta^-_{x_i}} \quad +1 = \frac{\left(x_1^o + \Delta^+_{x_i}\right) - x_1^o}{\Delta^+_{x_i}}$$

The CCD-design specifies a further variation $\Delta^{\pm\alpha}_{x_i}$ with respect to the base case which leads to the standard levels $\pm\alpha$ in a similar way as computed above. The value of α depends on the desired properties of the design and on the number of factors that are tested as it will be shown afterwards. These standardized levels specify the values that each parameter will assume for any configuration that will be tested during the campaign. The settings are collected in a design matrix. Since a full factorial and a CCD-design considers different samplings of the parameters levels, two different matrices can be defined as reported here below.

Table B.1: Design matrix of full factorial

test	x_1	x_2
#1	-1	+1
#2	+1	+1
#3	-1	-1
#4	+1	-1

Table B.2: Design matrix of CCD-design

test	x_1	x_2
#1	-1	+1
#2	+1	+1
#3	-1	-1
#4	+1	-1
#5	-α	0
#6	+α	0
#7	0	-α
#8	0	+α
#9	0	0

This example shows how the design matrix of a CCD-design is equivalent to the design matrix of a 2-level full factorial design plus additional star and central points. These additional points serve to calculate the curvature of the response surface, the central point is also important to assess the lack of fit of a regression model. Therefore the benefit to apply a CCD-design with respect to a full factorial design is more evident as the number of parameters increases. For instance if four parameters has to be tested on 3 levels each, a full factorial design would require $3^5 = 243$ runs while $24 + N_{center}$ runs are necessary for a CCD-design where N_{center} indicates the number of runs that should be repeated for the base configuration. This latter value can be equal to 1 for deterministic processes while it is usually much greater than one (~ 9) for experimental based runs since the variability in the process outcome at the center point can be used as a measure of the lack of fit. As the previous design matrices show, a CCD-design always takes more levels for each parameter even for a simple test case like the one considered here. A design matrix is created with the property of being orthogonal, namely none parameter configuration can appear twice within the same sequence of runs. However this matrix specifies the levels for each parameter in any configuration consequently the experimentalist is free to upset the order and to repeat each configuration a number of times in order to have a measure of the variance in the outputs. In the case of a CCD-design further properties can be achieved depending on how the design matrix is built:

+ type:
    - circumscribed: the star points are placed at distance α from the center point and represent new extreme levels for the parameters. The value of α depends on the desired properties of the design and on the number of factors involved in the analysis. This type of test explores the largest input space, it has a spherical symmetry and it defines 5 levels for each parameter.

  - inscribed: this design can be obtained from a circumscribed one by dividing the star point for α, namely the star points are added in such a way that they do not exceed the extreme values impose by the original factorial levels. This type comprises 5 levels for each factor.
  - face centered: in this design $\alpha = 1$ so just three levels for each factor are tested. This type explores the smallest input space since the value of α delimits the domain to be considered.
- rotatability: a design matrix is rotatable if the variance of the predicted output response at an input point X depends only on the distance between X and the center point. This property is important to apply a response surface methodology because it implies that the observations do not depend on the direction followed from the center point to define a parameter level.

The latter property holds by assigning a desired value of α. The following formula reports the desired value of α as function of the number of factorial runs which eventually depends on the number of parameters:

$$\alpha = [number\ of\ tests]^{1/4}$$

The number of experimental runs is related to either a full or a fractional factorial because the design matrix of a CCD-design is built upon a 2-level full or fractional design augmented with a number of star and central points. The following figures report the parameters levels for a 2-factor CCD-design for either a circumscribed or a face centered or an inscribed design.

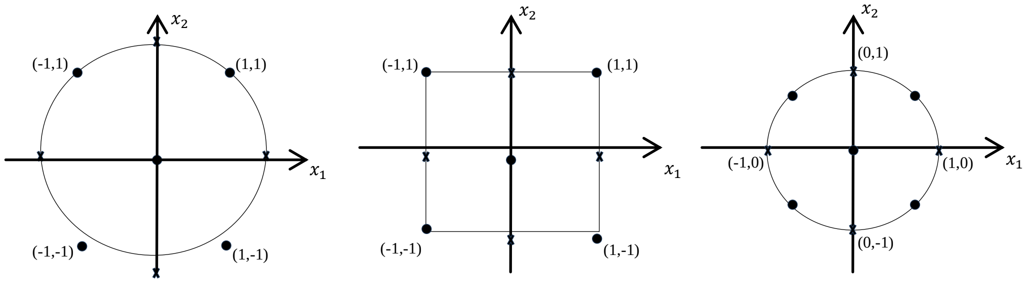

circumscribed face centered inscribed

Figure B.3: The test configurations taken by three different design matrices.

In an experimental based design the repetitions of runs at the center point allows assessing the lack of fit, namely if the analysis omits some important terms in the regression model. The lack of fit represents a steady error due to poor regression model and it is a different source of error than the random error due to random uncertainty.

The most advanced approach to analyze input-output relations is represented by random sampling techniques which are referred to as Monte Carlo simulations. In this approach the input space of parameters is better described since each parameter can assume several levels and the correspondent values are picked at random from the correspondent parameter domain. Due to the fact that more observations are available and parameters values are picked randomly about the correspondent base value it is possible to calculate the sensitivity coefficients using the analysis of variance or other detailed mathematical calculations like Fourier amplitude sensitivity. A base case is always specified and values are picked in the neighborhood; efficient optimized random sampling techniques like optimized Latin hypercube are employed to guarantee that the input space can be described well. Contrary to the previous case, the experimentalist has only to define the boundaries of the input space and not the discrete levels of each parameter. The drawback of this latter approach is the long time required for the whole simulation or experimentation due to the increased number of combinations to be evaluated. For experimental design it is often unfeasible applying this approach and even computer based design may become too long if the model is complex. Monte Carlo methods are applied to a variety of problems and their application to sensitivity analysis is mostly focused on the determination of a suitable regression model. They can also be directly applied to evaluate the robustness of a control strategy towards uncertainty in model parameters and measurement noise.

The regression analysis provides the most comprehensive sensitivity measure by deriving a mathematical regression model of the observations which can relate the inputs to the output. The unknowns of a regression analysis are the regression coefficients and a regression model is defined either linear or nonlinear depending on the relation between the system response and the regression coefficients. A linear regression model can include nonlinear relations between independent variables and system response. This model can be specified by any possible mathematical function but polynomial curves or surfaces of independent variables are utilized for the sake of simplicity. Moreover the resource available to conduct experimental runs are usually limited therefore for practical applications it is rare to have enough observations to derive a polynomial response surface of order higher than 2. A second order polynomial gives the possibility to find an optimum of the system response; nevertheless a response surface is always limited to a small domain around the initial base case meaning that inference on system response should be avoided outside the domain used to get the observations. The magnitude of the regression coefficients is a direct ranking of parameter influence over the system output; if the regression surface is to be used to rank the parameter influence the regression coefficients are usually standardized in order to take into account the relative units and place all parameters on an equal level. For the sake of simplicity it is common to start guessing a linear regression model. Linearity is assumed for the regression coefficients while each independent input variable can appear in the regression model through a nonlinear function. Once a suitable model is guessed, the regression coefficients are calculated by means of least square method in order to minimize the distance between the observed values and the values obtained from the regression model at the correspondent input configurations. A second order polynomial regression model can usually assume a form similar to the following one:

$$y = \beta_1 + \sum_{i=1}^{4} \beta_{2\ldots5} x_i + \sum_{i=1}^{4} \beta_{6\ldots9} {x_i}^2 + \frac{1}{2} \sum_{i=1}^{4} \sum_{\substack{j=1 \\ j \neq i}}^{4} \beta_{10\ldots18} x_i x_j \qquad \text{(B.3)}$$

where β_k with $k = 1 \ldots n$ are the regression coefficients while x_j, with $j = 1 \ldots m$, are the independent variables. Here y represents the response of the system. In order to assess the adequacy of the regression model, statistical test fit is usually applied. The analysis of variance (ANOVA) is an established technique to judge if there is high probability that the hypothesized regression model matches the observed values at a certain significance level.

ANOVA relies on three main assumptions:

- the levels of an independent variable are not influenced by the levels of the other input variables

- the residuals coming from the regression are assumed to be normally distributed having zero mean
- the variance in the data is assumed to remain constant among different populations of the input data

The first assumption can be validated by the user when the factor levels are chosen while the third assumption does not represent an issue when computer based simulations are considered due to the lack of intrinsic uncertainty in input data. On the other hand the second assumption can be used as starting point to check the adequacy of the regression model. Once the regression coefficients are calculated, the residuals of regression can be computed as:

$$e_i = y_i - \hat{y}_i$$

where $\hat{y}_i$ is the system response obtained at the *i-th* configuration of the parameters using the regression model and y_i is the *i-th* observation. If the second assumption holds a normal probability plot of the residuals should produce a plot where all points lie on a straight line. If the points are not ordered on a line but are randomly spread then it can be concluded that the regression model has poor quality. A more refined investigation appeals to hypothesis testing where through a statistical approach it is possible to infer some conclusions on regression coefficients. The null hypothesis that should be rejected is that the k-th regression coefficient β_k is null against the hypothesis that it is not null. ANOVA uses an F-test to evaluate this hypothesis and conclusions can be drawn on the null hypothesis from the p-value of the test. It is customary to assume that a p-value smaller than 0.05 sets moderate or high evidence against the null hypothesis, namely that there is high probability that the null hypothesis is wrong and the k-th regression coefficient is not null in the regression model. The threshold value 0.05 is called "significance of the test".

This hypothesis testing evaluates the hypothesis of having a constant model against a linear model.

Appendix C - Standard drive cycles

The velocity profiles of the standard drive cycles that have been considered throughout the analysis are reported below.

NEDC

- Road profile: flat
- Length of the cycle: 11.010 km

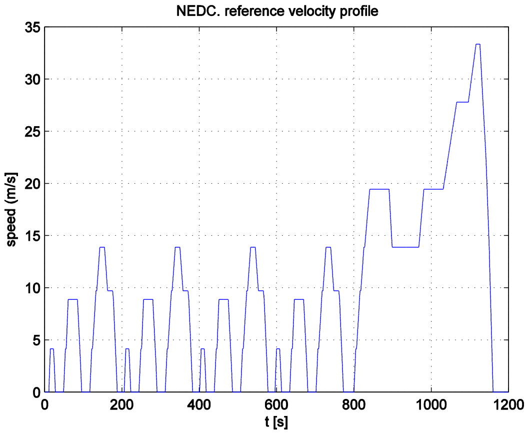

Figure C.1: Reference velocity profile of cycle NEDC

HWFET

- Road profile: flat
- Length of the cycle: 16.501 km

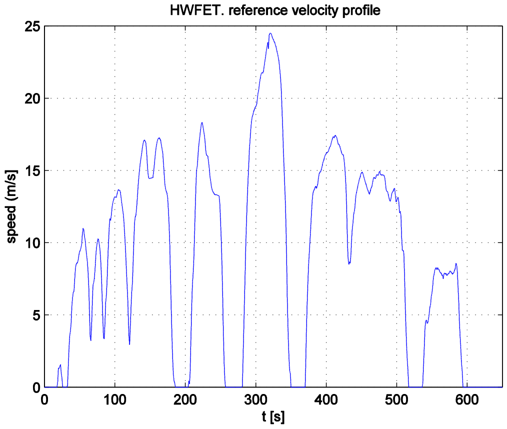

Figure C.2: Reference velocity profile of cycle HWFET

SC03

- Road profile: flat
- Length of the cycle: 5.758 km

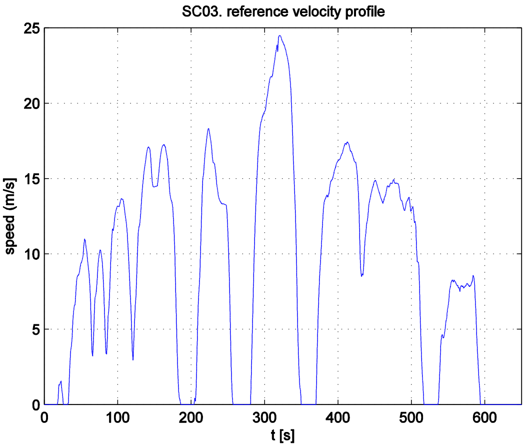

Figure C.3: Reference velocity profile of cycle SC03

UDDS

- Road profile: flat
- Length of the cycle: 11.985 km

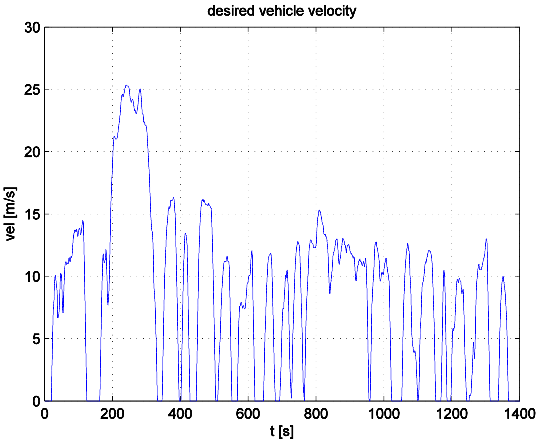

Figure C.4: Reference velocity profile of cycle UDDS

US06

- Road profile: flat
- Length of the cycle: 12.882 km

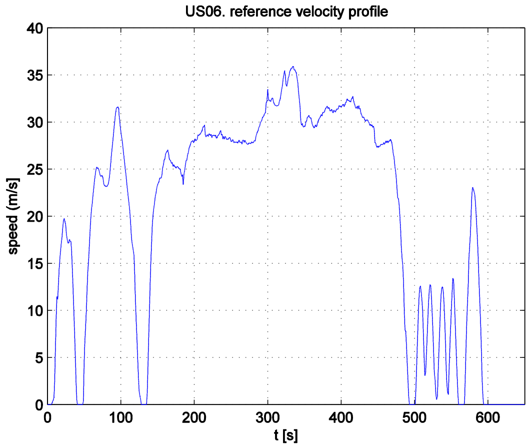

Figure C.5: Reference velocity profile of cycle US06

Bibliography

[1] I. Husain, Electric and Hybrid vehicles. Design and Fundamentals, Second Edition ed., CRC Press.

[2] G. Ferrari, Motori a combustione interna, Il Capitello.

[3] K. Govindswamy, T. Wellmann and G. Eisele, “Aspects of NVH integration in Hybrid Vehicles,” *SAE International.*

[4] P. J. Møller, “Seminar on Electric vehicle,” DTU, Lyngby, Denmark, 2011.

[5] L. Serrao, “"A comparative analysis of energy management strategies for hybrid electric vehicles.",” *Electronic Thesis or Dissertation. Ohio State University, 2009. https://etd.ohiolink.edu/.*

[6] P. Pisu and G. Rizzoni, “"A Comparative Study Of Supervisory Control Strategies for Hybrid Electric Vehicles,",” *Control Systems Technology, IEEE Transactions on,* vol. 15, no. 3, pp. 506-518, May 2007.

[7] A. Sciarretta and L. Guzzella, “Control of Hybrid electric vehicles,” *Control of Systems, IEEE,* vol. 27, no. 2, pp. 60-70, April 2007.

[8] D. V. Ngo, T. Hofman, M. Steinbuch and Serrarens, “"An optimal control-based algorithm for Hybrid Electric Vehicle using preview route information,",” *American Control Conference (ACC),* pp. 5818-5823, June 30th 2010-July 2nd 2010.

[9] S. P. B. E. L. Johannesson, “"Predictive energy management of a 4QT series-parallel hybrid electric bus",” *Control Engineering Practice,* vol. 17, pp. 1440-1453, 2009.

[10] G. Ripaccioli, D. Bernardini, S. Di Cairano, A. Bemporad e I. Kolmanovsky, «"A stochastic model predictive control approach for series hybrid electric vehicle power management,",» *American Control Conference (ACC),* pp. 5844-5849, June 30 2010-July 2 2010.

[11] R. G. Y. S. B. Musardo C, «“A-ECMS: An Adaptive Algorithm for Hybrid Electric Vehicle Energy Management”,» *European Journal of Control* , vol. 11, pp. 509-524, 2005.

[12] R. Beck, F. Richert, A. Bollig, D. Abel, S. Saenger, K. Neil, T. Scholt e K. Noreikat, «"Model Predictive Control of a Parallel Hybrid Vehicle Drivetrain,",» *Decision and Control, 2005 European Control Conference. CDC-ECC '05. 44th IEEE Conference,* vol. 12, n. 15, pp. 2670-2675.

[13] L. d. Re, Automotive model predictive control: Models, Methods and Applications, Springer-Verlag.

[14] S. Di Cairano, W. Liang, I. Kolmanovsky, M. Kuang and A. Phillips, “"Engine power smoothing energy management strategy for a series hybrid

electric vehicle,",” *American Control Conference (ACC),* pp. 2101-2106, June 29th 2011, July 1st 2011.

[15] H. A. Vahidi, A. Phillips, M. Kuang, I. Kolmanovsky e S. Di Cairano, «"MPC-Based Energy Management of a Power-Split Hybrid Electric Vehicle,",» *Control Systems Technology, IEEE Transactions,* vol. 20, n. 3, pp. 593-603, May 2012.

[16] M. M. a. T. K. K. Yu, «"Model predictive control of a power-split hybrid electric vehicle system, ",» *Artificial Life and Robotics,* vol. 17, n. 2, pp. 221-226, Dec 2012.

[17] L. Johannesson, M. Asbogard e B. Egardt, «"Assessing the Potential of Predictive Control for Hybrid Vehicle Powertrains Using Stochastic Dynamic Programming,",» *Intelligent Transportation Systems, IEEE Transactions* , vol. 18, n. 1, pp. 71-83, March 2007.

[18] D. Opila, D. Aswani, R. McGee, J. Cook e J. Grizzle, «"Incorporating drivability metrics into optimal energy management strategies for Hybrid Vehicles,",» *Decision and Control, 2008. CDC 2008. 47th IEEE Conference,* vol. 9, n. 11, pp. 4382-4389, Dec 2008.

[19] A. S. b. LMS, “Amesim User's Guide,” 2012.

[20] F. U. e. al., “Derivation and Experimental Validation of a Power-Split Hybrid Electric Vehicle Model,” *IEEE Transactions on vehicular technology,* vol. 55, no. 6, pp. 1734-1747, November 2006.

[21] L. Guzzella and A. Sciarretta, Vehicle Propulsion Systems. Introduction to Modeling and Optimization., Third Edition ed., Springer-Verlag, 2013.

[22] Toyota, «Toyota Hybrid system THS II,» May 2003.

[23] J. Maciejowski, Predictive control with constraints, Prentice Hall, 2002.

[24] L. Wang, Model Predictive Control System Design and Implementation Using Matlab®, Springer, 2009.

[25] Ferreau, Kirches, Potschka, Bock and Diehl, “qpOASES: A parametric active-set algorithm for quadratic programming,” *Mathematical Programming Computation,* 2014.

[26] “ISO 2631-1:1997 Mechanical vibration and shock - Evaluation of human exposure to whole-body vibration,” *International Organisation for Standardisation, Schweiz, 1997.*

[27] Q. Huang e H. Wang, «Fundamental Study of Jerk: Evaluation of Shift Quality and Ride Comfort.,» *SAE International,* 2004.

[28] A. Fassò and P. Perri, “Sensitivity analysis,” *Encyclopedia of Environmetrics,* 2006.

[29] N. Bradley, The Response Surface Methodology, Thesis in Applied mathematics & computer science, 2007.